THE RELATIONSHIP BETWEEN CARBON ISOTOPE FRACTIONATION AND CARBON CONCENTRATING MECHANISM ACTIVITY IN MARINE PHYTOPLANKTON

By

ANTHONY STEPHEN FIELDING

B.Sc. (Hons), Acadia University, Nova Scotia, 1992

A THESIS SUBMITTED IN PARTIAL FULFILLMENT OF
THE REQUIREMENTS FOR THE DEGREE OF

DOCTOR OF PHILOSOPHY

in

THE FACULTY OF GRADUATE STUDIES
(Department of Earth and Ocean Sciences)

We accept this thesis as conforming
To the required standard

THE UNIVERSITY OF BRITISH COLUMBIA

February 2000

In presenting this thesis in partial fulfillment of the requirements for an advanced degree at the University of British Columbia, I agree that the Library shall make it freely available for reference and study. I further agree that permission for extensive copying of this thesis for scholarly purposes may be granted by the head of my department or by his or her representatives. It is understood that copying or publication of this thesis for financial gain shall not be allowed without my written permission.

Department of Earth and Ocean Sciences

The University of British Columbia
Vancouver, Canada

Date February 22, 2000

Abstract

The ocean is the largest reservoir of carbon on the Earth's surface and hence ocean processes involving carbon are of great importance in light of the growing concern over global warming due to an increased greenhouse effect. Modern phytoplankton assemblages appear to record the CO_2 concentration in seawater through their carbon stable isotope content. Phytoplankton preserved in marine sediments could contain a record of atmospheric CO_2 concentrations dating back as much as 200 million years. However, before using a relationship between CO_2 concentration and the stable isotopic content of phytoplankton, the mechanism(s) behind this apparent relationship must be examined further.

Research on carbon isotope fractionation in marine phytoplankton has typically assumed that cells rely on CO_2 diffusion to supply photosynthetic carbon demand. The results of this thesis show that active carbon uptake has a strong influence on carbon isotope fractionation in six species of marine phytoplankton. A more detailed study of the marine diatom *Thalassiosira pseudonana* demonstrated that carbon concentrating mechanism (CCM) induction occurred over an ecologically relevant range of CO_2 concentrations (ca. 3 to 16.5 μM), and that fractionation decreased simultaneously with increased CCM induction. CCM induction in *T. pseudonana* appeared to be regulated by CO_2 concentration rather than DIC concentration. Based on the results of experiments and modeling, the CCM appears to involve extracellular carbonic anhydrase catalyzed CO_2 formation from bicarbonate and subsequent uptake of CO_2. A better understanding of factors that influence fractionation, including the involvement of CCM activity and species variability, must be gained before the isotopic composition of sedimentary organic matter can be used as a proxy for past atmospheric CO_2 concentrations.

Table of Contents

List of Tables

List of Figures

List of Abbreviations

α	Kinetic isotope fractionation factor
CA	Carbonic Anhydrase
CCM	Carbon concentrating mechanism
CO_2	Dissolved form of CO_2
CO_2g	Gaseous form of carbon dioxide
CO_3^{2-}	Carbonate (dissolved)
$\delta^{13}C$	A measure of carbon isotope content of a sample relative to a standard.
$\Delta\delta$	Fractionation during conversion of substrate to product
DIC	Dissolved Inorganic Carbon
ε_p	Fractionation relative to CO_2aq
HCO_3^-	Bicarbonate (dissolved)
$K_{1/2}DIC$	[DIC] required to give 50% of maximum photosynthesis
$K_{1/2}CO_2$	[CO_2] required to give 50% of maximum photosynthesis
K_m	Michaelis-Menten half-saturation constant for enzyme-substrate
PDB	Carbon isotope standard – Pee Dee Belemnite Limestone
PEPCase	Phosphoenolpyruvate Carboxylase
POC	Particulate organic carbon
R	Ratio of ^{13}C to ^{12}C
RuBisCO	Ribulose-1,5-Bisphosphate Carboxylase-Oxygenase
V_{max}	Maximum rate of reaction
‰	Notation for "per mil" measure of fractionation

ACKNOWLEDGEMENTS

There are many people to whom I owe a great deal of thanks. First, I wish to thank Dr. Paul J. Harrison who has been an excellent supervisor and who took me on after I was orphaned from another lab. I thank the isotope group consisting of Drs. Stephen E. Calvert, Robert D. Guy, Nathalie Waser and David H. Turpin for their input and discussions on stable isotope fractionation. I also appreciate the co-operative efforts of Dr. David W. Crawford and Lisa Lee with whom I spent long hours in the lab. I am grateful to the many fellow students from the Harrison lab, too many to mention, who were always there to help and provide input on my research. Special appreciation goes to Dr Robert D. Guy who seemed to be perpetually fixing the broken glass of the vacuum lines. My next mission is to attempt glass blowing. I also wish to thank Bente Nielsen for the isotope analysis and Dr. David Layzell who helped me to design the gas mixing system.

However, perhaps the most appreciation goes to my family. I wish to thank my parents Raymond and Gloria Fielding for their encouragement throughout my doctoral program. Thank you Dad for starting me on a career of science. I wish to thank my wife Sonya Budge for her support during my doctorate program. It is her and our daughter Meaghan who fill my life with love and enjoyment everyday. I dedicate this thesis to them both.

Chapter 1

General Introduction

1.1 Overview

Nitrogen has typically been viewed as the limiting nutrient for primary productivity in the ocean environment though recent studies have implicated many different nutrients as potential limiting factors (for example, Morel *et al.* 1994). One nutrient that has been suggested as a potential limiting resource is inorganic carbon (Riebesell *et al.* 1993b). While, at first glance, there appears to be ample carbon with which to supply the carbon required for photosynthesis, only about one percent is actually immediately available for use in the form of CO_2. This has led to speculation that phytoplankton can use alternate forms of inorganic carbon, namely bicarbonate. Close to half of global photosynthesis occurs in the ocean (Falkowski 1994) and the ocean's ability to absorb great amounts of carbon illustrates the importance of the ocean's role in the global carbon cycle. Given that organically fixed carbon is preserved in sediments, primary productivity in the ocean is of great importance to the regulation of global temperatures and, as of late, global warming. Preserved phytoplankton might also reveal a message which, when deciphered, could provide a record of the composition of the atmosphere in the past. Such information would be valuable in establishing relationships between atmospheric CO_2 concentration and global temperatures and climate. This message is preserved in the carbon isotope content of phytoplankton remains.

The carbon isotopic compositions of natural phytoplankton populations show considerable variation in the world's oceans. The importance of various factors in determining the isotopic content of phytoplankton remains a contentious issue with often conflicting results from laboratory studies depending on the species studied and the culturing conditions. In addition to laboratory studies, scientists have attempted to correlate various environmental conditions with the isotopic content of natural assemblages of phytoplankton in the ocean. Ultimately, an understanding of these factors would allow for interpretation of past environmental conditions based on preserved phytoplankton in marine sediments. However, there is still no clear model of carbon isotope fractionation by marine phytoplankton and, as a result, there is considerable current interest in learning more about the factors that influence this process.

All of the factors studied to date can ultimately be tied to photosynthesis. However, few studies have closely examined the photosynthetic physiology of phytoplankton while studying other environmental conditions. It can be argued that photosynthesis is the most important process in determining the isotopic content of phytoplankton since it is the process by which inorganic carbon is converted to organic carbon. Factors which influence growth rates ultimately regulate photosynthetic rate since cells must maintain an adequate photosynthetic rate to support a given growth rate. These factors may also influence the ability of cells to take up carbon and potentially the pathway of uptake. Some examples of factors that have been studied to date are dissolved inorganic carbon (DIC) and/or CO_2 concentration, light, pH and temperature. To further complicate matters, temperature and pH not only affect cell physiology, they also influence the inorganic carbon system itself. This results in uncertainty as to whether carbon isotope fractionation was influenced by changes in cell physiology or changes in the supply of carbon to the cells.

The research presented in this thesis attempts to clarify the factors that influence carbon isotope fractionation, especially carbon concentrating mechanism (CCM) activity, while simultaneously examining the photosynthetic physiology of phytoplankton cultures. The following sections will provide background information on carbon isotope fractionation by marine phytoplankton and the factors that influence the isotope content of cells. Various aspects of photosynthetic physiology will be introduced as well as models that attempt to predict the fractionation expressed by phytoplankton under a range of environmental conditions. Finally, the objectives of the thesis will be presented.

1.2 Carbon Isotope Fractionation

There are two stable isotopes of carbon: carbon-12, which makes up 98.9% of the total carbon and carbon-13, which makes up the remainder (O'Leary, 1988). The isotope content of a sample can be expressed as the ratio (R value) of ^{13}C to ^{12}C as per Equation 1; however, changes in isotope content are very small. As a result, Equation 2 is used to calculate isotope content of samples and the results are expressed as $\delta^{13}C$ with the units per mil (‰). This equation uses as a standard the isotope ratio of the Pee Dee Belemnite (PDB) Limestone from South Carolina and thus $\delta^{13}C$ values are often cited as relative to PDB. Positive $\delta^{13}C$ values indicate the sample is enriched in ^{13}C while negative values indicate that the sample is depleted in ^{13}C relative to the standard. The $\delta^{13}C$ values of naturally occurring organic materials are typically negative (O'Leary, 1988).

$$R_{sample} = \frac{^{13}C}{^{12}C} \quad (1)$$

$$\delta^{13}C\,(‰) = \left[\frac{R_{sample}}{R_{standard}} - 1\right] \times 1000 \quad (2)$$

Organic material contains less ^{13}C than the carbon in the physical environment because the processes that are responsible for carbon fixation generally discriminate against the heavier isotope. Discrimination against ^{13}C is a result of the extra atomic mass unit of ^{13}C and the fact that it forms stronger bonds than ^{12}C. The result of discrimination against ^{13}C during a process results in an expressed fractionation that can be calculated as per Equation 3. Differences in the isotope composition of substances can provide valuable insight into the processes involved in their formation, including physical, chemical and biological processes. For example, there are two major groups of terrestrial plants that can be distinguished by the primary means of initial carbon fixation. These are C_3 plants which rely primarily on the enzyme ribulose-1,5-bisphosphate carboxylase-oxygenase (RuBisCO) and C_4 plants which initially fix carbon via the enzyme phosphoenolpyruvate carboxylase (PEPCase). C_3 plants typically have $\delta^{13}C$ values in the vicinity of –28‰ while the $\delta^{13}C$ for C_4 plants tends to be in the range of -12 to -14‰. Since the isotopic content of the CO_2 source for these plants is relatively constant, the difference in $\delta^{13}C$ is the result of different fixation pathways and discrimination of the primary carboxylation enzymes possessed by these two groups of plants. In fact, the difference in $\delta^{13}C$ of these two groups was known prior to the elucidation of their carbon fixation pathways.

$$\Delta\delta = \frac{\left[\delta^{13}C_S - \delta^{13}C_P\right]}{1 + \left[\frac{\delta^{13}C_S}{1000}\right]} \qquad (3)$$

Where (S) and (P) represent source and product respectively.

Although enzyme discrimination is a major cause of fractionation, other factors, such as diffusion, also determine the expressed fractionation. Each process results in a unique fractionation value. In a more complex system, the expressed fractionation of the overall system typically reflects the fractionation of the rate-limiting step. Thus, although carbon fixation by RuBisCO results in a high fractionation of ca. 29‰ (varies depending upon species, Guy *et al.* 1987, 1989), limitation in the supply of carbon to the enzyme will result in an overall fractionation that is more consistent with that of the supply process. Since fractionation associated with diffusion in water is relatively small (0.7‰, O'Leary 1984), cells that are fully limited by the rate of carbon dioxide diffusion will express very little overall fractionation. The actual fractionation can be used to determine the fractional limitation on photosynthesis by diffusion and fixation and this model will be described later in the thesis.

A final consideration when studying fractionation is whether the process represents kinetic or thermodynamic isotope effects (O'Leary 1981). Kinetic isotope fractionation occurs when the transformations of substances containing different isotopes occur at different rates. In the case of ^{12}C and ^{13}C, substances containing the latter species will react more slowly than those containing the lighter isotope. Kinetic isotope fractionation values ultimately represent the ratio of the two rate constants for the transformation of a substance containing two different isotopes (Equation 4). Kinetic isotope fractionation is often

expressed in terms of an α value. For example, the kinetic isotope fractionation associated with fixation of CO_2 by eukaryotic RuBisCO (α) is 1.029. This means that $^{12}CO_2$ reacts 1.029 times faster than $^{13}CO_2$.

$$\alpha = \frac{\text{rate constant for process with } ^{12}C}{\text{rate constant for process with } ^{13}C} \qquad (4)$$

Thermodynamic isotope fractionation occurs when processes are in equilibrium. The equilibrium isotope effect is the result of the kinetic isotope fractionations associated with both the forward and backward reactions. The assumption of isotopic equilibrium is only valid when the particular transformation is very rapid relative to the steps immediately preceding and following it. This is especially important since isotopic equilibrium is attained more slowly than chemical equilibrium (O'Leary 1981). One isotope effect that might be assumed to be in equilibrium is the dissolution of CO_2 from the atmosphere into water. When equilibrium is in doubt, the kinetic isotope fractionation approach should be used.

If a single step unidirectional process is considered, one can determine the fractionation using Equation 3 if the substrate pool is infinitely large when compared to the product formed. However, in a closed system, one can model the changes in the isotope content of the substrate and product pools in accord with the Rayleigh distillation model (Mariotti *et al.* 1981). This technique uses the kinetic approach to isotope fractionation analysis and assumes that variation in fractionation with substrate concentration does not occur, a condition supported by O'Leary (1981). The relationship between the fraction of substrate remaining (f) and the isotope content of the accumulated product in a closed system is given by Equation 5 (Mariotti *et al.* 1981). The per mill enrichment factor, ε, represents

fractionation during the particular transformation in question. The problem with this approach is that isotopic changes in the accumulated product are slow. A better approach is to measure the isotopic content of the newly fixed (instantaneous) carbon; however, it is difficult to separate out newly fixed carbon from "old" carbon. Alternatively, one can use the isotopic content of the remaining substrate at a given time relative to that at the beginning of the experiment. Again, the Rayleigh distillation model can be used. Changes in the $\delta^{13}C$ of the substrate and product are illustrated in Figure 1.1A.

$$\delta^{13}C_{product} = \delta^{13}C_{substrate,\,t=0} - \varepsilon \times \left[\frac{(f \times \ln(f))}{1-f}\right] \qquad (5)$$

Given a constant fractionation, there is a linear relationship between the natural log of the ratio of the R values at a given time and the initial time, multiplied by 1000 (Y-axis) and the negative natural log of f (X-axis). This method is illustrated in Figure 1.1B. The slope of the resulting line generated in Figure 1.1B represents the fractionation in a closed system (Guy *et al.* 1992). The regression line used was fitted through the raw data without reference to the initial value (origin). This approach was used throughout this thesis as the method of determining fractionation. However, models of fractionation by marine phytoplankton ultimately require consideration of numerous processes including fractionation associated with carbon fixation, CO_2 diffusion through both the medium and the cell membrane, and active uptake. It is for these reasons that the experiments contained in this thesis were carried out.

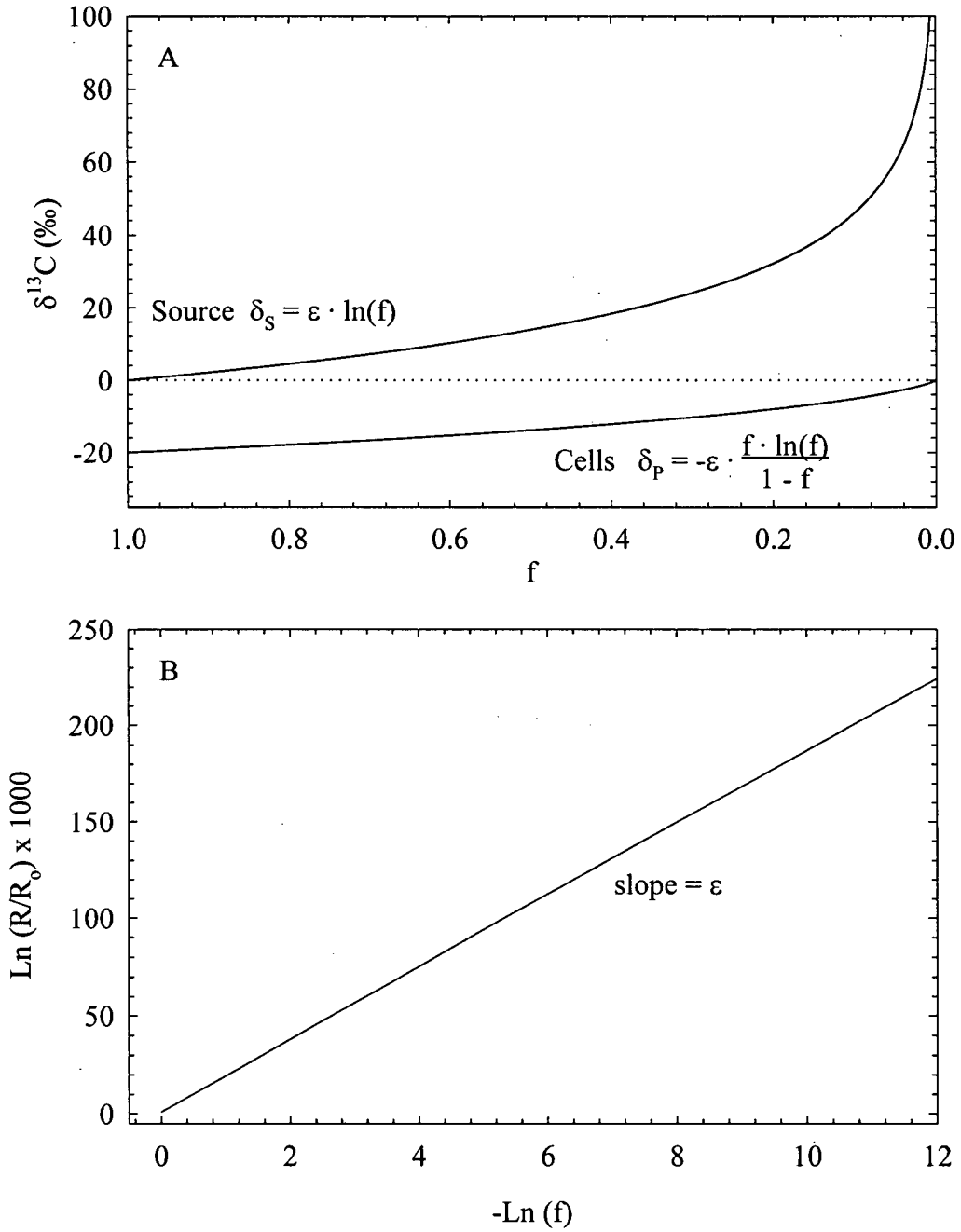

Figure 1.1. Methods for determining fractionation. Theoretical changes in the isotopic content of remaining substrate as taken from Mariotti *et al.* (1981) (A), and changes in $^{13}C/^{12}C$ as a function of the fraction of remaining substrate (f) as taken from Guy *et al.* (1989) (B). Both figures assume a constant fractionation of 20‰.

1.3 Photosynthetic Kinetics

Carbon isotope fractionation, and hence the isotopic content of phytoplankton cells, is ultimately determined by the processes involved in inorganic acquisition and, to a lesser extent, by the respiration processes which serve to reduce cell carbon. A proper understanding of phytoplankton carbon isotope fractionation thus requires some knowledge of phytoplankton photosynthesis. Photosynthesis in higher plants can be described as using C_3, C_4, or CAM mechanisms. In the case of C_3 and C_4 plants, the name comes from the number of carbon atoms contained in the initial fixation product. In C_3 photosynthesis, carbon dioxide is fixed by RuBisCO, resulting in the formation of the three-carbon compound phosphoglycerate. However, in C_4 photosynthesis, the four-carbon compound oxaloacetate acts as an intermediate between initial fixation and the ultimate carbon fixation by RuBisCO. Thus, even though the initial fixation process is different, the final carbon fixation steps are similar in both C_3 and C_4 plants.

The enzyme responsible for the initial fixation of carbon can have a strong influence on the overall fractionation during photosynthesis. Higher plants using the C_3 pathway typically exhibit fractionation 10 to 15‰ higher than C_4 plants due to the different initial carbon fixation enzyme (O'Leary 1988). CAM plants are somewhat similar to C_4 plants except that they fix carbon during dark periods when experiencing drought stress and use this stored carbon during the day to carry out the normal C_3 type pathway. When CAM plants use their ability to accumulate carbon at night, they will have a $\delta^{13}C$ value similar to C_4 plants since the pathways are similar. However, if they rely solely on daytime photosynthesis, they will exhibit fractionation similar to C_3 plants (O'Leary 1981).

The range in $\delta^{13}C$ values observed in phytoplankton is between –8.8 and –34.5‰ (Kerby & Raven 1985, Maberly *et al.* 1992). It was thought that such a range could be the result of different levels of β-carboxylation activity similar to that used by C_4 plants (Beardall *et al.* 1976, Descolas-Gros & Fontugne 1985). However, in marine phytoplankton, the C_3 photosynthetic pathway appears to be the most important one with no real evidence for an obligatory C_4 type mechanism available to date (Raven *et al.* 1993). Thus, most of the carbon fixed in phytoplankton is via the enzyme RuBisCO. This is not to say that PEPCase, and indeed other carboxylation enzymes, are not present in phytoplankton. There is evidence that alternative carboxylase enzymes contribute as much as 10% of the total carbon fixed by some marine phytoplankton (Raven *et al.* 1993). The diversity of these other carboxylase enzymes is a result of the range of products required for cellular metabolism as well as the evolutionary history of the group of phytoplankton (Raven *et al.* 1993). RuBisCO uses CO_2 as its carbon source while other carboxylase enzymes use either bicarbonate or CO_2.

The most logical method of carbon dioxide supply to the site of RuBisCO is diffusion of CO_2 across the phytoplankton cell membrane where it is then fixed. With a total dissolved inorganic carbon (DIC) concentration that stays fairly constant at around 2 mM in the present-day ocean, it would seem unlikely that carbon could limit photosynthesis. However, because of the complex speciation of inorganic carbon in seawater, cells relying on CO_2 diffusion are restricted to only a small portion of the carbon pool. Though the number varies with temperature, CO_2 represents only about 1% of the total inorganic carbon available. Complicating matters is the slow uncatalyzed rate of conversion from bicarbonate to CO_2. These factors have led some (Riebesell *et al.* 1993b) to speculate that carbon dioxide supply could actually limit the growth of phytoplankton in marine environments.

The question that remains is whether marine phytoplankton do indeed rely solely on diffusive uptake of CO_2. There is evidence that some alternative pathway of carbon uptake is possible under conditions where CO_2 diffusion would be insufficient to supply the carbon required to maintain a specific growth rate. The enzyme RuBisCO possesses both a carboxylase activity as well as an oxygenase activity. Phosphoglycolate is one of the products produced when RuBisCO fixes oxygen. During the steps used to eliminate this compound, CO_2 is released. Because of these competing processes, there exists a concentration of CO_2 at which the rates of the carboxylase and oxygenase are equal. This CO_2 concentration is referred to as the compensation concentration. However, the compensation point of marine phytoplankton appears to be lower than that predicted when carbon uptake is by diffusion (Raven 1993a, 1993b). This suggests that cells are able to suppress the oxygenase activity perhaps by elevating the CO_2 concentration at the site of RuBisCO activity.

Further evidence for non-diffusive CO_2 uptake comes from the affinity of cells for carbon. Some species appear to have a higher rate of photosynthesis as well as a greater affinity for carbon than that of the pure enzyme, suggesting that the site of fixation is flooded by CO_2 which allows the enzyme to function faster than predicted by the lower external carbon concentrations (Raven 1993a). Finally, the occurrence of a higher CO_2 concentration inside than outside the cell suggests that another mechanism besides CO_2 diffusion may come into play (Raven 1993a). These lines of evidence support the existence of some form of energy-dependent carbon uptake mechanism.

Raven *et al.* (1993) point out that one must be cautious when interpreting experiments suggesting that cells employ active uptake. The concern lies in the fact that while there is significant indirect evidence of CCM activity in marine phytoplankton, demonstration of

higher internal relative to external DIC concentrations have only been shown in a few species. Secondly, there is speculation about whether such mechanisms would operate under natural conditions when atmospheric CO_2 and the ocean inorganic carbon system are in equilibrium. Experimental cells are rarely cultured under natural conditions. Nonetheless, conditions do exist where CO_2 concentrations are significantly reduced, such as during high levels of primary productivity (Codispoti *et al.* 1982, Codispoti *et al.* 1986, Raven *et al.* 1993) or other oceanographic processes (Rau *et al.* 1989).

1.4 Objectives

The main objective of this thesis was to gain a better understanding of the interaction between the expression of CCM activity and carbon isotope fractionation in marine phytoplankton. Many species of phytoplankton are capable of actively concentrating carbon, but the effects of CCM induction on $CO_2 - \delta^{13}C$ relationships have, until recently, been ignored. With the apparent ubiquitous nature of CCM ability, the influence of active uptake on carbon isotope fractionation must be considered when developing such models of fractionation based on CO_2 concentration.

The culture conditions and experimental methods used throughout the thesis are presented in Chapter 2. The fractionation of several species of marine phytoplankton under both high and low DIC levels is examined in Chapter 3. The degree of CCM induction is also presented for these phytoplankters. The objective of the fourth chapter was to examine how fractionation and CCM induction varied over a range of DIC levels for the marine diatom *Thalassiosira pseudonana* grown under steady state culture conditions. The influence

of growth-mediated changes in the DIC concentration in a closed culture system on both fractionation and CCM induction is also examined in this chapter. The final chapter attempts to gain a better understanding of the mechanism of active uptake used by *T. pseudonana.* Temperature can influence fractionation both directly through changes in growth rate and indirectly through its effects on the inorganic carbon system. The direct effect of temperature, independent of the carbon system, was therefore investigated. This chapter also attempts to assimilate the results of the thesis and compares the results to models of carbon isotope fractionation from the literature.

These studies will greatly enhance our understanding of the role that CCM induction plays in determining the $\delta^{13}C$ values of modern phytoplankton species and, as a result, the influence it might have had on phytoplankton preserved in ancient marine sediments. The implications of CCM induction and species variability on models used to predict CO_2 concentration will be discussed.

Chapter 2

General Methods

2.1 Culture Conditions

The phytoplankton used in the experiments described in this thesis were cultured in enriched artificial seawater medium (ESAW) prepared in 20 L batches as described by Harrison *et al.* (1980), and modified by Thompson *et al.* (1991). In order to prevent possible macronutrient limitation, the concentrations of $NaNO_3$ and $Na_2SiO_3.9H_2O$ were increased to 500 μM and NaH_2PO_4 to 100 μM. The silicate was dissolved separately in deionized distilled water (DDW) and adjusted to an approximate pH of 8.2 using 50% HCl. Nitrate and phosphate were dissolved in the silicate solution and the mixture was then added to the rest of the medium. A salinity of 35 ppt was used to allow the use of published rate constants for the inorganic carbon system, which are based on this salinity. Unless otherwise stated, the medium was buffered with 20 mM N-[2-hydroxyethyl]piperazine-N'-[2-ethanesulfonic acid] (HEPES) and adjusted to a final pH of 8.2 using 4N NaOH. The medium was then bubbled with 5% CO_2 balanced in air obtained from a gas cylinder. The same cylinder was used to supply CO_2 to the cultures, as described later in the methods. This was done to establish a total dissolved inorganic carbon (DIC) concentration desired for each experiment. The pH was measured and adjusted to 8.2, as described above. The medium was then filtered through a sterilized 0.22 μM Millipore™ GS membrane filter into a 20 L sterile polypropylene carboy.

The primary phytoplankton species used for these experiments was *Thalassiosira pseudonana* (Clone 3H, NEPCC No. 58, Northeast Pacific Culture Collection, University of British Columbia). Other species used in the thesis are listed where appropriate. Axenic stock cultures were maintained at 18°C in 40 mL culture tubes containing medium similar to that described above and a DIC concentration of 2 mM. Cultures were illuminated with a bank of 40 Watt Vitalite™ fluorescent tubes providing a photosynthetic photon flux density of 200 μmol quanta m^{-2} s^{-1}, as measured with a Biospherical Instruments™ (San Diego, USA) light meter fitted with a QSL-100 probe. Stock cultures were diluted approximately every 7 days to ensure an actively growing population of cells.

During experiments, cells were grown in either 2 L or 3 L borosilicate round bottom flasks unless otherwise stated. Cultures were maintained under the same temperature and light conditions as stock cultures, with the exception of the temperature response study where cultures were grown under temperatures ranging from 10 to 22°C. Typically, ca. 10 mL of actively growing axenic stock culture was used to inoculate the experimental culture flask. Aseptic conditions were used so that bacterial contamination was minimized. Each flask was sealed with a sterile silicon stopper containing 7 mm glass tubing necessary to aerate the cultures and for the withdrawal of samples. Sterile silicon tubing was used to connect the cultures to the 20 L carboy containing the dilution medium. A series of three-way valves on the stopper apparatus was used to allow aeration, sample withdrawal and dilution without the removal of stoppers. The carboy was equipped with a screw-cap and glass tubing to allow bubbling of the medium reservoir as well as three-way valves to allow dilution of the cultures. The cultures were stirred with a magnetic stir bar at a speed of approximately 120

rpm to ensure adequate mixing of the aeration gas as well as to maintain the cells in suspension.

2.2 Growth Measurements

Culture density was measured using a Coulter Counter™ model TAII particle counter fitted with a population accessory and using a 70 μm aperture sampler. Culture samples were diluted 20-fold with freshly filtered 3% NaCl prior to counting. Dense cultures were further diluted with the same NaCl solution as required. In addition, biomass was approximated by measuring *in vivo* fluorescence using a Turner Designs™ Model 10 fluorometer. Cultures were maintained at an *in vivo* fluorescence no higher than 2 representing a cell density of ca. 1.0×10^5 cells ml^{-1}. Culture samples were placed in a 10 mL disposable glass culture tube and placed directly into the fluorometer. A reading was taken once a steady value was obtained. Unless otherwise stated, cultures were maintained in logarithmic growth phase by periodically diluting the culture. Since dense cultures have the ability to use CO_2 faster than it can be supplied by aeration, they were diluted frequently (at least daily for fast growing species) to prevent deviation from DIC:CO_2 equilibrium.

2.3 Gas Mixing System and Carbon Measurement

All of the experiments described in this thesis relied on accurate mixing of gases in order to establish constant carbon concentrations in the cultures. Thus, a great deal of time was spent on designing a gas mixing system that could provide a steady concentration of CO_2

in the aeration gas. Two such systems were designed. The general design of the gas mixing system is illustrated in Figure 2.1. CO_2-free gas was obtained by passing building air through two soda lime columns and a cotton wool filter which was used to remove dust and debris from the building air supply. This was then mixed with 5% CO_2 (balanced in air) to obtain the desired CO_2 concentration. Two methods were used to mix the gases. The first used gas flow meters (Cole-Parmer, Vernon Hills, Illinois) to supply the amounts of gasses to be mixed. The difficulty with this method arises when pressure fluctuations occur at the endpoint of the system. Flow rate of gases is dependent on both the upstream and downstream pressure. Cultures in these experiments were aerated with a glass airstone to provide small bubbles. However, these airstones plugged quickly with cells resulting in higher flow resistance and thus an increase in the downstream pressure at the point of gas mixing. This caused significant fluctuations in the CO_2 concentration of the mixed gas.

To alleviate this problem, a second system was designed which used mass flow meters (models FMA-762-V-5%CO_2/95%Air and FMA-769-V-Air) and a model FMA-78P2 controller (Omega Engineering, Stamford, Conn.) to force a known amount of the two gasses into the mixing flask. This system enabled a more precise and constant supply rate of the gases prior to mixing since it was unaffected by fluctuations in downstream pressure. All experiments requiring precise pCO_2 levels used the more precise mixing system. The mixed gas was then passed though a 0.22 μM cartridge filter (Millipore Corp, Bedford, Mass., USA.), humidified, then bubbled through the 20 L medium reservoir. A pressure regulator and relief valve were used to prevent excessive pressure build up between the mixing stage and the cultures. This system allowed precise mixing and delivery of an aeration gas to the cultures. Gas was passed from the mixing system through the medium reservoir and finally into the cultures. This ensured that both the stock medium and culture medium were in

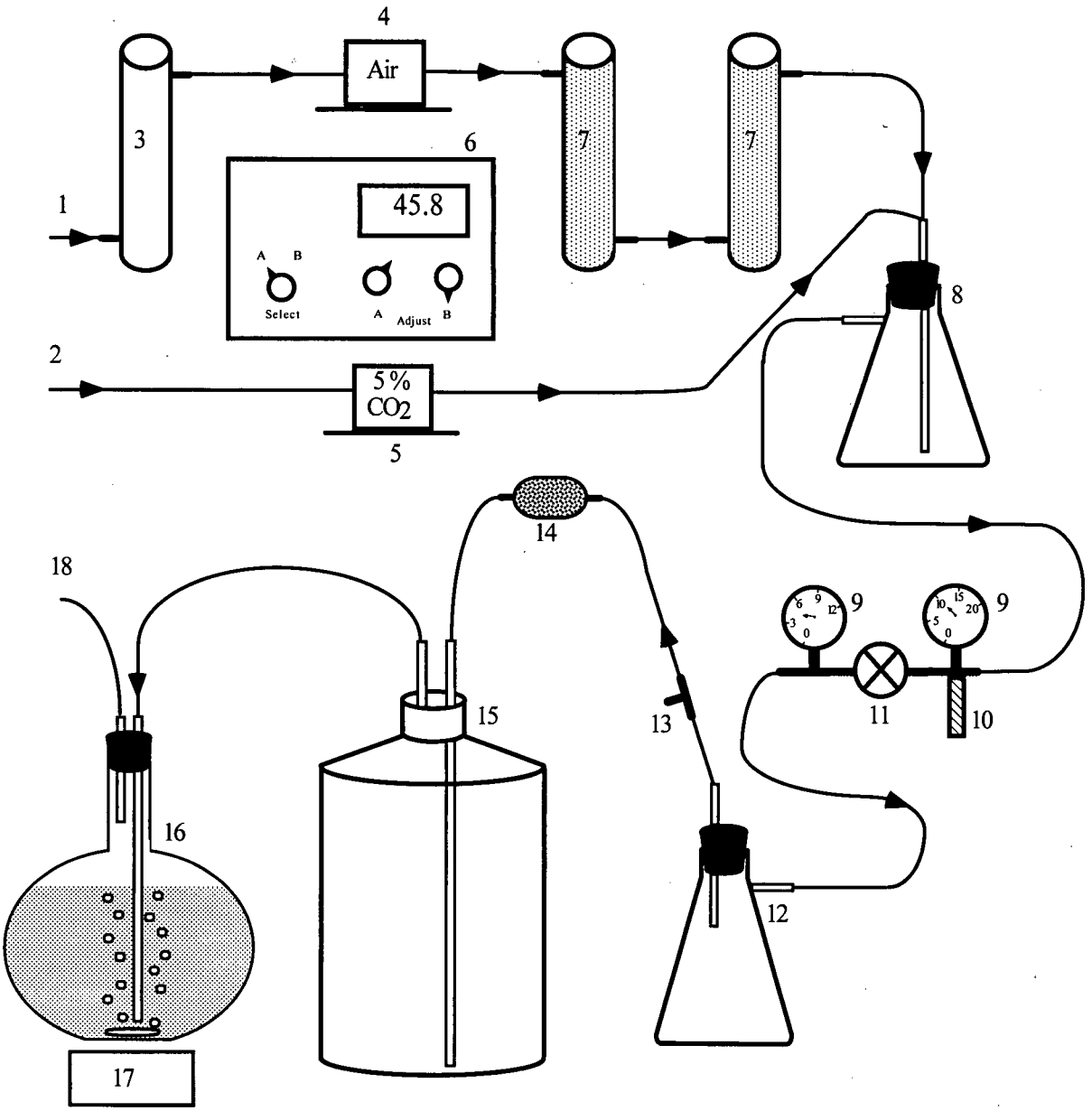

Figure 2.1. Schematic diagram of the culturing system used. Parts are: 1) Building air inflow, 2) 5% CO_2 balanced in air from a gas cylinder, 3) Drying column, 4) Air mass flow controller, 5) 5% CO_2 mass flow controller, 6) Mass flow control unit, 7) Soda lime column, 8) Gas mixing flask, 9) Pressure gauges, 10) Pressure relief valve, 11) Pressure regulator, 12) Emergency media backflow collection flask, 13) Gas sampling septum, 14) Sterile cartridge air filter, 15) 20 L medium stock flask, 16) 3 L culture flask, 17) Magnetic stir motor, 18) Exhaust gas outflow.

equilibrium in terms of the carbon system and subsequent dilution of the cultures was with medium with a similar DIC concentration as the undiluted culture.

Carbon concentrations were measured with an infrared gas analyzer (IRGA) (Analytical Development Company, Hoddesdon, England) calibrated by injecting volumes of known CO_2 concentration gas directly into the IRGA. Gas samples from the mixing system and culture outflow were also measured by injection of the sample into the IRGA. The samples were injected into a continuous flow of nitrogen carrier gas. Peak height was compared to that of standard gas injections and represented a concentration of CO_2 in the injected gas sample. Gas concentrations were found to vary by less than 5% from the desired value when mixed with the mass flow system. The CO_2 concentrations of the exit gas were also within 5% of the inflow gas. Significant deviations indicated either that the medium pH had changed or that there was significant bacterial growth in the cultures with the latter causing an elevated CO_2 level in the exit gas due to high respiration rates. Such cultures were discarded in favour of freshly inoculated ones.

DIC concentrations were determined by acidifying 2.8 mL of medium and measuring the CO_2 gas released with the IRGA. The medium sample was pipetted into a 44 mL, N_2-flushed amber bottle. The bottle was then sealed with a teflon-lined septum and 0.2 mL of concentrated phosphoric acid was injected into the bottle. A 1 mL syringe was used to remove a gas sample and the DIC concentration was calculated as per Equation 6. Again, good agreement was achieved between expected [DIC] and measured values with deviations generally within 5%. Larger deviations again indicated pH problems or bacterial growth.

$$\text{DIC (mM)} = \frac{\text{ppm}\,CO_2 \times V_C}{V_I \times V_A \times V_M} \qquad (6)$$

where

V_C = gas volume collected (mL)

V_I = gas volume injected (mL)

V_A = aqueous sample volume (mL)

V_M = ideal gas volume, 22,414 (ml mol^{-1})

Finally, cultures had to be bubbled rapidly to ensure that DIC concentrations remained constant and at equilibrium throughout the time course of the experiments. To achieve this, aeration flow rates were between 500 mL and 1 L min^{-1}, depending on the flask size, and whether air stones were used. Culture density was kept sufficiently low such that the rate of dissolution of CO_2 into the medium was greater than the rate of removal by phytoplankton cells. Along with biomass measurements, cultures were monitored daily for various parameters such as pH, DIC concentration and pCO_2 for both the mixed gas and the outflow from the cultures.

A detailed knowledge of carbon conditions within the cultures was required for each experiment described in this thesis. The dissolution of CO_2 in seawater, based on Henry's Law, depends on the partial pressure (pCO_2) and the constant α as described by Equation 7 (Broecker and Peng 1982). The production of HCO_3^- from CO_2 is controlled by the hydrogen ion concentration, CO_2 concentrations, and the constant K_1 as described by Equation 8 (Broecker and Peng 1982). The conversion of HCO_3^- to CO_3^{-2} is described by Equation 9 (Broecker and Peng 1982). Constants were taken from Broecker (1982) for various temperatures and polynomial quadratic equations (Marquardt-Levenberg algorithm, Jandel Scientific) were fitted through the values to determine temperature-dependent

equations. Figure 2.2 illustrates the results of the curve fits for α, K_1, and K_2. The r^2 value for all three regressions was 1.0.

$$[CO_2aq] = \frac{pCO_2}{\alpha} \quad (7)$$

$$[HCO_3^-] = K_1 \times \frac{[CO_2aq]}{[H^+]} \quad (8)$$

$$[CO_3^{-2}] = K_2 \times \frac{[HCO_3^-aq]}{[H^+]} \quad (9)$$

Based on the constants determined from the regression equations shown in Figure 2.2, the concentrations of CO_2, HCO_3^-, CO_3^{-2}, and total carbon (DIC) were determined for a range of partial pressures of CO_2 at 18°C and a pH of 8.2 and are shown in Figure 2.3. The data points shown in Figure 2.3B represent actual measurements taken from cultures. The scatter around the expected line likely represents the fluctuations in pCO_2 produced by the gas mixing system, the variability in the total DIC measurement, and, most importantly, slight fluctuations in pH. The latter was found to vary by no more than 0.02 pH units, although this variability can produce close to a 5% change in the total DIC concentration. pH was measured using a pH/ion analyzer (Corning Model 350 fitted with a Corning 3 in 1 probe, Corning, New York). Dense algal growth can cause the pH of growth medium to increase (Goldman 1999); however, low culture biomass in these experiments along with the use of the artificial buffer prevented significant changes in pH.

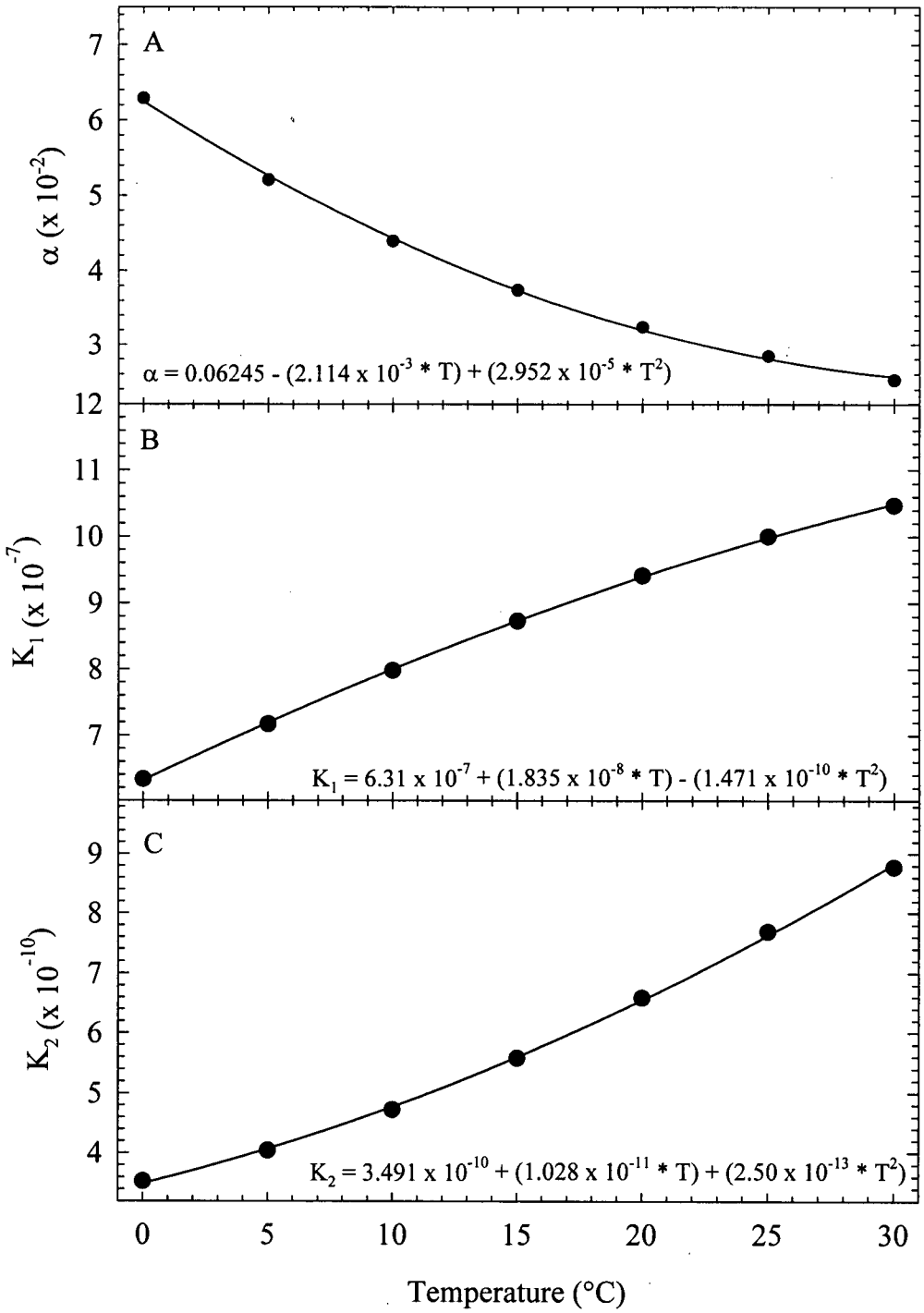

Figure 2.2. Determination of constants used to calculate the concentration of various forms of inorganic carbon at temperatures ranging from 0 to 30°C and at a salinity of 35 ppt. Points represent values from Broecker and Peng (1982). (A) α for CO_2aq concentration (B) K_1 for HCO_3^- concentration, and (C) K_2 for CO_3^{-2} concentration. Equations are second order polynomial regression fits through values from Broecker and Peng (1982). T = temperature in °C.

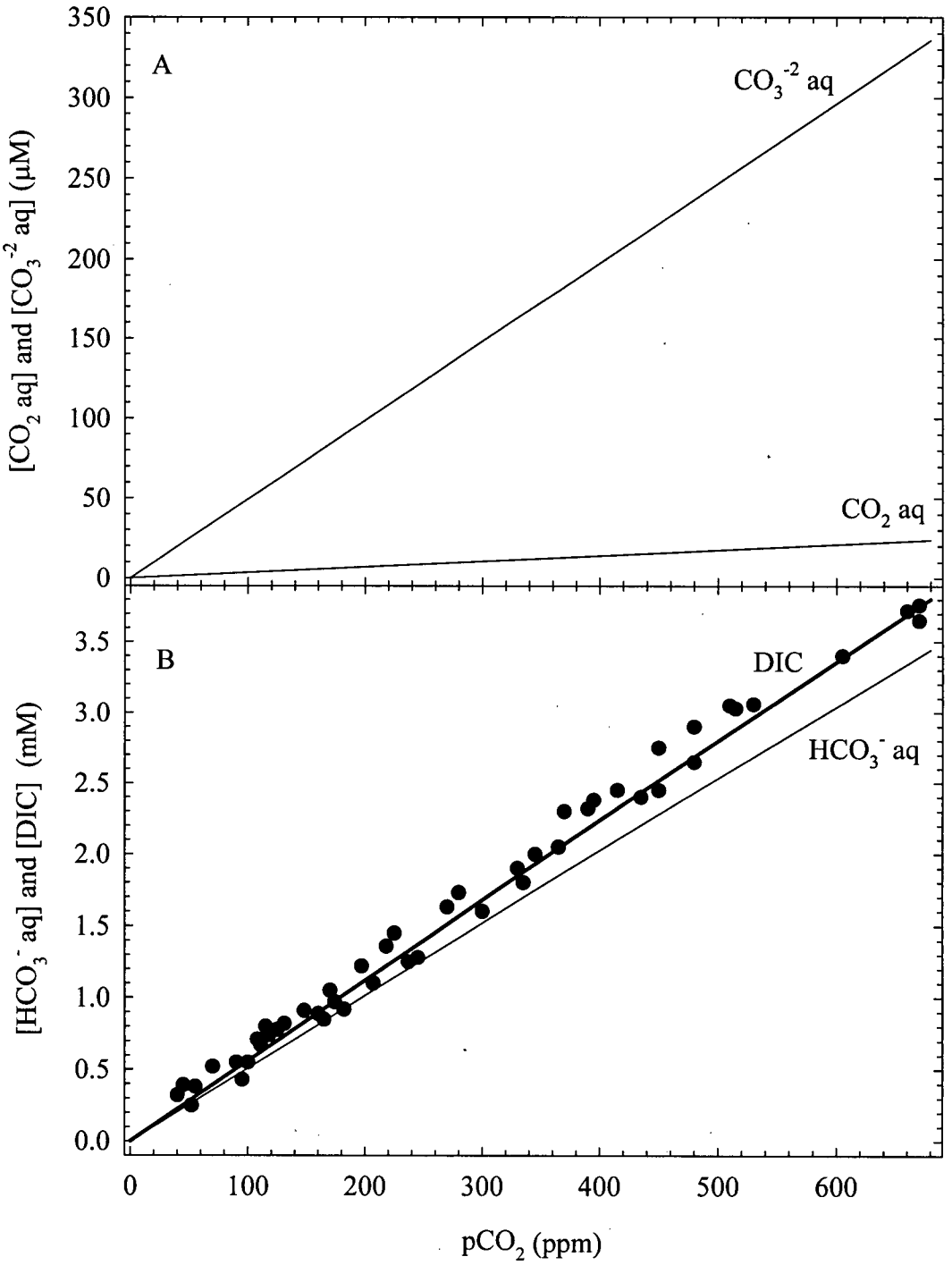

Figure 2.3. The theoretical concentrations of inorganic carbon species in seawater medium at a pH of 8.2 and a temperature of 18°C in response to varying pCO_2. (A) CO_2 and CO_3^{-2}, (B) HCO_3^- and DIC. Points represent actual measured values from culture experiments.

2.4 Isotopic Analysis

Cell particulate organic carbon was obtained by gently filtering a sample of the culture through a precombusted (600°C) 13 mm Gelman™ A/E glass fiber filter. The filters were frozen until measured. Prior to measurement, the filter was dried at 40°C for 5 h, rolled in aluminum foil and combusted using a model NA1500 NC (Fisons Instruments, Milano, Italy) combustion device. The resulting gas was injected into a Prism triple collector (VG Isotech, Manchester, U.K.) mass spectrometer for isotope analysis.

Medium was sampled by evacuating a 20 mL glass sampling ampoule equipped with a high vacuum stopcock at each end and containing 2 mL of concentrated phosphoric acid. The sampling end was flushed with N_2 gas and a Cajon™ connector placed tightly on the same end. An N_2-flushed 1 mL syringe was placed on the other end of the Cajon™ coupling. A sample of the medium was then "sucked up" due to the vacuum created when the stopcock was opened. Once collected, the sample was placed into a vacuum isolation line as illustrated in Figure 2.4 using helium as the carrier gas. The vacuum line was equipped with a dry ice-ethanol (-98°C) trap to remove water and two liquid nitrogen traps (-198°C) to trap the carbon dioxide released due to acidification and stripping from the sample by helium bubbling. The quantity of CO_2 released, and hence the original DIC concentration of the medium, was determined by transferring the CO_2 into a closed arm (of known volume) of the vacuum line system equipped with a pressure transducer. Once isolated, the gas was melted and the pressure measured. The quantity of gas was determined using Equation 10. The original medium DIC concentration was calculated using the weight of the medium sample and the medium density as per Equation 11. Finally, the sample was trapped in a glass tube,

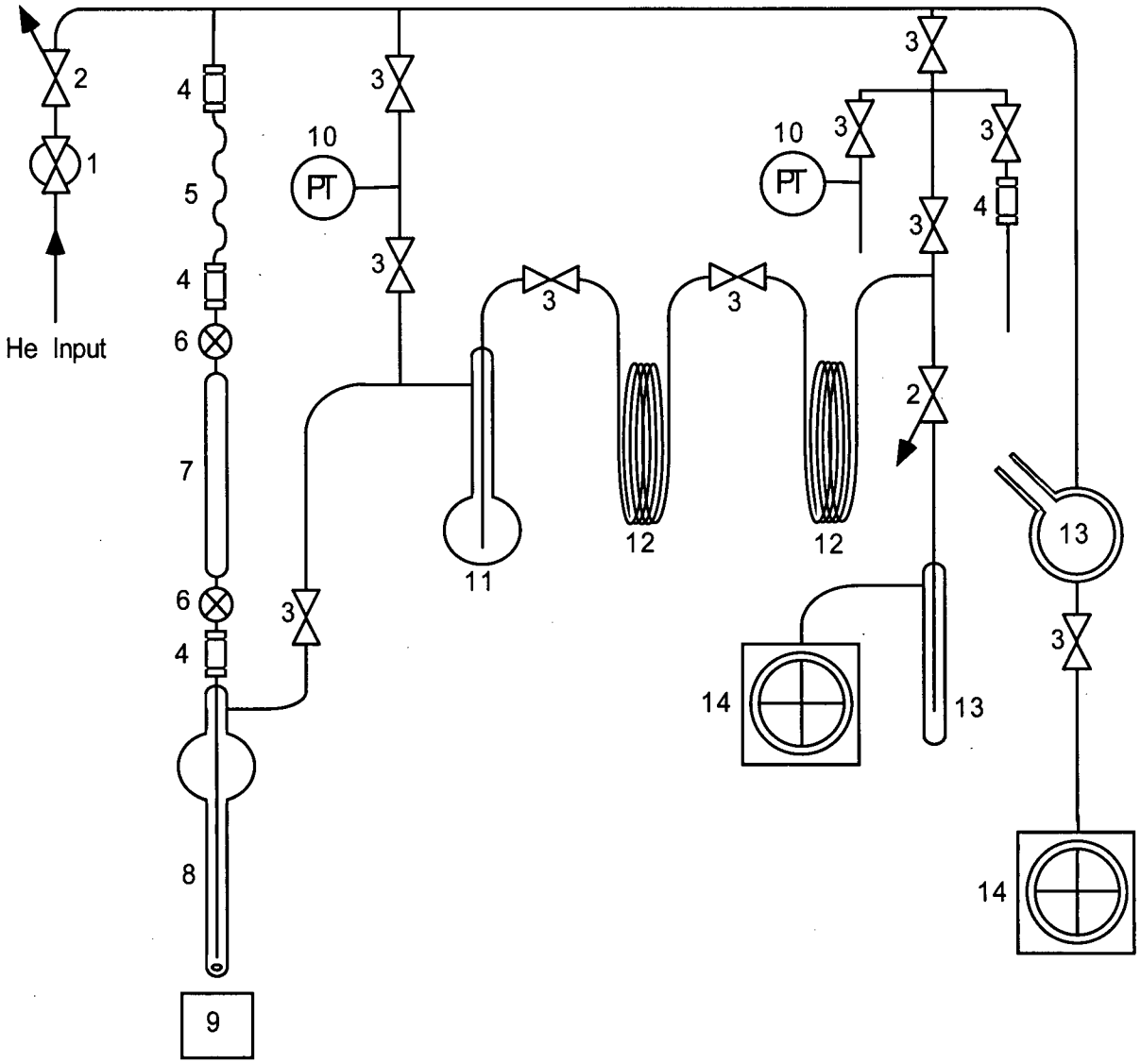

Figure 2.4. Schematic diagram of the vacuum line used for isolation of DIC samples for isotopic analysis. Parts are: 1) Solenoid valve, 2) Variable flow valves, 3) Two-way vacuum stopcocks or valves, 4) Cajon™ couplings, 5) Flexible bellows tubing, 6) High-vacuum valves on ampoule, 7) 20 mL ampoule, 8) Receiving vessel allowing bubbling of sample with He, 9) Magnetic stirrer, 10) Pressure transducers, 11) Water vapour trap, 12) Multiple-loop liquid N_2 traps to collect CO_2, 13) Liquid N_2 traps to prevent CO_2 from exiting vacuum pumps, and 14) Rotary vacuum pumps.

sealed off using a torch, and the resulting gas sample transferred to the mass spectrometer as described above for isotope analysis.

$$G = \frac{[A_P \times S \times S_R \times V]}{[A \times A_R \times R \times T]} \quad (10)$$

Where

G = moles of gas

A_P = atmospheric pressure (Torr)

S = sample reading (mv)

S_R = sample range on recorder (mv)

V = volume of closed arm of vacuum line (cm^3)

A = atmosphere reading (mv)

A_R = atmosphere range on recorder (mv)

R = ideal gas law constant (6.23656×10^4 Torr cm^3 $°K^{-1}$ mol^{-1})

T = sample temperature (°K)

$$C = \frac{G \times D}{[W_F - W_E]} \times 10^6 \quad (11)$$

Where

C = [DIC] (mM)

W_F = ampule weight with sample

W_E = ampule weight without sample

D = density of medium (g mL^{-1})

2.5 Fractionation Measurements

Unless otherwise stated, fractionation was determined using closed system short-term source depletion experiments. This involved filtering a large volume of culture gently through a 3 μm pore size membrane (type HA) filter with a vacuum applied to aid in filtration and resuspending the cells in a smaller (100 mL) volume of the same medium using a vortex mixer. The concentrated culture was then injected into a clear previously evacuated, gas-impermeable bag equipped with a septum sampling port. The cell culture was stirred during the depletion experiments at 240 rpm. Throughout the depletion experiment, samples were taken for photosynthetic kinetics. Single medium samples were also obtained for isotopic analysis at various stages of the depletion experiment. The $\delta^{13}C$ of the source medium was determined as described above, and the results plotted as in Guy *et al.* (1992) and illustrated in Figure 1.1B. In all cases, at least four points were taken. The value and standard error of the slope were determined from the resulting linear regression (least squares method) using functions in Excel (Version 97 SR-1, Microsoft Corporation, Redmond, USA). In the case of the detailed *Thalassiosira pseudonana* study (Chapter 4), five points were used to determine fractionation.

One assumption of the source depletion method is that fractionation is constant over the time course of the source depletion period. This condition might not be met if changes in the induction state of the CCM had occurred. To guard against this, depletion experiments were short in duration (ca. 2 h) while still providing sufficient source depletion to enable an accurate determination of fractionation. Results demonstrated that CCM induction did not occur within 2 h following transfer from high to low DIC concentrations (Figure 2.5). Depletion experiments typically lasted 2 h, during which source carbon depletion amounted

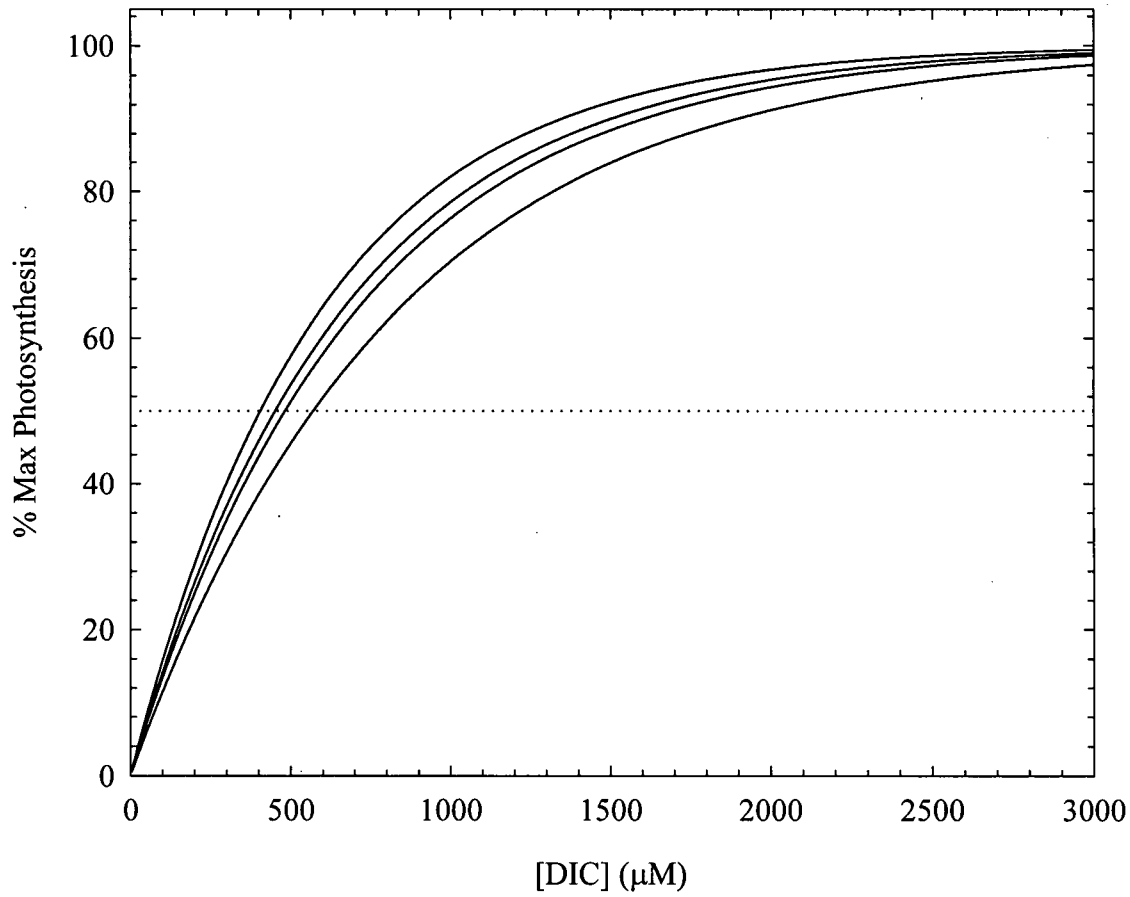

Figure 2.5. Single sample DIC curves for *Thalassiosira pseudonana* grown at a [DIC] of 2.00 mM. Curves were done at various points in a time course depletion experiment lasting a total of 120 min during which [DIC] decreased from 2.00 to 1.63 mM. Curves are from left to right: 40, 120, 0, and 80 min from the start of the experiment. The data indicate no detectable trend in $K_{1/2}$DIC values throughout the time course of the depletion. Curves were fitted to the P vs. I equation from Platt and Gallegos (1980) as outlined in the methods.

to 15 – 20%. The effect of respiratory carbon release on the calculation of fractionation was between 0.8 and 1.8‰ (R. Guy, pers. comm.) resulting in a possible underestimation of fractionation. The depletion approach was used to avoid the problems associated with maintaining steady-state carbon conditions in the growth medium as well as the carry-over effect of old carbon in the particulate samples.

2.6 Photosynthetic Kinetics

Samples of the culture medium containing the phytoplankton cells were obtained and concentrated by centrifugation at maximum speed in an International Clinical Equipment (ICE) benchtop centrifuge for 2 min. The cells were then re-suspended in carbon-free medium using a vortex mixer. The procedure was repeated three times. All manipulations were done under nitrogen gas. Carbon-free medium was obtained by using unbuffered medium, acidifying with dilute HCl, bubbling with N_2 gas for 1 h followed by addition of the HEPES buffer which resulted in a final pH of 8.2. This medium was otherwise identical to the growth medium. The final re-suspension volume was 1mL and this was injected into a 2 mL water-jacketed transparent cuvette. The sample was sealed with a fitted plunger, thus preventing gas exchange with the atmosphere. No carbonic anhydrase was added to this sample. The temperature was maintained at a level similar to ambient culture conditions. Measurements of oxygen concentration were made using a Clarke-type oxygen electrode (Hansatech plc, King's Lynn, Norfolk, U.K.). Light was supplied using a Hansatech projector light at an intensity of 500 μmol m^{-2} s^{-1}. Cultures were stirred with a magnetic flea

at approximately 240 rpm. Each DIC curve took no longer than 25 minutes to perform, thus limiting the potential change in the photosynthetic physiology of the cells during the process.

The rate of oxygen evolution was measured in response to externally added standard HCO_3^- solutions injected using a 10 µL Hamilton™ syringe. $K_{1/2}$DIC values, similar to K_m values in Michaelis-Menten enzyme kinetics, were determined by fitting the data to a form of the P versus I relationship (Equation 12) taken from Platt and Gallegos (1980). Since this equation does not have a 50% maximum rate parameter, the standard error around the initial slope parameter (k) was used to calculate the standard error of the extrapolated $K_{1/2}$DIC values. The Michaelis-Menten equation, which is commonly used for studies of this type, was found not to fit the data as effectively when cultures were acclimated to high DIC levels. It is not surprising that the equation did not fit the data from high DIC-acclimated cells since the latter might be relying on passive DIC uptake and not on an enzyme (or carrier)-mediated process best described by the Michaelis-Menten equation.

$$P = M \times \left[1 - e^{\left(\frac{-K \times S}{M} \right)} \right] \qquad (12)$$

Where

P = photosynthetic rate at a given carbon concentration (µmol O_2 L^{-1} min^{-1})

M = maximum photosynthetic rate (µmol O_2 L^{-1} min^{-1})

e = 2.71828

K = initial slope of the regression (min^{-1})

S = DIC concentration (µM)

For chlorophyll a determination, 0.5 mL of the culture was combined with 9.5 mL of 95% acetone thus creating a 90% acetone solution. The mixture was stored at 4°C for 24 hours to allow complete chlorophyll extraction from the cells which settled on the bottom of the tube. The extract was then analyzed fluorometrically as described by Parsons *et al.* (1984).

Chapter 3

Response of Six Species of Marine Phytoplankton to High and Low DIC: Fractionation and CCM Induction

3.1 Introduction

It is well established that the $\delta^{13}C$ values of phytoplankton in colder waters are more negative than in warmer, equatorial waters (Deuser *et al.* 1968, Freeman and Hayes 1992, Mizutani and Wada 1982, Rau *et al.* 1989, Rau *et al.* 1992, Wada *et al.* 1987). Although a relationship does appear to exist between phytoplankton isotope content and temperature, it has long been postulated that the true relationship is between CO_2 concentration and phytoplankton $\delta^{13}C$ (Degens *et al.* 1968b, McCabe 1985, Pardue *et al.* 1976, Rau *et al.* 1989, Rau *et al.* 1992, Sackett 1991). This is particularly appealing since such a relationship could allow palaeoceanographers to measure the $\delta^{13}C$ of preserved phytoplankton in sediments to infer the concentration of CO_2 in the ocean in the past. Using samples of marine particulate organic matter collected over a range of latitudes, Freeman and Hayes (1992) were able to demonstrate a correlation between phytoplankton isotope fractionation and the CO_2 concentration of modern oceans. This relationship was then used to estimate concentrations of CO_2 in ancient oceans.

While it is appealing to establish such a correlation, there are many problems with this approach (Goericke and Fry 1994). The first and most obvious concern is the existence of species variability across the range of latitudes examined. A tight relationship between surface water CO_2 concentration and phytoplankton isotopic composition has not been

observed (Goericke and Fry 1994), possibly because of the variability in isotope fractionation by different species of phytoplankton. Even at given latitudes, there is considerable variability in phytoplankton isotopic ratios (Goericke and Fry 1994). This is most likely due to species variability at different horizontal and vertical scales at particular latitudes.

Some species of phytoplankton predominate in coastal areas while others might be dominant at the same latitude but in the open ocean. Typically, coastal phytoplankton assemblages are made up of large diatoms, whereas the open ocean assemblage is made up of smaller species, including cyanobacteria (Chisholm 1992). Smaller phytoplankton species are believed to thrive in the open ocean due to a scarcity of nutrients because they have a larger surface area to volume ratio (Morel 1987). The higher nutrient content of coastal waters leads to less nutrient limitation, thus favoring the larger fast growing diatoms.

A final concern with respect to species variability is whether phytoplankton species of ancient oceans responded to CO_2 concentration in a manner similar to modern species. Palaeoceanographers are interested in preserved phytoplankton from marine sediments and, in particular, specific biomarkers originating from these phytoplankton (Hayes *et al.* 1987, 1989, 1990, Jasper and Hayes 1990). One would expect such phytoplankton to accumulate in the sediments only when there is a significantly high sedimentation rate such as might occur during a bloom (Thompson and Calvert 1994). If this is true, larger species that typically make up bloom assemblages should be more frequently preserved in the sediments. Laboratory research should focus on which species are most likely to be found in the sediments and then examine the isotope content of these species. Water column particulate organic matter samples usually contain many phytoplankton species, thus averaging out the isotope values of the individual species (Fry 1996). In the open ocean, it is difficult to isolate field samples of individual species for separate isotopic analysis.

There have been numerous laboratory studies on carbon isotope fractionation of phytoplankton. However, different culturing conditions make it difficult to compare results. For example, Wong and Sackett (1978) found considerable variability in phytoplankton isotope fractionation; however, they used artificially high DIC concentrations. Falkowski (1991) looked at isotope fractionation of 13 different species of phytoplankton in an attempt to determine which species were capable of using bicarbonate as a carbon source. The approach is similar to the one used for terrestrial plants where less negative $\delta^{13}C$ values indicate a C_4 (β-carboxylation) mode of photosynthesis. Most carbon fixation using β-carboxylation uses bicarbonate as the carbon source, depending on the enzyme (Raven *et al.* 1993). Falkowski (1991) found a range of isotope ratios, indicating that phytoplankton species cannot be classified as either C_3- or C_4-like and concluded that species variability of phytoplankton isotope fractionation, potentially caused by different degrees of β-carboxylation, could explain the range of $\delta^{13}C$ values observed in natural assemblages. Even with these two studies, there is no good comparison of phytoplankton fractionation for several species under well-defined natural carbon concentrations.

The difficulty with laboratory experiments is the regulation and monitoring of the carbon system. Falkowski (1991) found that an increase in pH of 0.5 units resulted in a 7‰ decrease in fractionation. Such sensitivity to environmental variables highlights the importance of proper control and measurement of pH, temperature, and carbon concentrations in the growth medium. Crawford and Harrison (1997) found considerable variability when measuring pH in seawater. Two electrodes can give sample pH readings differing by 0.17 units, thus increasing the difficulty of accurately determining culture conditions. It is possible that some of the variability in the $\delta^{13}C$ values of the species in

Falkowski's study (1991) was the result of small changes in the pH or CO_2 concentration. However, the DIC concentration was not measured and this limits the usefulness of his data.

A further complication is that the method of calculating fractionation can influence results. For example, Fry (1996) suggests that near complete consumption of inflow CO_2 by dense algal cultures can result in an underestimate of fractionation when the isotope content of the inflow gas is used as a reference for calculating fractionation. If the aeration rate is sufficiently low, the DIC level of the medium can actually decrease (Johnston and Raven 1992). Fry (1996) also points out that phytoplankton growth often results in increased pH which in turn causes higher DIC levels, thus complicating the carbon system considerably. Data presented by Johnston and Raven (1992) appear to support this idea in that as biomass increased in well-aerated batch cultures, the DIC level also increased, although pH was not monitored. Ideal culture experiments should use natural, well-monitored carbon concentrations, maintain low biomass, and always measure the concentration and isotope content of the source carbon in the medium (Fry 1996).

Given the assumption that phytoplankton carbon isotope content does vary with CO_2 concentration, the question remains as to the mechanism that controls the fractionation. There are currently two widely held hypotheses regarding the dependence of carbon isotope content on CO_2 concentration. The first hypothesis suggests that phytoplankton cells rely on diffusion of CO_2 from the growth medium across the cell membrane and into the cell where it is fixed by RuBisCO (Goericke *et al.* 1994, Laws *et al.* 1995, Rau *et al.* 1996). Diffusional models of fractionation are based on the supply rate of CO_2 relative to the cell's demand for carbon. They have incorporated growth rate, cell size, temperature, and pH, among other parameters.

While such models might appear to explain much of the variability of isotope content of phytoplankton, they fail to recognize that many species possess the capacity to actively concentrate carbon. Beardall *et al.* (1982) were among the first to suspect that isotope fractionation was influenced by the activity of a carbon concentrating mechanism. Sharkey and Berry (1985) were the first to present a model of isotope fractionation by phytoplankton incorporating the concept of active carbon uptake. There is only one detailed model incorporating the effects of CCM activity (Keller and Morel 1999) though these authors have a second model that is yet unpublished. Induction of a carbon concentrating mechanism should cause reduced fractionation, since active transport should produce little fractionation (Berry 1989, Kerby and Raven 1985). Thus, both active transport and CO_2 diffusion limitation predict reduced fractionation under low CO_2 conditions.

Some of the best evidence for the interaction between carbon uptake ability and fractionation comes from Sharkey and Berry (1985) who found that as *Chlamydomonas reinhardtii* cells acclimated to low carbon levels, their affinity for carbon increased while fractionation decreased. Higher affinity for carbon is assumed to represent induction of a CCM. The difficulty with this study was that a 5% CO_2 concentration was used to establish a high DIC concentration. While there have been significant fluctuations in the atmospheric CO_2 level in the past, recent (last 800 million years) concentrations have remained below 1% CO_2 (Raven 1991b). A study using the freshwater cyanobacterium *Synechococcus leopoliensis* by Mayo *et al.* (1986) found that induction of the carbon concentrating mechanism was gradual and that cells could exist in states of partial induction. This study supports the idea that small changes in DIC concentration can result in varying degrees of CCM induction. A decrease in fractionation has also been shown for this species as CCM activity was induced (Erez *et al.* 1998). However, it is not known whether small changes in

CCM induction can cause the range of $\delta^{13}C$ values currently observed in natural phytoplankton populations. Furthermore, the results of the studies mentioned above are for freshwater species. There are no studies that have attempted to establish a link between CCM induction and fractionation in marine phytoplankton. Before relying on a correlation between CO_2 concentration and phytoplankton $\delta^{13}C$ values, one must understand the mechanism by which CO_2 concentration exerts an influence on carbon isotope fractionation.

The goal of the experiments described in this chapter was to examine the response of carbon isotope fractionation and cell carbon affinity to high and low DIC concentration. With the exception of Falkowski (1991), other studies have examined only a limited number of species. The literature is lacking a careful comparison of fractionation by numerous species under well defined, ecologically relevant carbon concentrations. It would be useful to know the range of fractionation expressed by various species of marine phytoplankton in response to changing DIC concentrations regardless of the mechanism of carbon uptake. This would make it easier to assess the influence of species variability on the $\delta^{13}C$ values of particulate organic carbon (POC) observed in the ocean. In this study, several species of marine phytoplankton were tested to determine if both fractionation and carbon uptake affinity responded to changes in DIC concentration. In selecting the species, a number of considerations were taken into account. An attempt was made to select species for which there was existing laboratory data on fractionation. However, a requirement for a successful experiment was species that could withstand rapid bubbling, stirring and centrifugation. An attempt was made to test species across several classes of phytoplankton. Temperature and pH were held constant such that the only variable was the concentration of CO_2/DIC.

3.2 Methods

The species tested included *Phaeodactylum tricornutum* (clone CCMP630, Provasoli-Guillard Center for Culture of Marine Phytoplankton, Bigelow Laboratory for Ocean Sciences, West Boothbay Harbor, Maine, USA), *Thalassiosira pseudonana* (NEPCC # 58 Clone 3H), *Dunaliella tertiolecta* (NEPCC # 001 Clone DUN), *Thalassiosira weissflogii* (NEPCC # 741 Clone ACTIN), *Skeletonema costatum* (NEPCC # 18), and *Synechococcus bacillaris* (NEPCC # 539). All NEPCC clones were obtained from the Northeast Pacific Culture Collection, University of British Columbia, Vancouver. These species were able to withstand the high aeration rates and substantial agitation required for both the culturing and isolation phases of the experiments.

Cultures were grown at both low (0.5 mM) and high (2.7 mM) DIC concentrations to determine if substantial changes in DIC concentration influenced fractionation. Medium DIC concentration was held in equilibrium with aeration gas which was adjusted to either ca. 85 ppm (low DIC) or 475 ppm (high DIC). The medium pH was held constant at 8.2. Cultures were rapidly aerated at a rate of 0.5 L min^{-1} and stirred with a magnetic stirrer at 120 rpm to insure equilibrium.

All short term depletion experiments and photosynthetic kinetic experiments were performed as described in the general methods with the exception of *Dunaliella tertiolecta* which was found to adhere to the type HA filters used during the concentrating process. Thus, the culture was centrifuged at 3000 rpm in a refrigerated centrifuge (model PR-J, International Equipment Co, Needham Heights, USA). Cells of all species were then re-suspended using a vortex mixer in 100 mL of the original medium and 35 μg mL^{-1} carbonic anhydrase (Bovine Erythrocyte EC 4.2.1.1, Sigma Chemical Company, St Louis, USA) was

added to assure chemical and isotopic equilibrium between the CO_2 and bicarbonate. Growth rates for all species were calculated from *in vivo* fluorescence measurements using a Turner Designs™ Model 10 fluorometer.

3.3 Results

Growth rates for the six species tested are shown in Figure 3.1. There was no significant difference (paired-sample t-test) between the high and low DIC culture growth rates. Cultures were diluted daily to prevent high biomass accumulation. As a result, it was not possible to obtain an extended series of points between dilutions and thus growth rates showed considerable variability. For each species tested, fractionation for the high DIC culture was greater than for the low DIC culture (Figure 3.2). As a group, there was a significant difference in fractionation between the two DIC levels (paired-sample t-test, α=0.002).

There was no consistency across species in the fractionation values at either the low or high DIC conditions, with values ranging from 11.69 to 25.98‰ and from 21.83 to 36.60‰, respectively. All fractionation values are expressed relative to source DIC since it is unclear whether these species were using bicarbonate or CO_2 as their carbon source. *Synechococcus bacillaris* exhibited the highest fractionation under both high and low DIC conditions. The largest difference in fractionation between high and low DIC conditions occurred in the diatom *Thalassiosira weissflogii*, while *Phaeodactylum tricornutum* showed the smallest difference. Interestingly, if one ranks the fractionation values of the six species from lowest (1) to highest (6), the same order is obtained under both DIC concentrations with the exception of the two *Thalassiosira* species that are reversed.

For each species at both DIC levels, at least four replicate DIC curves were performed. Interestingly, the per unit chlorophyll maximum photosynthetic rates for each replicate exhibited considerable variability (Figure 3.3A); however, the $K_{1/2}$DIC values were fairly consistent (Figure 3.3B). Sample chlorophyll-a measurements were taken for each

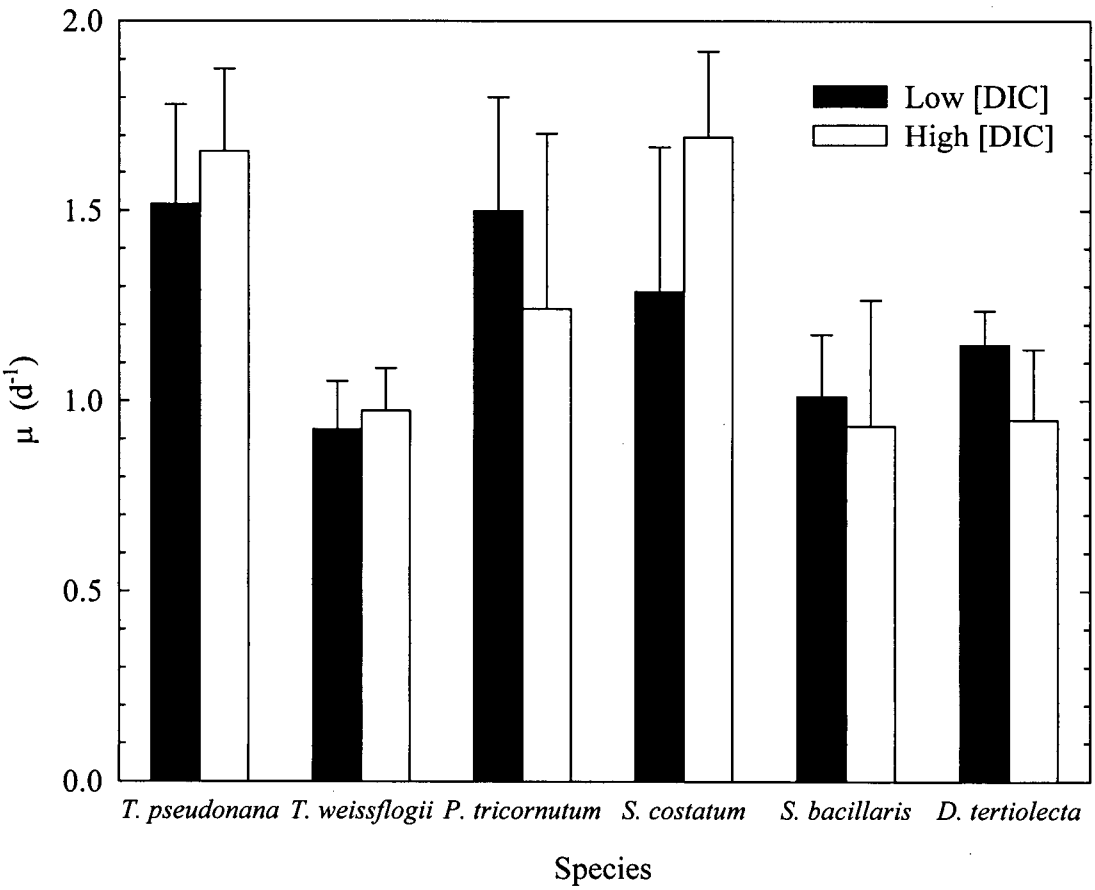

Figure 3.1. Growth rates for six species of phytoplankton grown under low (0.5 mM) or high (2.7 mM) DIC concentration. Growth rates are based on fluorescence measurements. Error bars represent ± 1 standard deviation of two point growth rate calculations (n=4).

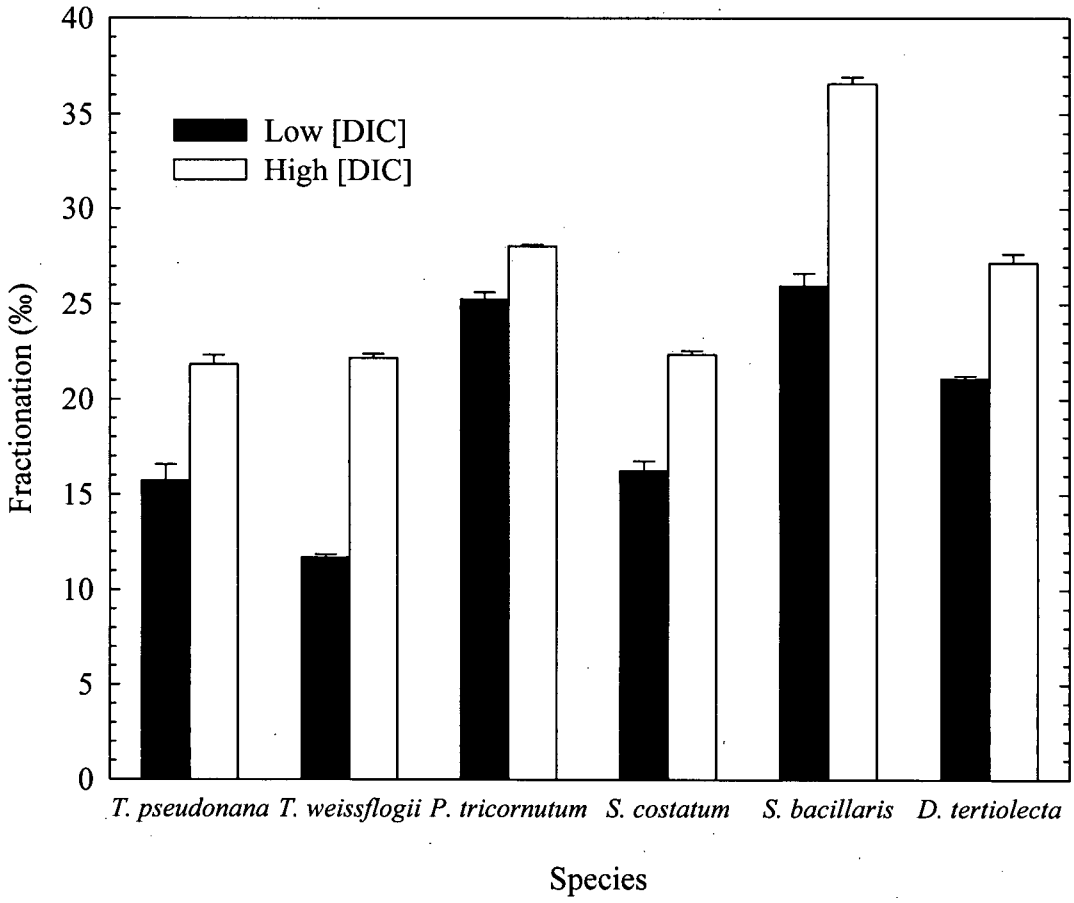

Figure 3.2. Fractionation of six species of phytoplankton grown under low (0.5 mM) or high (2.7 mM) DIC concentration. Fractionation is expressed relative to DIC. Error bars represent ± 1 standard error of the regression fitted through the raw data.

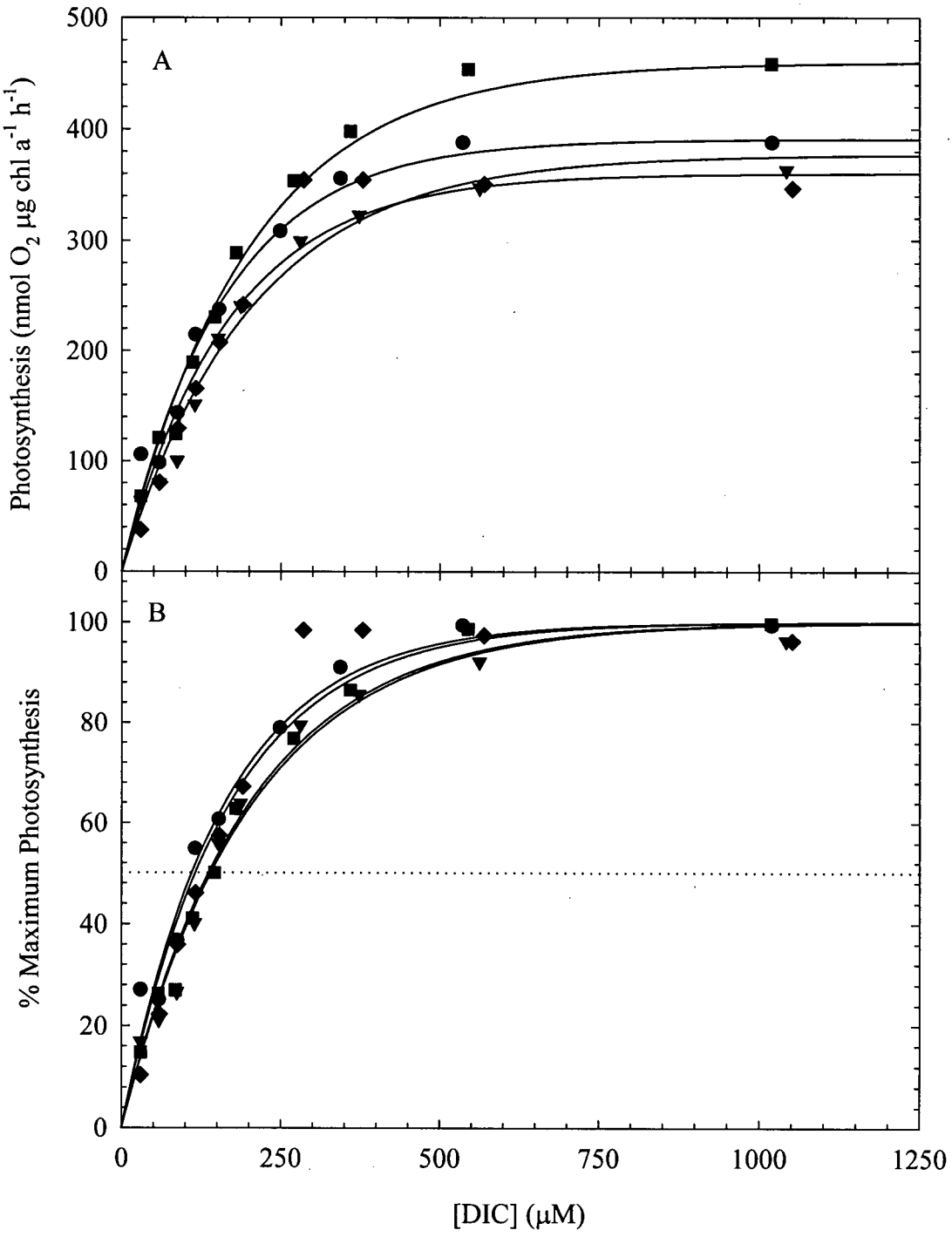

Figure 3.3. Comparison of replicate DIC curves expressed as oxygen production per unit chl-a (A), or normalized as percent maximum photosynthetic rates (B), for *Thalassiosira pseudonana* cultures grown at a DIC concentration of 0.5 mM. Curves were fitted to the P vs. I equation from Platt and Gallegos (1980) as outlined in the methods.

DIC curve. While everything was done to ensure that the sample preparation process was consistent across replicates, it is possible that differing numbers of viable cells might have influenced the maximum photosynthetic rate calculated for individual replicates. Replicates were normalized to 100% maximum photosynthetic rate to avoid the variability in absolute photosynthetic rates. In any case, the $K_{1/2}$DIC was unaffected by normalization.

Photosynthetic kinetics for each species acclimated to both high and low DIC concentrations are illustrated in Figures 3.4 and 3.5. A $K_{1/2}$DIC value represents the DIC concentration required to produce 50% maximum photosynthesis with lower values indicating higher cell affinity for carbon. In each species, cultures acclimated to low DIC exhibited a significantly higher affinity for DIC than those acclimated to the high DIC conditions (Figure 3.6). When results for all six species were pooled, $K_{1/2}$DIC values were significantly lower when cells were grown at low DIC concentrations (paired-sample t test, $\alpha = 0.0006$). It is interesting that *Phaeodactylum tricornutum*, the species that showed the smallest range in fractionation, exhibited a large range in $K_{1/2}$DIC. *Skeletonema costatum* showed the smallest change in $K_{1/2}$DIC; however, the $K_{1/2}$DIC at low DIC was still only 33% of the high DIC cells.

The correlation between fractionation values and the $K_{1/2}$DIC was not significant when data from all six species were pooled (Figure 3.7). The r^2 value for the linear regression was 0.158. The relationship between fractionation and $K_{1/2}$DIC was stronger for diatoms, but still not significant ($r^2 = 0.395$). Despite the lack of a significant correlation in the pooled data, both fractionation and $K_{1/2}$DIC values were higher when cultures were acclimated to high DIC concentrations suggesting that they might be related. There was no significant correlation between fractionation and cell volume at either DIC concentration (Figure 3.8).

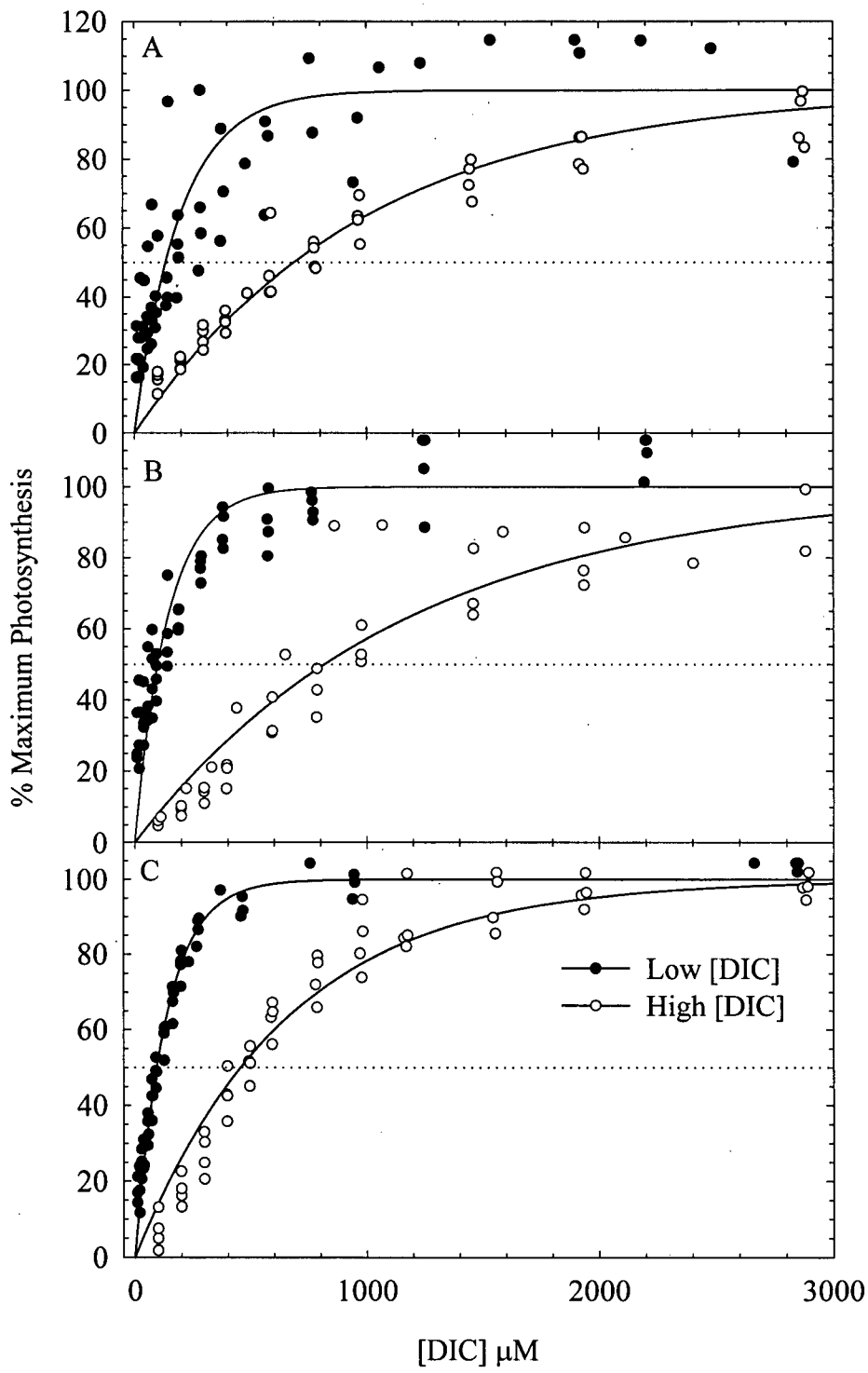

Figure 3.4. DIC curves for *Phaeodactylum tricornutum* (A), *Thalassiosira pseudonana* (B), and *Thalassiosira weissflogii* (C), grown under low (0.5 mM) or high (2.7 mM) DIC concentration. Data points represent at least three replicate curves. Curves were fitted to the P vs. I equation from Platt and Gallegos (1980) as outlined in the methods.

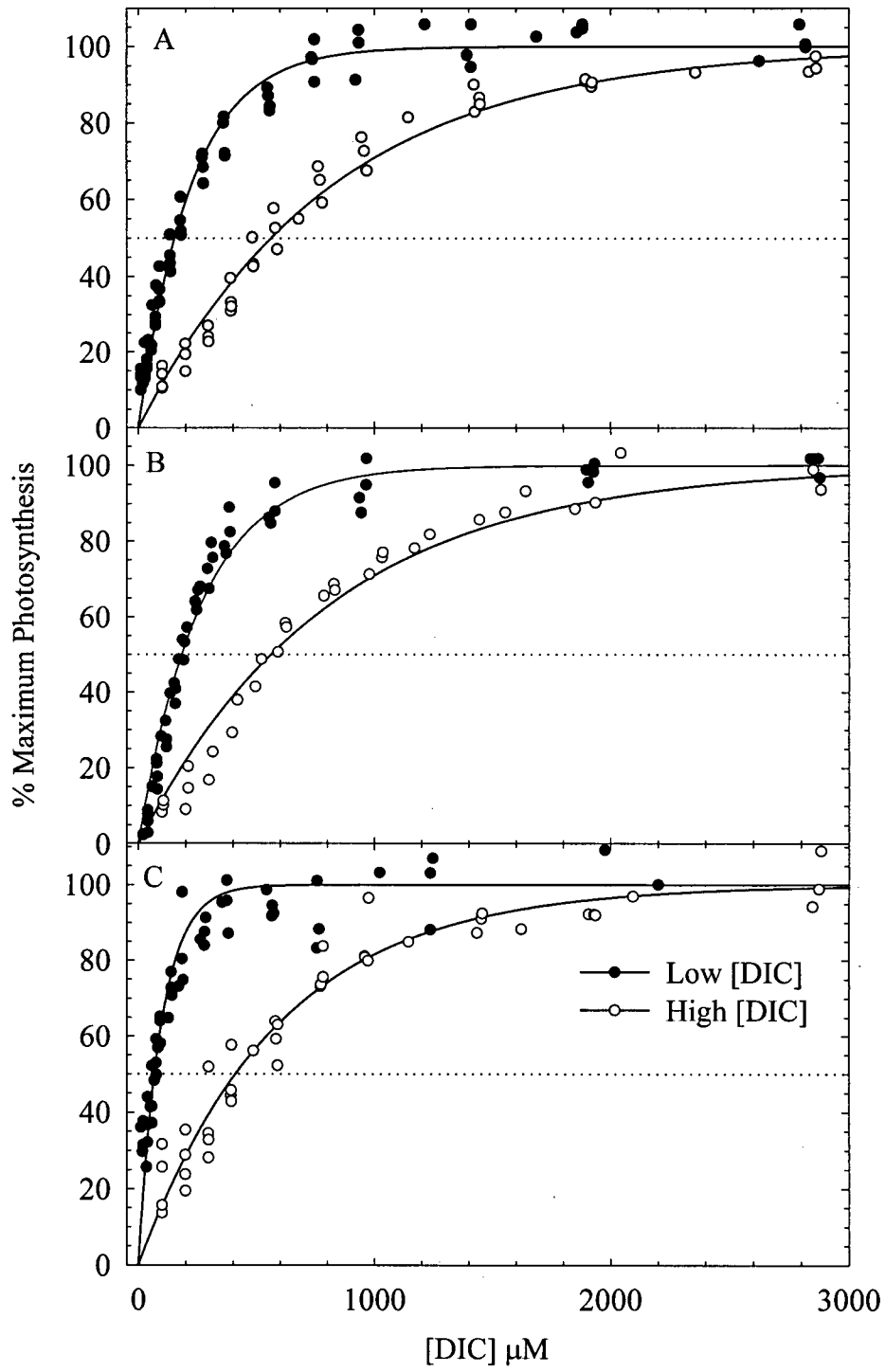

Figure 3.5. DIC curves for *Dunaliella tertiolecta* (A), *Skeletonema costatum* (B), and *Synechococcus bacillaris* (C), grown under low (0.5 mM) or high (2.7 mM) DIC concentration. Data points represent at least three replicate curves. Curves were fitted to the P vs. I equation from Platt and Gallegos (1980) as outlined in the methods.

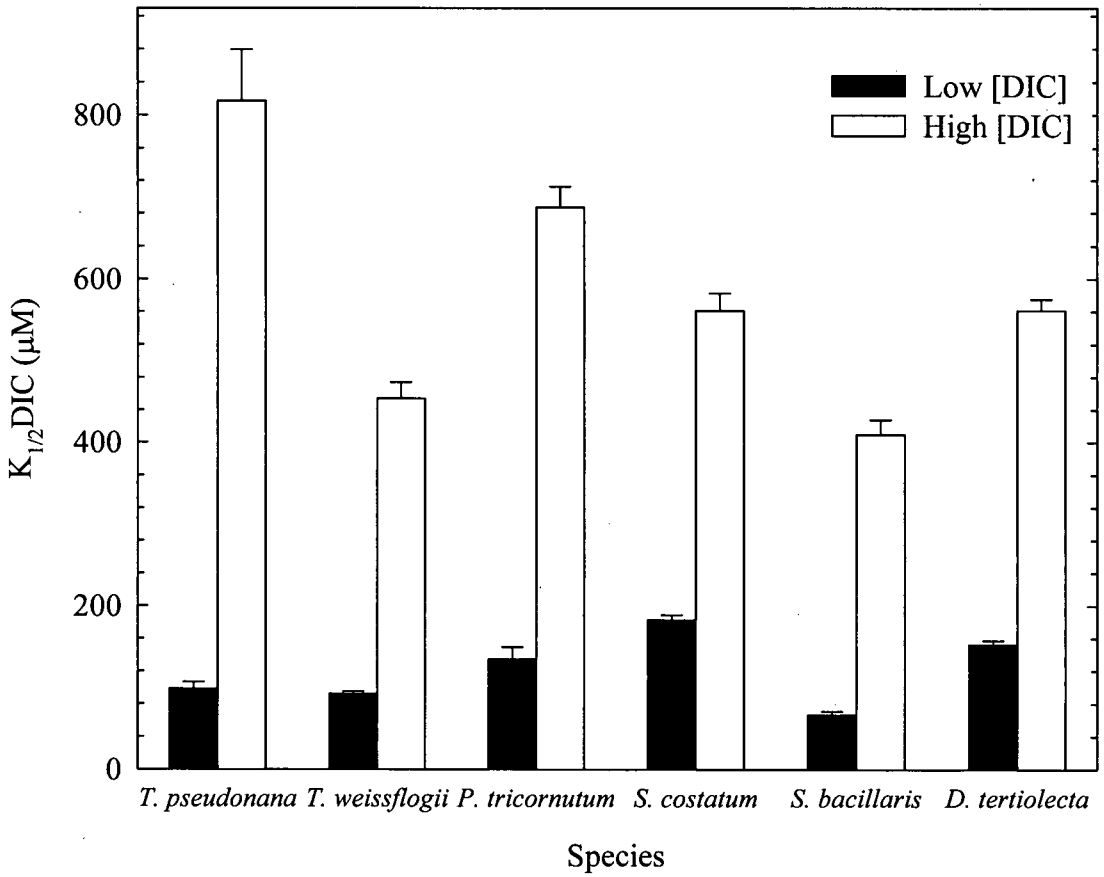

Figure 3.6. $K_{1/2}$DIC values for six species of phytoplankton grown under low (0.5 mM) or high (2.7 mM) DIC concentration. Error bars represent ± 1 standard error of the regression fitted through the raw data.

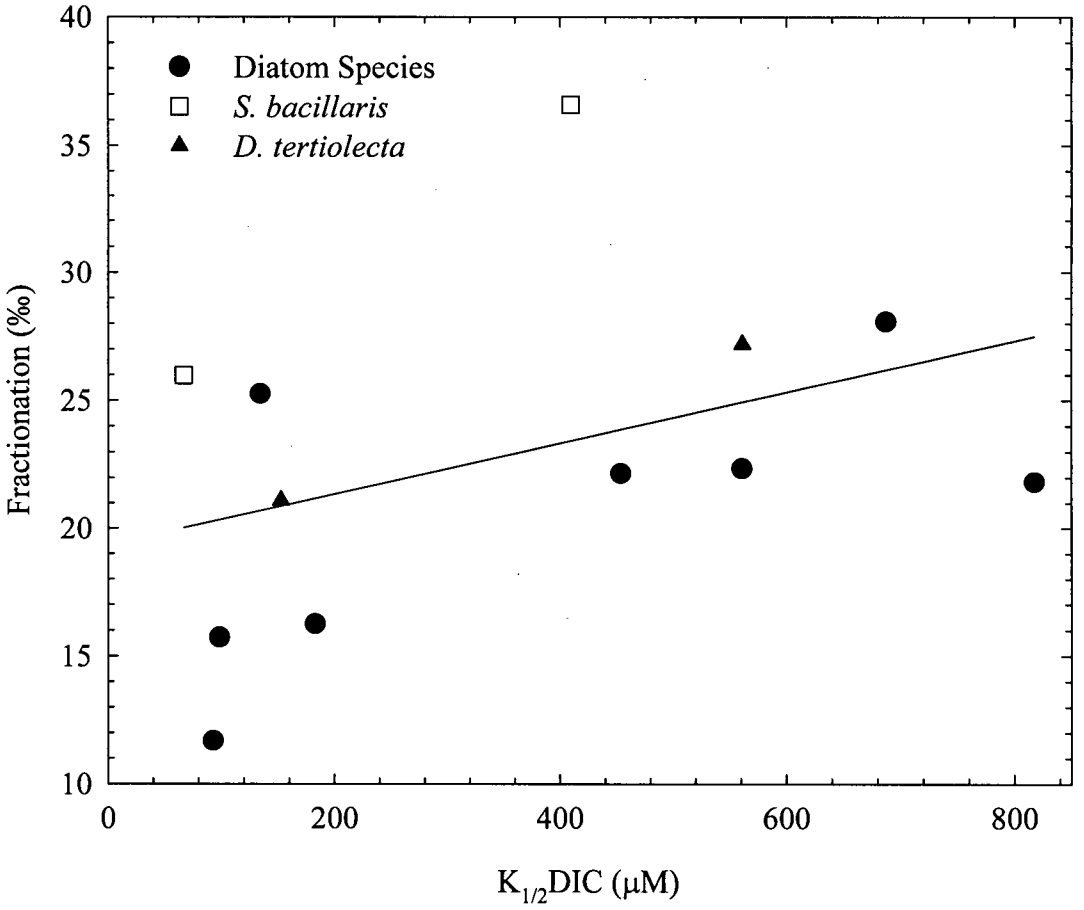

Figure 3.7. Relationship between fractionation and $K_{1/2}$DIC values for all six species tested under both low (0.5 mM) and high (2.7 mM) DIC concentration. The linear regression is through all data points. The equation is: Fractionation = 0.01($K_{1/2}$DIC) + 19.36 (r^2 = 0.158).

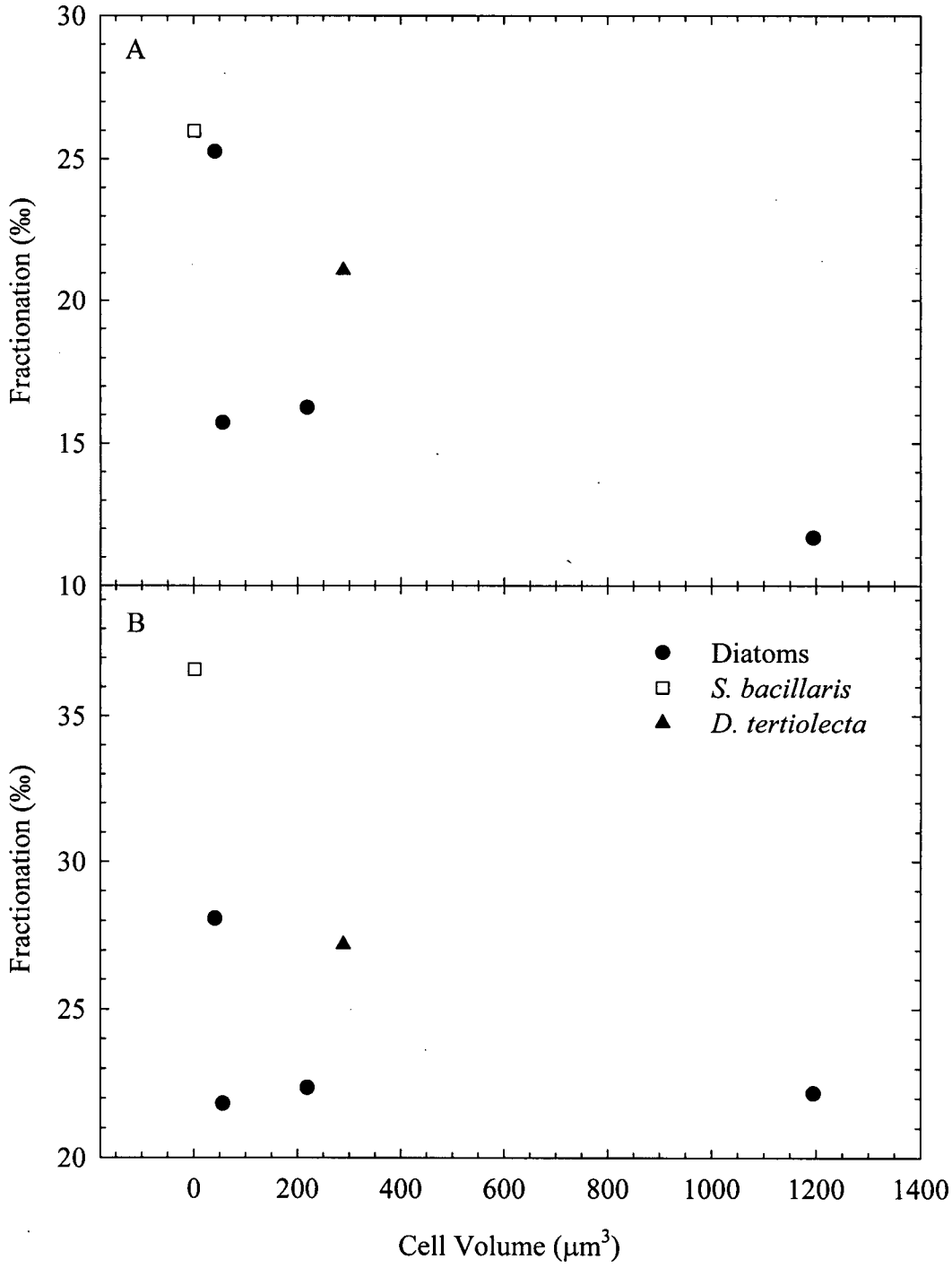

Figure 3.8. Relationship between fractionation and cell volume for all six species under low (0.5 mM) DIC concentration (A), and high (2.7 mM) DIC concentration (B).

3.4 Discussion

3.4.1 Influence of DIC Concentration on Fractionation

Many factors have been suggested to explain the trend toward more negative $\delta^{13}C$ values of phytoplankton as one moves away from the equator towards the poles in the modern ocean. The most notable of these factors are temperature (Sackett *et al.* 1965, Wong and Sackett 1978) and CO_2 (Degens *et al.* 1968b, McCabe 1985, Pardue *et al.* 1976, Rau *et al.* 1989, Rau *et al.* 1992, Sackett 1991). The difficulty with field measurements is that temperature of the surface water varies with latitude, but this temperature difference also produces a carbon system difference because colder waters are more carbon rich than warmer equatorial waters (Fry and Wainright 1991, Rau *et al.* 1989, Sackett 1991). This makes it difficult to determine if the latitudinal trend in phytoplankton $\delta^{13}C$ values is the result of temperature, inorganic carbon concentrations, or both. What is needed to separate the effects of temperature and DIC conditions are experiments that change DIC concentrations independently of temperature, an approach already used by Johnston and Raven (1992).

The data presented in this chapter indicate that cells exhibit higher fractionation when grown at higher medium DIC concentration. This suggests that the carbon concentration of ocean water does influence the $\delta^{13}C$ values of phytoplankton. Since all of the experiments were conducted at 18°C, the only variable was the concentration of DIC and the various inorganic carbon species. The high DIC cells were grown under a DIC concentration of 2.7 mM. This was generated by using a gas concentration of 480 ppm CO_2 and resulted in a aqueous CO_2 concentration of 16.8 μM. The low DIC cultures were aerated with 90 ppm CO_2, resulting in DIC and aqueous CO_2 concentrations of 0.5 mM and 3.1 μM, respectively. Interestingly, while the range in DIC concentrations in the ocean is typically

only 2.0 to 2.3 mM, free CO_2 ranges from 6.5 to 12.9 μM (Goldman and Carpenter 1974). In the case of some coccolithophore blooms, CO_2 levels of 4.8 μM have been observed (Codspoti *et al.* 1986, Cooper *et al.* 1998, Robertson *et al.* 1994). Upwelling of CO_2 enriched waters could potentially result in elevated CO_2 concentrations above 12.9 μM. An unanswered question is whether phytoplankton fractionation responds to the free CO_2 concentration or the total inorganic carbon concentration.

The results of these experiments were intended to demonstrate both the maximum and minimum fractionation values for the species tested. The two CO_2 concentrations used are within the range of potential concentrations in nature. It is tempting to use an abnormally high concentration of CO_2, such as that obtained by bubbling cultures with 5% CO_2, since this extreme concentration should result in maximum fractionation. However, this concentration is purely artificial since such high concentrations are never observed in the ocean (Thompson and Calvert 1994). In addition, attempts to establish equilibrium between high (greater than 1%) CO_2 concentrations and total DIC concentration while maintaining a natural pH of 8.2 were unsuccessful. Bubbling culture medium with high concentrations of CO_2 resulted in a drop in medium pH (data not shown). The effects of pH changes on cell physiology would further complicate the findings of such an experiment.

Many of the previously reported fractionation values for various species of phytoplankton are difficult to interpret due to the lack of carefully controlled medium carbon conditions (Fry 1996). Thus care must be used when interpreting these results. For studies where conditions were reasonably similar to those of this study, these fractionation values are summarized in Table 3.1. Fractionation is commonly expressed relative to either source DIC or CO_2 with the latter referred to as ε_p. Where literature values are expressed as ε_p, they have

Table 3.1. Fractionation values from the literature and growth conditions for the six species tested in this study. *Synechococcus* sp. represents various marine isolates. An "n/a" indicates that the condition is not disclosed in the paper. The $\delta^{13}C$ CO_2 is converted to $\delta^{13}C$ DIC using the equations of Mook *et al.* (1974). Where a range in phytoplankton $\delta^{13}C$ values is included, two fractionation values were calculated. Fractionation is expressed relative to source DIC.

Reference	Species	[DIC]	Temp (°C)	pH	Light	Stir	μ (d^{-1})	$\delta^{13}C$ CO_2 (‰)	$\delta^{13}C$ DIC (‰)	$\delta^{13}C$ POC (‰)	Fract (‰)
Falkowski 1991	*D. tertiolecta*	n/a air	15	8.2	14:10 LD	gentle	n/a	-6.9	3.2191	-23.3	26.43
Burkhardt *et al.* 1999	*P. tricornutum*	2.05 mM	15	7.8	24 L	n/a	1.6	-10.3	-0.1809	-26.6	26.42
Johnston & Raven 1992	*P. tricornutum*	air	20	n/a	24 L	air bubble	1.58	n/a	-2.2	-22.8 to -24.3	20.65 to 22.15
Johnston 1996	*P. tricornutum*	[CO2] 11.3 μM	20	8.2	16:8 LD	air bubble	1.75	-9.06	0.4751	-21	21.46
Laws *et al.* 1995	*P. tricornutum*	[CO2] 13 μM	22	n/a	24 L	air bubble	1.4	n/a	-8	-35	27.22
Laws *et al.* 1995	*P. tricornutum*	[CO2] 31 μM	22	n/a	24 L	air bubble	0.5	n/a	-16	-47	31.50
Burkhardt *et al.* 1999	*S. costatum*	2.10 mM	15	7.98	24 L	n/a	1.9	-10.7	-0.5809	-24.5	23.93
Falkowski 1991	*S. costatum*	n/a air	15	8.2	14:10 LD	gentle	n/a	-6.9	3.2191	-16.4	19.56
Hinga *et al.* 1994	*S. costatum*	2.215 mM	15	8.26	14:10 LD	gentle stir	n/a	n/a	1.6	-20.92	22.48
Hinga *et al.* 1994	*S. costatum*	1.112 mM	15	7.51	14:10 LD	gentle stir	n/a	n/a	3.91	-25.11	28.91
Popp *et al.* 1998	*Synechococcus*	1.887 mM	22	n/a	24 L	air bubble	0.9	-9.65	-0.3429	-27.25	26.92
Popp *et al.* 1998	*Synechococcus*	2.182 mM	22	n/a	24 L	air bubble	0.1	-16.89	-7.5829	-32.03	24.63
Falkowski 1991	*T. pseudonana*	n/a air	15	8.3	14:10 LD	gentle	n/a	-6.9	3.2191	-7.5	10.68
Thompson & Calvert 1994	*T. pseudonana*	1.4-2 mM	18	8.2	24 L	inversion	1.5-2	-13.4	-3.6337	-20 to -25	16.43 to 21.44
Burkhardt *et al.* 1999	*T. weissflogii*	2.07 mM	15	7.97	24 L	n/a	1.6	-10.7	-0.5809	-24.6	24.03

been converted to fractionation relative to DIC since it is unknown whether phytoplankton possess the capacity to use bicarbonate in addition to CO_2 (Fry 1996).

Though Thompson and Calvert (1994) did not find a relationship between DIC concentration and fractionation in *Thalassiosira pseudonana*, they did report a range of fractionation values of 16.4 to 21.4‰. This range appears to be consistent with the results of these experiments. Both the values of Thompson and Calvert (1994) and this study are higher than those reported by Falkowski (1991) who found that fractionation by *T. pseudonana* was only 10.68‰. However, the carbon conditions were not monitored in Falkowski's experiments. Unlike the low fractionation Falkowski (1991) found for *T. pseudonana*, *Dunaliella tertiolecta* fractionation was similar to the value found in this study under high DIC conditions. It is possible that his *T. pseudonana* cultures were grown to a higher density, thus resulting in CO_2 limitation, a condition that can lead to reduced apparent fractionation (Fry 1996).

Fractionation by *Skeletonema costatum* has been previously reported to range from 19.6 to 28.9‰ (Burkhardt *et al.* 1999, Falkowski 1991, Hinga *et al.* 1994). In the study of Burkhardt *et al.* (1999), the carbon conditions were carefully monitored and their conditions under continuous light were similar to those used in my experiments for the high carbon cultures. Fractionation values for *Thalassiosira weissflogii* (22.17‰) and *S. costatum* (22.36‰) in this study were also similar to that found by Burkhardt *et al.* (1999).

Reported fractionation by *Phaeodactylum tricornutum* ranges from 20.7‰ (Johnston and Raven 1992) to 31.5‰ (Laws *et al.* 1995), whereas in this study, fractionation showed a considerably smaller range of 25.2 to 28.1‰. Finally, the fractionation value for *Synechococcus bacillaris* grown under high DIC conditions was considerably higher

(36.6‰) than the values obtained by Popp *et al.* (1998) (24.63 – 26.92‰). However, the DIC concentration used in this study was 0.7 mM higher than that used by Popp *et al.* (1998).

There is conflicting evidence as to whether CO_2 and/or DIC concentration influences fractionation in laboratory cultures. Thompson and Calvert (1994) found that *Thalassiosira pseudonana* fractionation did not respond to DIC concentration. Burkhardt *et al.* (1999) found that CO_2 concentration had little effect on fractionation for *Thalassiosira weissflogii* and *Skeletonema costatum*. These findings contradict data from Wong and Sackett (1978) and Hinga (1994) which suggest that *Skeletonema costatum* fractionation is influenced by DIC concentration (see Fry 1996). Experiments using *Phaeodactylum tricornutum* also suggest that fractionation increases with CO_2 concentrations (Laws *et al.* 1995, 1997).

The range over which changes in DIC result in changes in fractionation by phytoplankton is unclear. The *Synechococcus* data reported here indicate that even above 2 mM DIC, increasing DIC concentration can result in increased fractionation. This is in contrast to the literature fractionation values for the other five species at a DIC concentration of ca. 2.0 mM that correspond well to data from this study which are for 2.7 mM DIC. Fractionation in natural populations of phytoplankton relative to source DIC is typically in the range of 10 to 30‰ (Degens *et al.* 1968a, Park and Epstein 1961, Rau *et al.* 1982, Sackett *et al.* 1965, Wong 1976). The range in fractionation measured in laboratory studies, both in the literature and in this study, is considerably less than that observed in nature. It is difficult to say why this discrepancy exists (Fry 1996).

3.4.2 Influence of Cell Size and Growth Rate on Fractionation

A further question deals with why different species, when grown under similar conditions, have different fractionation values. One factor that might influence carbon isotope fractionation is cell size. Assuming cells are not actively transporting carbon, then the size of the cell would influence the size of the boundary layer surrounding the cell (Raven 1994). The larger the boundary layer, the more limiting the rate of diffusion of CO_2 becomes since the boundary layer essentially acts as a semi-closed system which restricts movement of CO_2 from the bulk medium to the cell surface (France 1995, Korb *et al.* 1996, Smith and Walker 1980).

Appendix A provides information regarding cell dimensions and volume for the six species tested in this study. Assuming similar photosynthetic capacities, one might expect that larger species would have a lower fractionation than smaller species if the rate of CO_2 uptake was faster than the rate of supply of CO_2 to the boundary layer (Korb *et al.* 1996). However, there was no significant relationship between cell volume and fractionation at either DIC concentration used in my experiments (Figure 3.8). This is true both within the diatom group as well as the complete set of species tested. Of the diatom species tested, *Thalassiosira weissflogii* was the largest in terms of volume, yet fractionation for this species was not markedly different from that of the smaller *Thalassiosira pseudonana*. *Synechococcus bacillaris*, the smallest species tested, exhibited the largest fractionation under the high DIC concentration, as expected. However, at low DIC, its fractionation is similar to that of *Phaeodactylum tricornutum*, which has a much larger cell volume. Finally, *Dunaliella tertiolecta* is the second largest species tested yet it does not have low fractionation relative to the others. Although cell volume likely imparts some influence on

fractionation, other factors are probably more important. The issue is further complicated since cell shape might also influence fractionation (Popp *et al.* 1998).

The second factor used to explain fractionation differences is growth rate (Bidigare *et al.* 1997, Fry and Wainright 1991, Hinga *et al.* 1994, Johnston and Raven 1992, Korb *et al.* 1996, Laws *et al.* 1995, 1997), although Johnston (1996) found only a small growth rate effect on fractionation with *Phaeodactylum tricornutum*. However, it remains to be seen whether interspecific growth rate differences can explain any of the variability in phytoplankton fractionation (Korb *et al.* 1996). One would expect that faster growing species would be more likely to experience CO_2 limitation and thus express reduced fractionation if they were relying on diffusion for carbon uptake. No such relationship was observed in this study. To further test this hypothesis, species exhibiting a wider range of growth rates than observed in my experiments must be tested.

All of the species tested in this study are fast growing, with growth rates at or above 1 d^{-1} (Figure 3.1). One would expect that cells relying on CO_2 diffusion might become CO_2 limited at low DIC concentrations and thus reduce their growth rates accordingly. This would result in reduced fractionation, as was observed here. However, none of the species tested exhibited significantly reduced growth rates under the low DIC concentration relative to the high DIC concentration. This is in agreement with Burkhardt *et al.* (1999) who also found that decreasing CO_2 concentrations did not result in decreased growth rates. However, Riebesell *et al.* (1993b) found evidence that low CO_2 concentrations (below 10 μM) resulted in growth rate decreases for three diatom species, although the effect on fractionation was not determined in their study.

A final consideration is that the six species of phytoplankton tested might possess different forms of RuBisCO. Guy *et al.* (1993) found that isotope fractionation by isolated

RuBisCO varied depending on the source species. The assumption that phytoplankton RuBisCO fractionation is 29‰ might not be appropriate. For example, fractionation by RuBisCO isolated from the cyanobacterium *Anacystis nidulans* was only 22‰. Surprisingly, this is lower than the fractionation under high DIC exhibited by the cyanobacterium from this study. Nevertheless, some of the species variability in fractionation might be the result of different forms of RuBisCO.

3.4.3 The Carbon Concentrating Mechanism and Fractionation

Many species of marine phytoplankton appear to possess an inducible carbon concentrating mechanism (Badger and Price 1992, Raven *et al.* 1993). These algae have suppressed photorespiration, a high affinity for DIC, and low CO_2 compensation points (Johnston and Raven 1992, Raven *et al.* 1993). One of the best lines of evidence for active carbon uptake is a higher CO_2 concentration inside relative to outside the cell (Raven 1993a). Another indication is an increased affinity for carbon relative to the primary carboxylation enzyme RuBisCO (Raven *et al.* 1993). Indeed, changes in the affinity of cells for carbon are an indicator that cells are either up-regulating or supressing their carbon concentrating mechanism. In all six species tested, cells grown under low DIC concentrations possessed a higher affinity for DIC (reduced $K_{1/2}$DIC). The most dramatic response was in the diatom *Thalassiosira pseudonana* that had an eight-fold higher affinity when acclimated to a low DIC concentration than cells acclimated to a high DIC concentration.

Although it is difficult to ascertain the nature of the carbon concentrating mechanism in these species, it is clear that the photosynthetic physiology of cells grown under low DIC concentrations is dramatically different from those grown under the high DIC conditions.

Several models have been proposed to describe the carbon concentrating mechanism and all of these might be used by marine phytoplankton (Figure 3.9). Cells ultimately require CO_2 as the substrate for RuBisCO, the major carbon-fixing enzyme (Raven *et. al.* 1993). One possibility is that cells actively take up CO_2. However, cells with large boundary layers might still become carbon-limited as CO_2 is depleted within this layer. A more plausible model suggests that cells produce extracellular carbonic anhydrase (CA) that can quickly convert bicarbonate into CO_2 within the boundary layer. This CO_2 then diffuses across the plasmalemma into the cell as a result of the larger concentration gradient. Alternatively, the cell could actively take up bicarbonate directly and later, via intracellular CA, convert the bicarbonate to CO_2 for RuBisCO. This process might occur within the cytoplasm or within the chloroplast.

The data from the experiments presented in this chapter suggest that phytoplankton exhibit reduced fractionation under low DIC concentrations and that this is accompanied by an increased affinity for carbon. It is likely that the increased affinity represents at least partial induction of a carbon concentrating mechanism. Whether the two processes are linked remains to be proven. No significant relationship was demonstrated within the group of species tested in this thesis. However, given the importance of photosynthetic processes in carbon isotope fractionation, there is likely a connection between CCM induction and fractionation. If CO_2 diffusion limitation was causing the change in fractionation, one might expect growth rates to drop under the CO_2-limiting conditions. This was not observed for any of the species tested. It is possible that, while cells did not become CO_2 limited, the pool of CO_2 within the boundary layer became depleted and potentially enriched in ^{13}C. Such enrichment can result in reduced apparent fractionation (Fry 1996). However, this

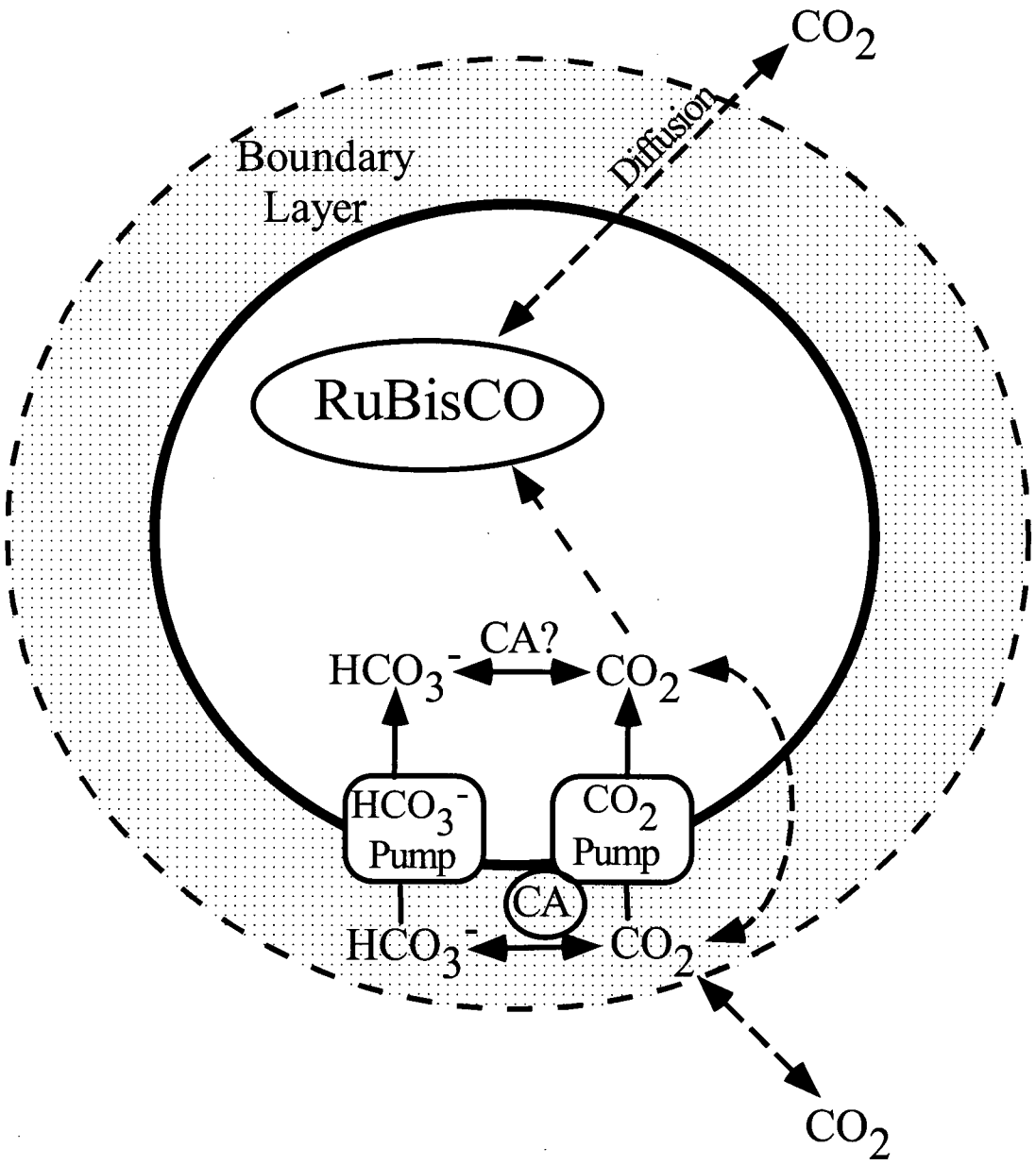

Figure 3.9. Simplified model of carbon entry into a phytoplankton cell including the potential involvement of active transport and carbonic anhydrase.

hypothesis does not explain the change in cell affinity for carbon observed in this study. Thus, although reduced apparent fractionation without growth rate changes may be in accordance with the CO_2 diffusion model, active carbon uptake complicates the issue. The relationship between carbon isotope fractionation and CCM induction will be explored further in Chapter 4.

Chapter 4

Relationship Between $K_{1/2}$DIC and Fractionation in the Marine Diatom *Thalassiosira pseudonana*: Steady State and Closed System Drawdown Experiments

4.1 Introduction

Though numerous attempts have been made to model the relationship between carbon isotope fractionation and CO_2 supply to phytoplankton, it has been difficult to incorporate all aspects of algal physiology. Surprisingly, active uptake of carbon is generally not considered in these models. The prospect of marine phytoplankton requiring an active carbon uptake mechanism may seem unlikely given the abundance of inorganic carbon in marine environments (Raven 1993a, Wolf-Gladrow and Riebesell 1997). However, as illustrated in Figure 2.3A and B, the concentration of free CO_2 is less than 1% of the total inorganic carbon present in seawater. The potential for CO_2 limitation of phytoplankton growth was first suggested by Riebesell *et al.* (1993b). Their suggestion has resulted in an open debate as to whether CO_2 limitation is possible in the marine environment (Raven 1993b, Raven *et al.* 1993, Riebesell *et al.* 1993a, Turpin 1993).

The controversy essentially resides around the ability of marine phytoplankton to actively take up carbon. The major carbon-fixing enzyme in marine phytoplankton is ribulose-1,5-bisphosphate carboxylase-oxygenase (RuBisCO) (Raven *et al.* 1993). Though β-carboxylation enzymes can, at times, be responsible for a substantial proportion of carbon fixation (Guy *et al.* 1989, Turpin *et al.* 1988), RuBisCO is thought to be responsible for at

least 90% of total carbon fixation by marine phytoplankton (Raven *et al.* 1993). The other carboxylation enzymes function predominantly in an anaplerotic mode to replenish the TCA cycle and likely refix CO_2 released during respiration (See Raven *et al.* 1993 for a review of the various carboxylase enzymes).

The enzyme RuBisCO is thought to have evolved at a time when the atmospheric CO_2 concentration was likely two orders of magnitude higher than current levels. This is probably the reason why it has such a low affinity for CO_2 (Badger *et al.* 1998, Raven 1993a). The half-saturation constant (K_m) for phytoplankton RuBisCO is estimated to range between 40 to 100 μM CO_2 (Badger *et al.* 1998). This means that under an ambient CO_2 concentration of approximately 12 μM that is typically found in the ocean, RuBisCO would be operating well below its maximum catalytic capacity if cells relied only on diffusional CO_2 uptake. A further characteristic of RuBisCO is that it can also catalyze oxygen fixation when CO_2 concentrations are low. The resulting glycolate pathway is energetically costly and it releases carbon already fixed (Falkowski and Raven 1998).

Many marine phytoplankton species exhibit characteristics that indicate the presence of a carbon concentrating mechanism (CCM). These characteristics include higher affinity for carbon dioxide than that of RuBisCO, insensitivity to oxygen, and accumulation of inorganic carbon inside the cell (Raven 1993a, Raven *et al.* 1993). A good review of the evidence for the occurrence of CCM in phytoplankton can be found in Badger *et al.* (1998). It is likely that most species at least possess the ability to use some form of a CCM. However, what remains unclear is whether these mechanisms are functional at ecologically relevant DIC (CO_2) levels (Raven *et al.* 1993). It is possible that CCM activity is only present under conditions of significant photosynthetic CO_2 drawdown (Codispoti *et al.* 1982, 1986) or low CO_2 concentrations generated by physical oceanographic processes (Rau *et al.*

1989). However, even intense algal bloom conditions rarely draw CO_2 levels down to less than half the ambient concentration (Codispoti *et al.* 1986, Cooper *et al.* 1998, Wanninkhof and Feely 1998).

Given an equilibrium between the atmosphere and ocean water, one must also consider that the rate of diffusion in water is much less than in air (Descolas-Gros and Fontugne 1990). The presence of a boundary layer around phytoplankton cells that restricts diffusion of CO_2 from the medium into the cell might make active uptake more important. Based on a model of diffusion to this boundary layer, through the layer, and across the plasmalemma, Riebesell *et al.* (1993b) suggested that growth rate could become limited by CO_2 supply. However, the ability of phytoplankton to induce a CCM might prevent any limitation of growth (Raven *et al.* 1993). Phytoplankton could maintain high photosynthetic rates under low CO_2 concentrations by increasing their affinity for carbon, perhaps by using bicarbonate. However, CCM induction would likely be accompanied by higher energetic costs, both in terms of extra enzyme synthesis and in the transport of carbon against a concentration gradient. This cost, however, would presumably be less than that incurred as a result of photorespiration. Either way, one can conclude that carbon limitation of photosynthesis and the subsequent induction of active carbon transport would not necessarily lead to significant growth limitation (Raven *et al.* 1993).

While the ecological significance of carbon concentrating mechanisms in marine phytoplankton is somewhat debatable, their degree of influence on carbon isotope fractionation remains unresolved. At high CO_2 concentrations, cells would likely rely on diffusion of CO_2 across the membrane. Models based on CO_2 diffusion essentially compare the rates of diffusional supply to CO_2 fixation. The latter is based on growth rate and cell carbon quota. Table 4.1 shows the fractionation associated with various partial processes

Table 4.1. Fractionation values (both kinetic and equilibrium) for various partial processes relevant to models of carbon isotope fractionation by phytoplankton. Unless otherwise indicated, values are for 25°C. CA = carbonic anhydrase, PEPCase = phosphoenol pyruvate carboxylase, CPSase = carbamyl phosphate synthetase. ? = Uncertain. Table modified from Raven *et al.* (1993).

Process	Fract. (‰) (Kinetic)	Fract. (‰) (Equil.)	Reference
CO_2 diffusion in solution	0.7		O'Leary (1984)
CO_2 flux through membranes	0.0?		Raven *et al.* (1993)
Active DIC uptake	0.0?		Berry (1989), Kerby and Raven (1985)
Uncatalyzed $CO_2 \rightarrow HCO_3^-$	13		O'Leary *et al.* (1992)
Uncatalyzed $HCO_3^- \rightarrow CO_2$	22		O'Leary *et al.* (1992)
$CO_2 \rightarrow HCO_3^-$ catalyzed by CA	0.1		O'Leary *et al.* (1992)
$HCO_3^- \rightarrow CO_2$ catalyzed by CA	10.1		O'Leary *et al.* (1992)
CO_2 fixation by RuBisCO I (Spinach) §	29		Guy *et al.* (1987, 1993), Roeske and O'Leary (1984)
CO_2 fixation by RuBisCO II*	17.8		Roeske and O'Leary (1985)
Fixation of HCO_3^- by PEPCase (vs CO_2)	4.7		O'Leary *et al.* (1992)
Fixation of HCO_3^- by CPSase (vs CO_2)	1?		Raven and Farquhar (1990)
Fixation of CO_2 by PEPCKase	24 - 40		Arnelle and O'Leary (1992)
Carboxylation reactions (intrinsic)	6		Arnelle and O'Leary (1992)
Decarboxylation reactions (intrinsic)	6		Arnelle and O'Leary (1992)
Respiration (general)	0?		Laws *et al.* (1995), others
$CO_2(aq) + H_2O \leftrightarrow HCO_3^- + H^+$ (18°C)		9.77	Mook *et al.* (1974)
$CO_2(g) \leftrightarrow CO_2(aq)$ (18°C)		-1.09	Mook *et al.* (1974)
$CO_2(aq) + RH \leftrightarrow RCO_2^- + H^+$ (25°C)		3	O'Leary *et al.* (1992)

§ Fractionation in marine phytoplankton by form I RuBisCO may differ from 29‰

* RuBisCO II is found in dinoflagellates (Morse *et al.* 1995), otherwise, phytoplankton possess form I.

relevant to carbon uptake and assimilation by marine phytoplankton. The important fractionation values are for diffusion (0.7‰), active uptake (0.0‰) and carbon fixation by RuBisCO (assumed to be 29‰ for diatoms).

Conceptually, models of fractionation for diffusional CO_2 uptake by phytoplankton cells are relatively simple and involve at least two major processes (Figure 3.9). The first process is the supply of CO_2 to the cell and through the cell membrane. The second process is the actual fixation of the CO_2 by RuBisCO. Fractionation by the cell is ultimately determined by the rate limiting process. If diffusion is the rate limiting process, the cell will exhibit an apparent fractionation close to 0.7‰ relative to the source CO_2. Since CO_2 is ca. 10‰ more negative than total DIC, a fractionation of ca. 11‰ relative to the source DIC pool should be observed. However, if the rate of CO_2 supply to RuBisCO is infinitely large relative to the carbon fixation rate, the fractionation of RuBisCO will be fully expressed. This would result in a fractionation of 29‰ relative to CO_2 (ca. 39‰ relative to total DIC). Of course, such extreme cases rarely exist and phytoplankton fractionation typically falls within a range of 10 to 30‰ relative to source DIC depending on the relative limitations imposed by the two processes (Degens *et al.* 1968a, Park and Epstein 1961, Rau *et al.* 1982, Sackett *et al.* 1965, Wong 1976).

Models of isotope fractionation based on active uptake of carbon assume that phytoplankton rely on diffusion of CO_2 at high DIC carbon concentrations. As a result, high fractionation should be expressed under these conditions. However, under low CO_2 concentrations, the rate of diffusion might be insufficient to supply enough carbon to meet levels required to support a given growth rate. One response might be to reduce growth rate. A more likely response is to induce a CCM.

There are several possible forms a CCM might take (Figure 3.9). If CO_2 was transported directly, one would expect whole cell isotopic fractionation to decrease to near zero relative to CO_2 or ca. 10‰ relative to DIC. Alternatively, direct transport of bicarbonate would cause a fractionation of close to zero relative to DIC. A final possibility is that cells possess external carbonic anhydrase (CA) that can speed up the rate of CO_2 production from bicarbonate. Since CO_2 produced by CA catalysis will have an identical isotopic content to the existing CO_2 pool, fractionation relative to the CO_2 should again approach zero.

Regardless of the nature of the CCM, its induction should result in reduced fractionation. This is because fractionation during active carbon uptake is thought to be zero (Berry 1989, Kerby and Raven 1985). This assumes that once transported into the cell, carbon is immediately fixed or sequestered and therefore it cannot diffuse back out of the cell. Indeed, it seems unlikely that cells would expend energy to transport carbon only to have it leak back out. If a mechanism did not exist to prevent leakage, the discrimination by RuBisCO would not be masked and the resulting whole cell fractionation would approach the RuBisCO value of 29‰. The exact nature of the mechanism preventing leakage is unknown but might involve either a change in membrane permeability of the plasmalemma to CO_2 (Sharkey and Berry 1985) or sequestering of the carbon within an internal organelle perhaps by means of an internal carbon pump (Badger and Price 1992). Both mechanisms would reduce efflux of CO_2. As a result, RuBisCO fixes what is transported and the apparent fractionation is much lower than that of RuBisCO. This is, of course, also true for diffusion models since RuBisCO immediately fixes CO_2 supplied by a slow diffusion rate.

There are only two studies that have linked gradual changes in the CCM induction state with fractionation. Sharkey and Berry (1985) found that the assimilation rate of CO_2 by

the freshwater green alga *Chlamydomonas reinhardtii* decreased upon transfer from high (5%) to low (0.03%) CO_2, however, it recovered within three hours. This was a result of a gradually increasing affinity for CO_2, an indication of CCM induction. CCM induction was accompanied by a reduction in fractionation. The addition of Diamox, an inhibitor of CA activity, caused a subsequent decrease in carbon assimilation rate. These results suggest that a CCM involving external CA was induced upon transfer to low DIC conditions. Erez *et al.* (1998) also found a link between CCM induction and reduced fractionation in a freshwater *Synechococcus* species. A demonstration of reduced fractionation as a result of CCM induction has not been attempted in marine phytoplankton.

It is difficult to determine from phytoplankton $\delta^{13}C$ values whether a reduction in fractionation caused by low CO_2 concentrations is due to diffusional limitation of CO_2 supply or CCM induction. The results of Chapter 3 suggest that phytoplankton grown under low DIC have a higher affinity for DIC while fractionating less against ^{13}C. This might indicate that CCM induction is accompanied by reduced fractionation. In this chapter, more detailed studies of fractionation and CCM induction are described. These include steady state experiments over a range of DIC concentrations as well as closed system drawdown experiments. Fractionation models based on CO_2 diffusion include parameters such as growth rate, external CO_2 concentration, cell size, and temperature. These important parameters were monitored throughout my experiments.

4.2 Methods

4.2.1 Steady State Experiments

Cultures of the marine diatom *Thalassiosira pseudonana* (Clone 3H, NEPCC # 58, Northeast Pacific Culture Collection, University of British Columbia) were grown at ambient DIC concentrations ranging from 0.2 to 2.75 mM total DIC. DIC levels were obtained using the relationship between pCO_2 and DIC as described in Figure 2.3. Cultures were maintained in logarithmic growth for at least six generations prior to sampling. Isotope fractionation and photosynthetic kinetics were determined for the cultures as described in the general methods. Five medium samples were taken during the closed system fractionation experiments. At least four replicate DIC curves were performed for each culture.

4.2.2 Closed System Drawdown Experiments

These experiments were essentially larger and longer-term versions of the smaller closed system depletion experiments used to determine fractionation in the steady state experiments in this chapter. The goal was to allow an exponentially growing culture to completely deplete the source carbon and, as a result, go into carbon limited growth. The two drawdown experiments differed only in that one used unbuffered medium.

The culturing apparatus is illustrated in Figure 4.1. A 10 L flask of artificial medium was inoculated with a small volume (10 mL) of logarithmic phase cultures of *Thalassiosira pseudonana*. The culture was then sealed with a high-density silicon stopper equipped with a sampling tube, an inflow tube for aeration and an outflow tube. To reduce potential contamination by external CO_2 from the laboratory air, gas impermeable Tygon™ tubing was

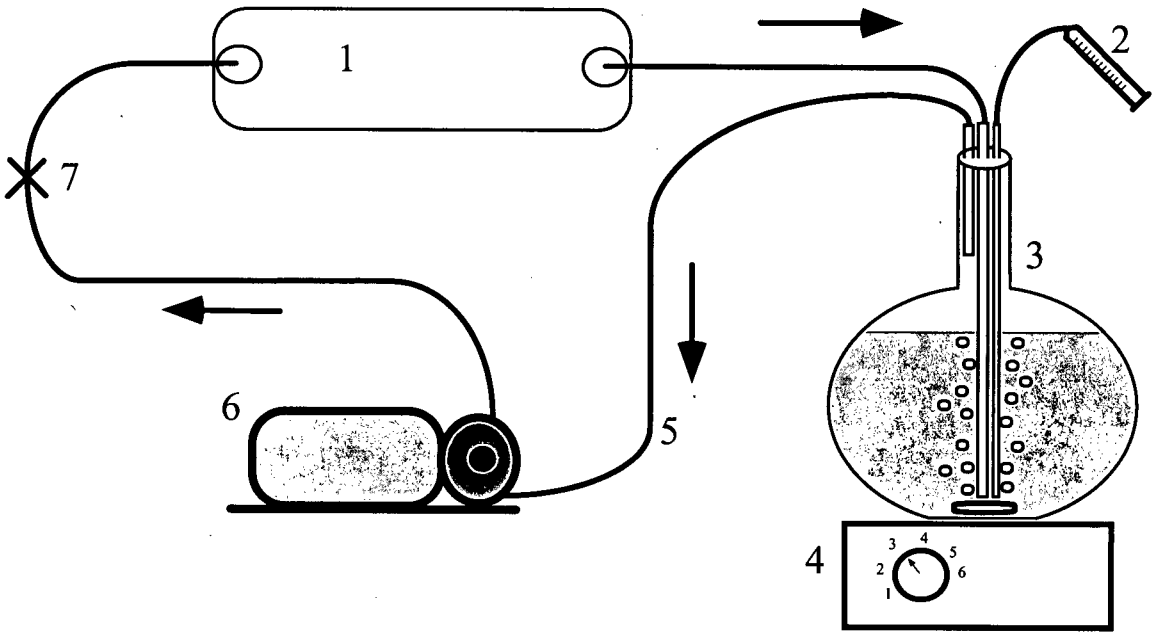

Figure 4.1. Culture apparatus for the closed system drawdown experiments. The component parts are: 1) Collapsible bag, 2) Sampling syringe, 3) 10 L culture flask fitted with a stopper and three glass tubes, 4) Magnetic stir motor, 5) Gas impermeable Tygon™ tubing, 6) Gas tight recirculating pump, and 7) Quick disconnect fittings.

used. The system was tested for CO_2 leakage by recirculating nitrogen gas for an extended (3 days) period of time and no measurable CO_2 contamination was observed. The gas was recirculated using an air-tight pump (Model 7015, Cole-Parmer, Vernon Hills, Illinois). The tubing contained air-tight quick-disconnect fittings to allow the insertion of the IRGA in-line with the aeration system. This allowed non-obtrusive monitoring of the pCO_2 throughout the time course of the experiments. Finally, a 10 L gas impermeable bag was placed in-line to allow sampling of the culture medium without creating a negative pressure in the system due to volume changes. Gas was recirculated at a rate of 1 L min^{-1} and the culture stirred at 120 rpm. The cultures were grown under conditions similar to those used for the steady state experiments with the exception of the unbuffered drawdown culture. The medium used for this experiment lacked the artificial buffer, but was otherwise identical to the buffered medium.

Throughout the time course of the experiments, sampling was performed for cell density, fluorescence, DIC concentration, pCO_2, pH, POC isotope content, medium isotope content, and photosynthetic kinetics. For isotope content of the medium, three replicate samples were taken at each point and the average used for determination of fractionation. In all cases, the replicates were extremely consistent with a standard deviation of no more than ca. 1% of the mean. Fractionation was determined between each pair of sampling points during which there was at least 10% DIC drawdown. The calculation used for fractionation was similar to that used in the steady state experiments except that only two points were used rather than five. At least four replicate DIC curves were performed at each sampling point. The experiments were terminated when culture growth ceased. This occurred when DIC was nearly completely exhausted in the buffered culture but when only half of the DIC was used up in the unbuffered experiment.

In addition to the drawdown experiments using cells, two drawdown experiments were conducted without cells. One of these experiments used buffered medium while the other used unbuffered medium. Otherwise, the medium was similar to that used in the drawdown experiments with cells. The CO_2 removal was accomplished by continuous sparging with N_2 gas. The experiments lasted 5 to 7 days with CO_2 removal rates significantly (less than 10%) lower than the uncatalyzed rate of CO_2 production from bicarbonate. These experiments were conducted in order to compare fractionation produced by the two methods of CO_2 removal.

4.3 Results

4.3.1 Steady State Experiments

The results presented in Chapter 3 indicate that *Thalassiosira pseudonana* was capable of increasing its affinity for carbon when acclimated to a low DIC concentration. This was accompanied by a decrease in fractionation. Cultures were acclimated over a range of ambient DIC concentrations and the resulting photosynthetic kinetics and fractionation were determined. The results presented in Figure 4.2 further demonstrate the ability of *T. pseudonana* to induce a CCM. A series of DIC curves (only three shown here) resulting from cultures acclimated to DIC concentrations ranging from 0.2 mM to 2.75 mM revealed that CCM induction varied in magnitude. Figure 4.3 summarizes the response in $K_{1/2}$DIC values to changing ambient DIC concentrations. There was a significant linear relationship ($p<0.001$) between $K_{1/2}$DIC and ambient DIC.

There was also a significant linear relationship ($p<0.001$) between fractionation and ambient DIC concentration (Figure 4.4). There appeared to have been a leveling off at around 2.0 mM DIC. To reflect this, the highest ambient DIC point was excluded from the regression. When fractionation was plotted against $K_{1/2}$DIC, a significant linear relationship ($p=0.002$) was also observed (Figure 4.5). It has been suggested that reduced carbon levels might limit growth rates of marine phytoplankton, and therefore the growth rate of cultures grown at each ambient DIC concentration was determined (Figure 4.6). Due to the frequent dilution of the cultures, reliable estimates of growth rates were not possible for these cultures as is indicated by the magnitude of the standard deviation values. None of the rates was significantly different from one another (t-test) indicating that fractionation was not dependent on growth rate.

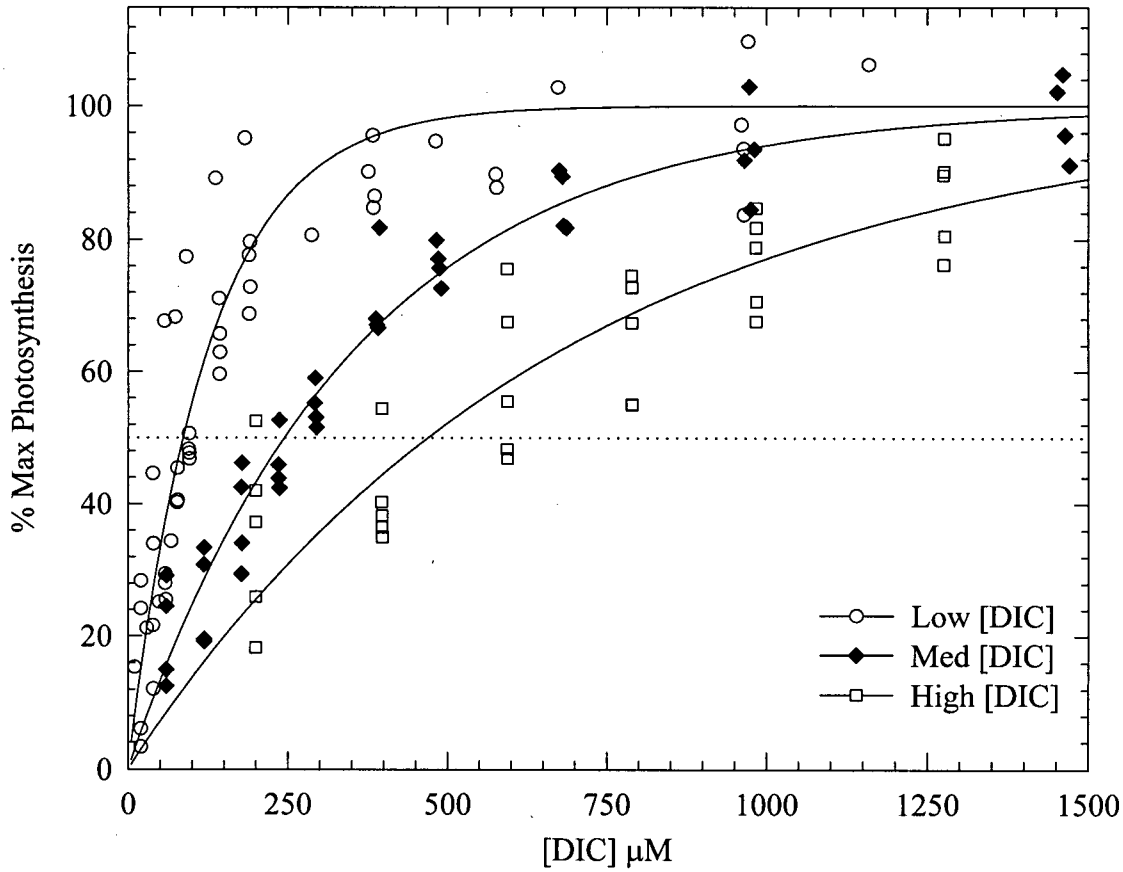

Figure 4.2. Photosynthetic kinetics of *Thalassiosira pseudonana* cultures grown under low (0.2 mM), medium (1.45 mM), and high (2.75 mM) DIC concentrations. Regressions are fitted through the data from at least three replicate DIC curves for each DIC level using the P vs. I equation (Platt and Gallegos 1980) and are normalized to percent maximum photosynthesis.

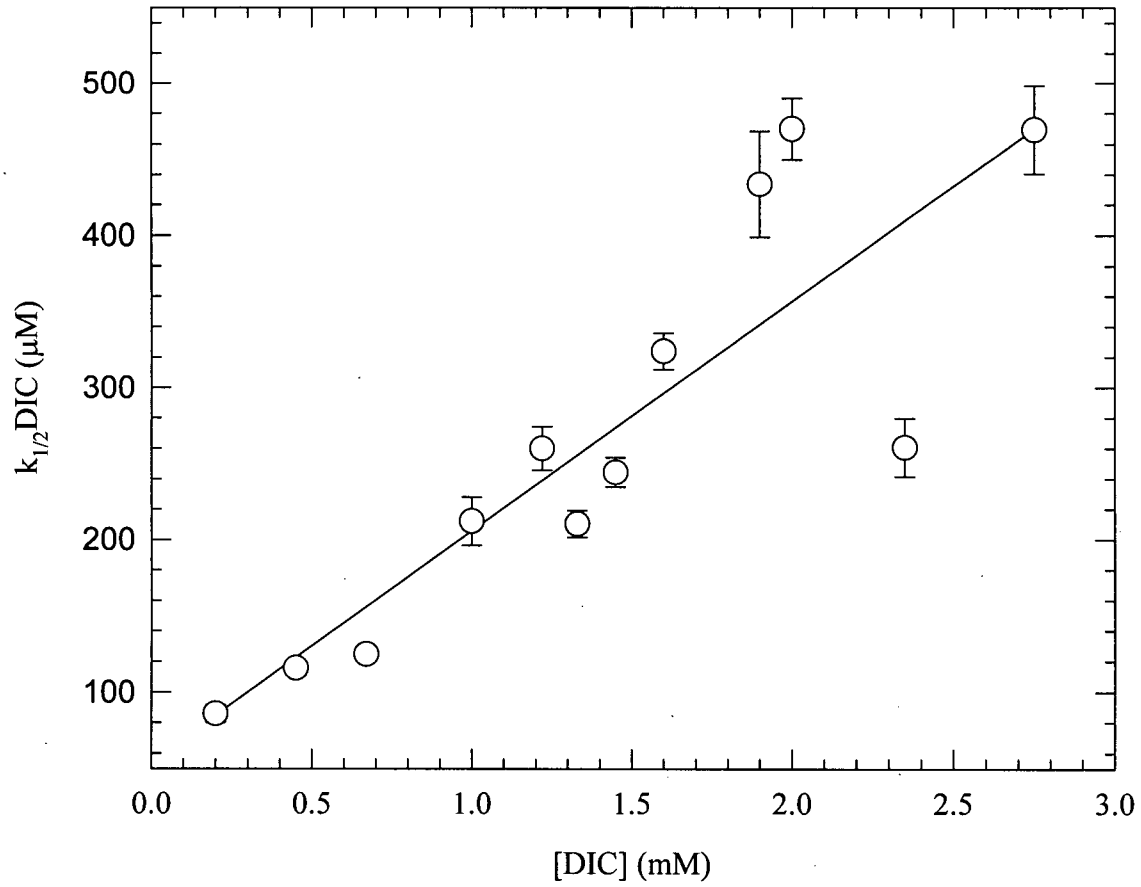

Figure 4.3. $K_{1/2}$DIC values for *Thalassiosira pseudonana* cultures grown at various ambient DIC concentrations ranging from 0.20 to 2.75 mM. Error bars represent ± 1 standard error of the regressions through the raw data. Where error bars are not visible they fit within the symbols. The regression equation is $K_{1/2}DIC = 151.1\ [DIC] + 54.5$ ($r^2 = 0.7517$).

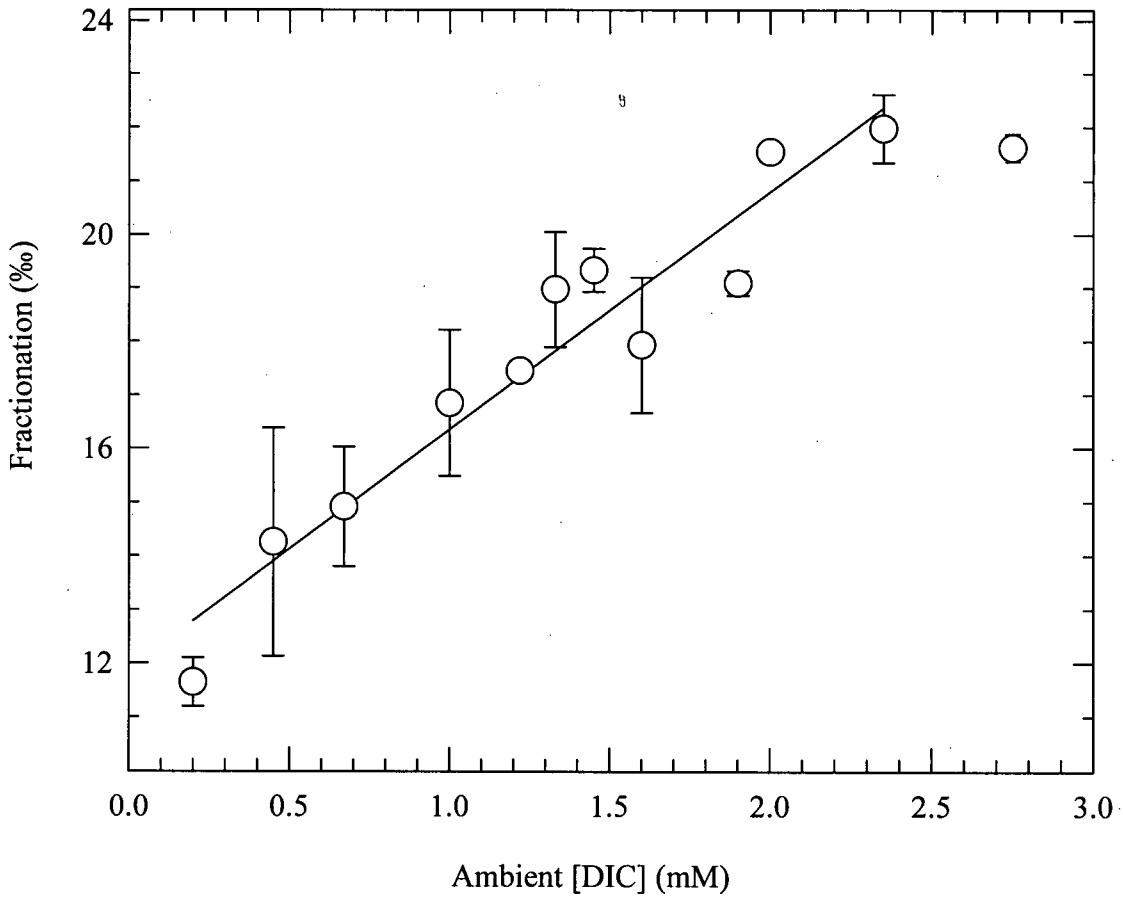

Figure 4.4. Fractionation values for *Thalassiosira pseudonana* cultures grown at various ambient DIC concentrations ranging from 0.20 to 2.75 mM. Error bars represent ± 1 standard error of the regression through the raw data. Where error bars are not visible they fit within the symbols. The regression line is through all data with the exception of the 2.75 mM sample point. The regression equation is: Fractionation = 4.45[DIC] + 11.90 (r^2 = 0.9224).

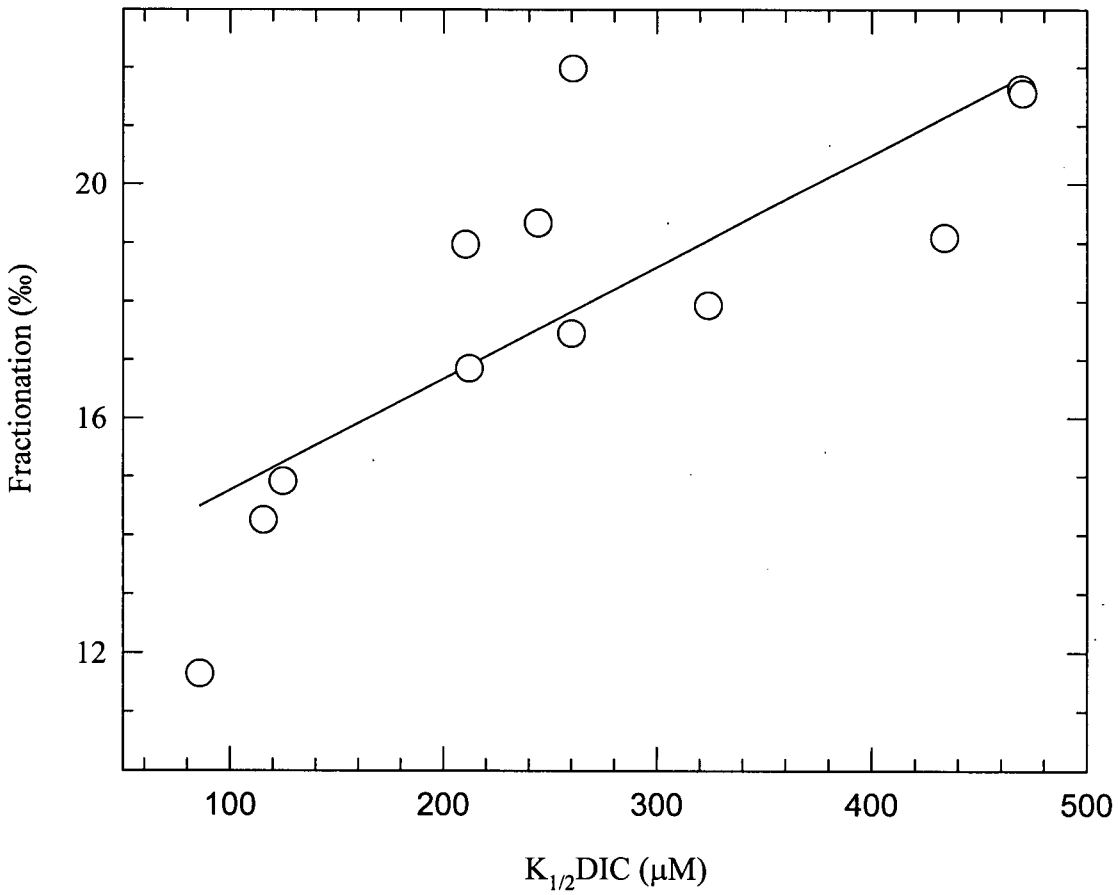

Figure 4.5. Relationship between fractionation and CCM induction (as represented by $K_{1/2}$DIC values) in cultures of *Thalassiosira pseudonana* grown at various ambient DIC concentrations ranging from 0.20 to 2.75 mM. The regression equation is: Fractionation = 0.019 ($K_{1/2}$DIC) + 12.85 (r^2 = 0.6448).

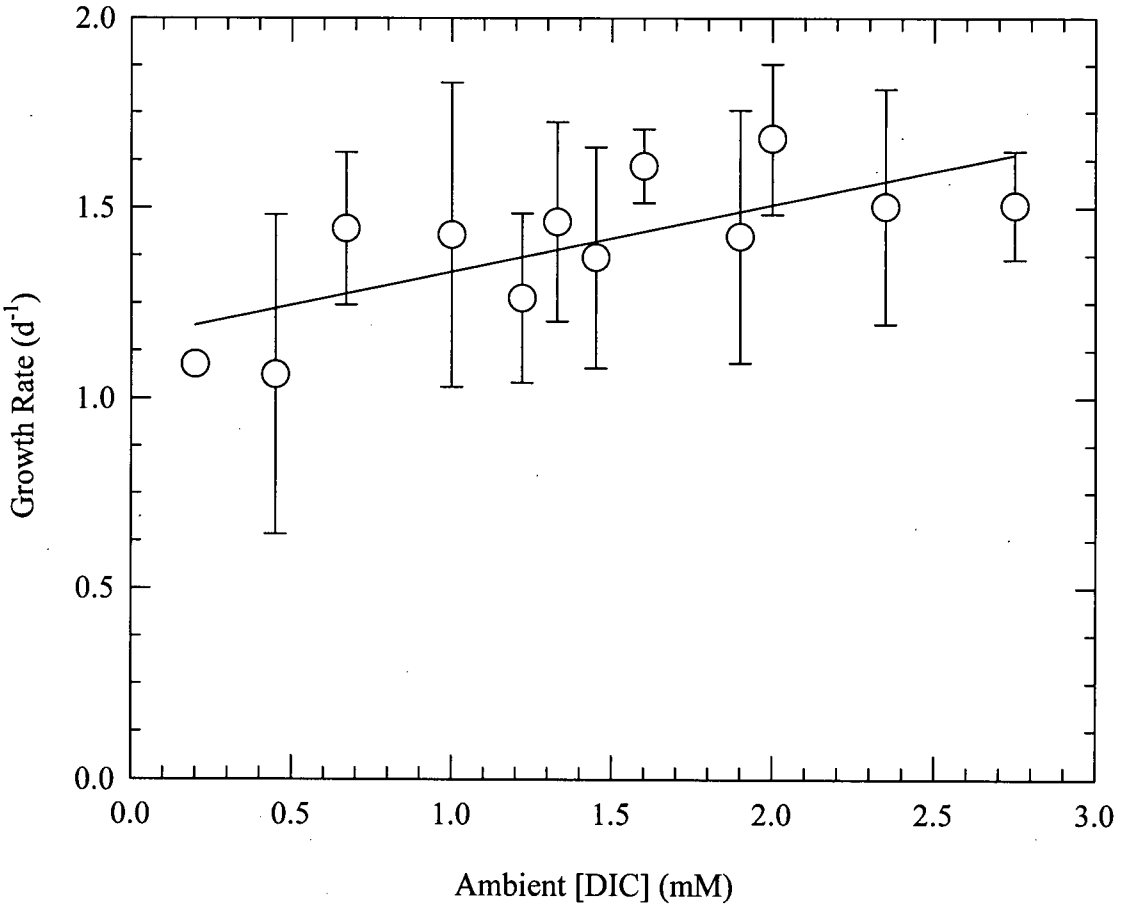

Figure 4.6. Growth rates of *Thalassiosira pseudonana* cultures grown at various ambient DIC concentrations ranging from 0.20 to 2.75 mM. Error bars represent ± 1 standard deviation of two point growth rate calculations ($n \geq 3$). Where error bars are not visible they fall within the symbols. The regression equation is: Growth Rate = 0.175 [DIC] + 1.156 (r^2 = 0.519).

4.3.2 Closed System Drawdown Experiments

These experiments were designed to assess the changes in both photosynthetic kinetics and fractionation over the duration of the logarithmic growth phase of a culture, ultimately ending in carbon limitation. The first drawdown experiment used artificially buffered medium similar to that used in the steady state experiments. Although dense phytoplankton growth usually results in dramatic increases in pH, with the artificial buffer, a rise of only 0.5 units was observed (Figure 4.7A). Similar experiments with unbuffered medium resulted in more than double this pH increase (Figure 4.13A). The growth rate of the culture was 1.36 ± 0.17 d^{-1}. Growth rate began to slow when the medium DIC reached 0.3 mM (Figure 4.7B). Both DIC and CO_2 decreased based on cell density as expected. The culture removed 95% of the total DIC (Figure 4.7B). At this DIC concentration and a pH of 8.7, free CO_2 was essentially zero (Figure 4.7B).

The photosynthetic kinetics of the culture changed markedly throughout the time course of the drawdown experiment. DIC curves at different points during the drawdown (Figure 4.8) illustrate the changing affinity of the cells for carbon. $K_{1/2}$DIC values decreased from more than 700 μM to less than 200 μM (Figure 4.9). The $K_{1/2}$DIC appeared to level off at ca. 125 μM. The range in $K_{1/2}$DIC from this experiment agrees well with that from Chapter 3 for this species; however, in the steady state experiments, a maximum $K_{1/2}$DIC of ca. 500 mM was observed (Figure 4.3). No apparent reason for this discrepancy was found.

Changes in fractionation throughout the time course of the experiment are presented in Figure 4.10 along with the DIC concentrations. One must be careful when interpreting the fractionation data as these points do not represent discrete points in time, but rather average

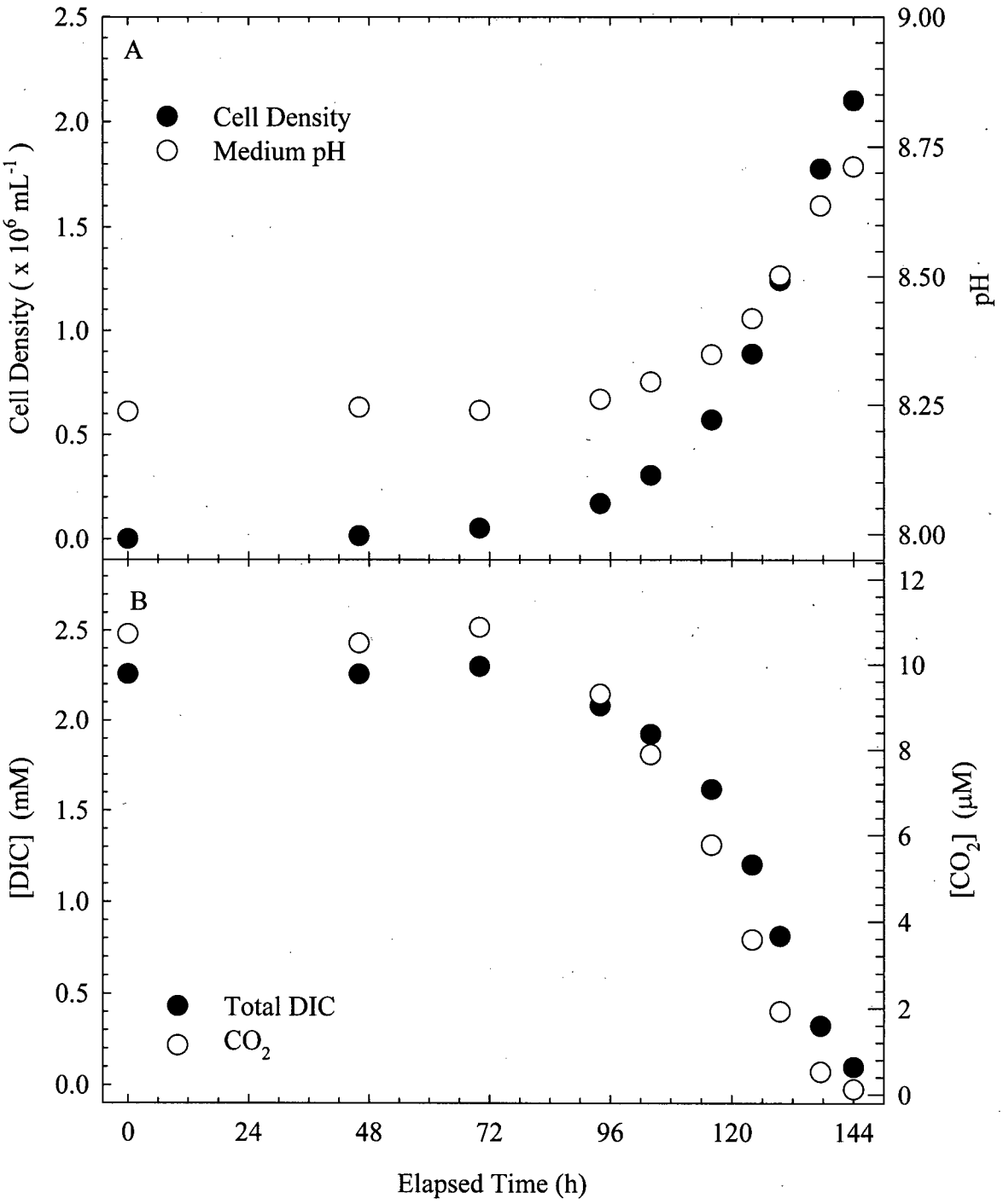

Figure 4.7. Changes in *Thalassiosira pseudonana* cell abundance and medium pH (A), and total DIC and CO_2 concentrations (B), during the closed system drawdown (buffered medium) experiment. Error bars represent ± 1 standard deviation ($n \geq 3$). Where error bars are not visible they fit within the symbols.

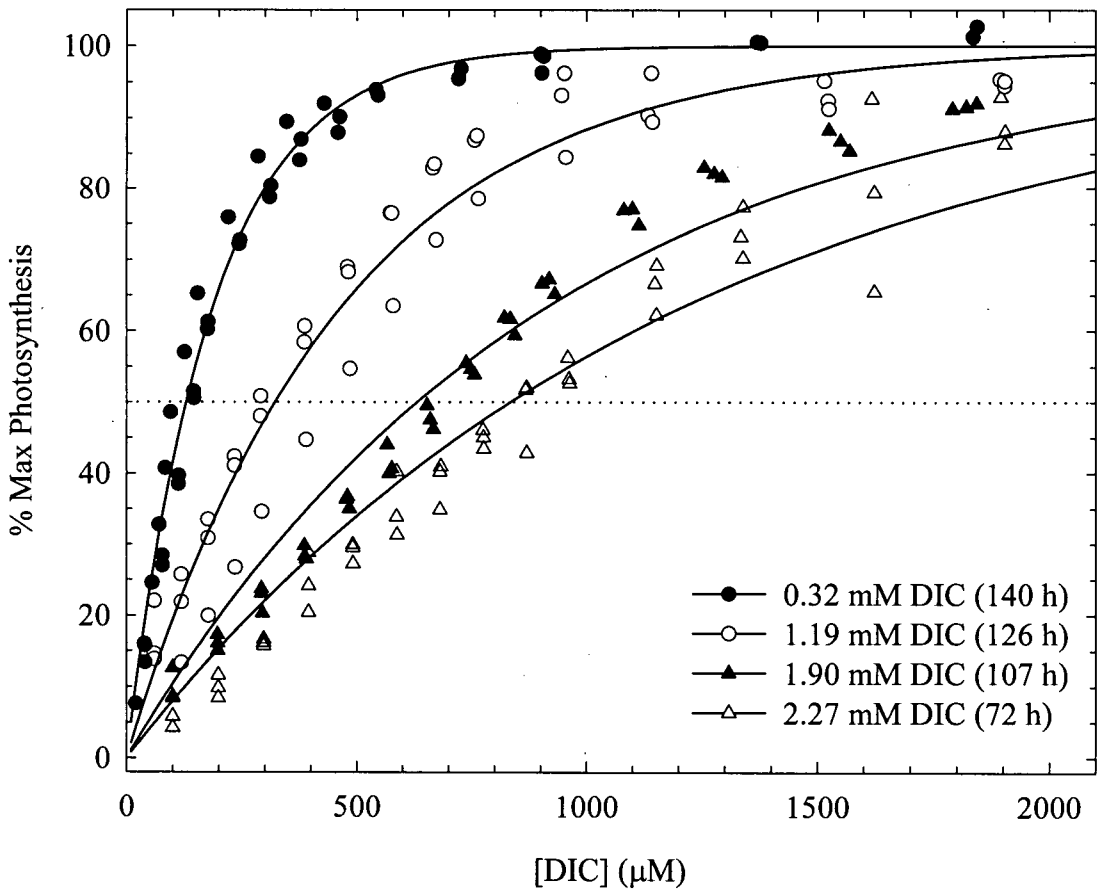

Figure 4.8. Photosynthetic kinetics of *Thalassiosira pseudonana* cultures at various DIC concentrations during the time course drawdown (buffered medium) experiment (see Figure 4.7). Regressions are fitted through the data from at least three replicate DIC curves for each DIC level using the P vs. I equation (Platt and Gallegos 1980) and are normalized to percent maximum photosynthesis.

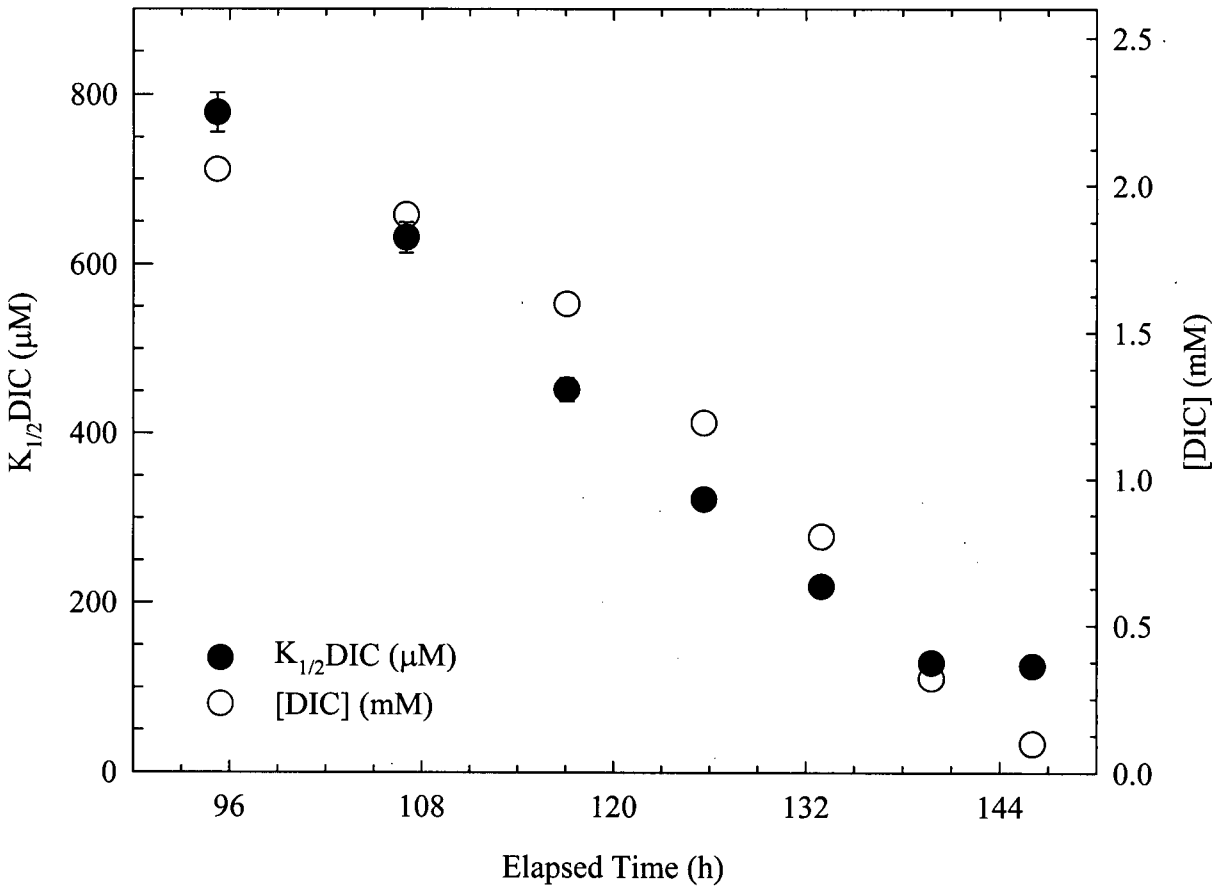

Figure 4.9. Changes in the DIC concentration and $K_{1/2}$DIC values for *Thalassiosira pseudonana* cells during the closed system drawdown (buffered medium) experiment. Error bars represent ± 1 standard deviation of DIC measurements (n=3) and ± 1 standard error of the regression through the raw data ($K_{1/2}$DIC). Where error bars are not visible they fall within the symbols.

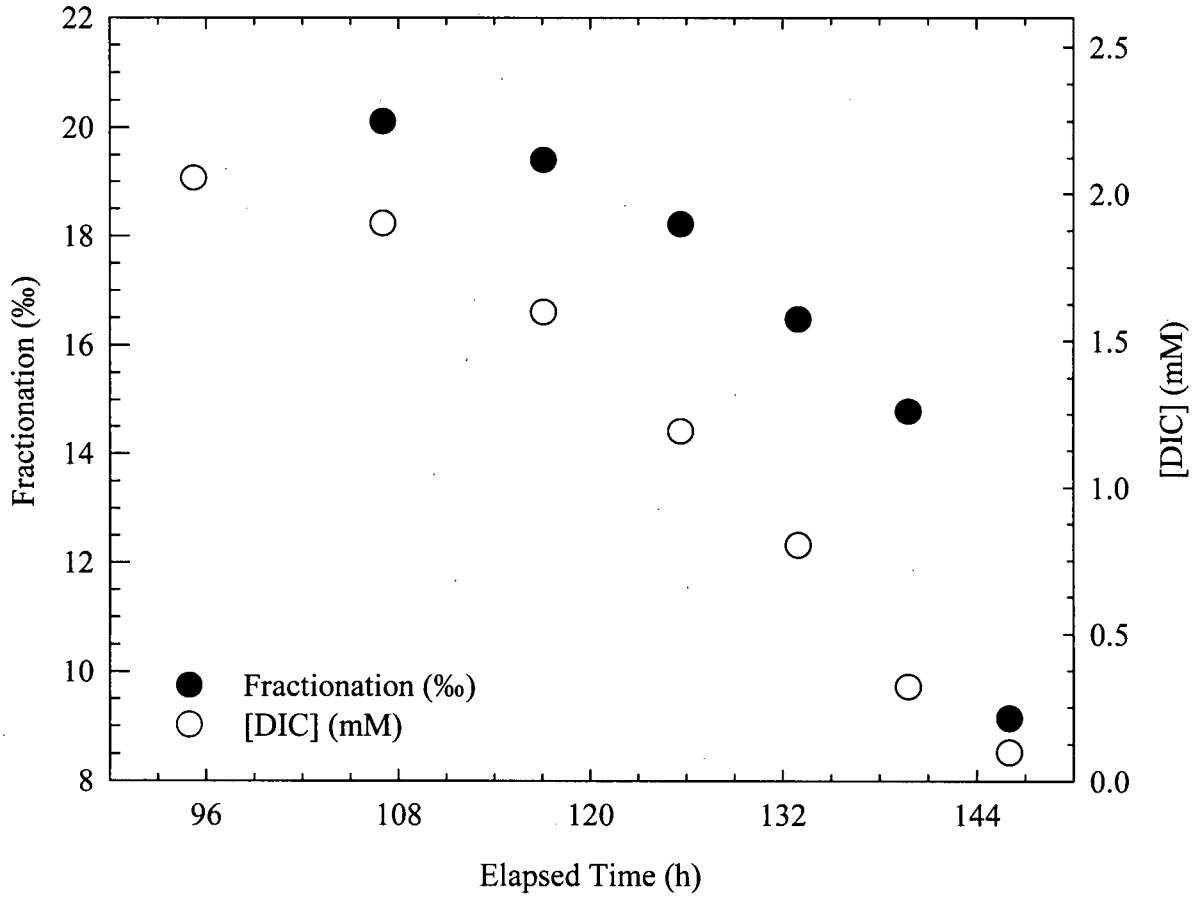

Figure 4.10. Changes in the DIC concentration and fractionation for *Thalassiosira pseudonana* cells during the closed system drawdown (buffered medium) experiment. Error bars represent ± 1 standard deviation of DIC measurements (n=3). Where error bars are not visible they fall within the symbols. Standard error was not calculated for fractionation values since only two points were used in the calculation. There is no datum point for fractionation at 96 h since fractionation was only calculated where at least 10% DIC depletion had occurred from the previous sampling time and this did not occur until ca. 108h.

fractionation by the culture during the time interval from the previous sampling point to the present measurement. Nevertheless, the results do indicate that fractionation decreased over the growth phase of the culture.

A better way to analyze the fractionation data is to draw a linear regression through the data as described in the general introduction, Figure 1.1, and Guy *et al.* (1989). The connected points represent the actual data from the experiment. Though a significant linear regression ($p<0.001$, slope = 13.78‰) was found to exist between $[\ln(R/R_o)x1000]$ and $[-\ln(f)]$ (Figure 4.11), a consistent decrease in the slope (fractionation) between subsequent sets of points indicates that fractionation is changing during the time course of the drawdown experiment. If fractionation was constant throughout the depletion period, a straight line should result with the slope representing the fractionation value. If one assumes a constant fractionation of 20‰ as was the case in the early stages of the experiment, the actual data drift progressively further below the line during the time course of the DIC depletion. This figure provides some of the best evidence of the difficulty in obtaining an accurate estimate of fractionation. When CO_2 was removed from the buffered medium using N_2 sparging as opposed to phytoplankton growth, there appeared to be a constant fractionation of 13.41‰ (Figure 4.12). A significant linear relationship ($P<0.001$, slope = 13.41‰) and no change in slope throughout the experiment indicate a constant fractionation occurred throughout the course of the drawdown.

A similar drawdown experiment was conducted where the culture medium lacked an artificial buffer. There was more than double the change in pH when the culture medium was not buffered (Figure 4.13A). This has a dramatic effect on the inorganic carbon speciation as the majority of the inorganic carbon is in the form of carbonate at this pH. Also of interest is that the final cell density was about half that of the buffered drawdown

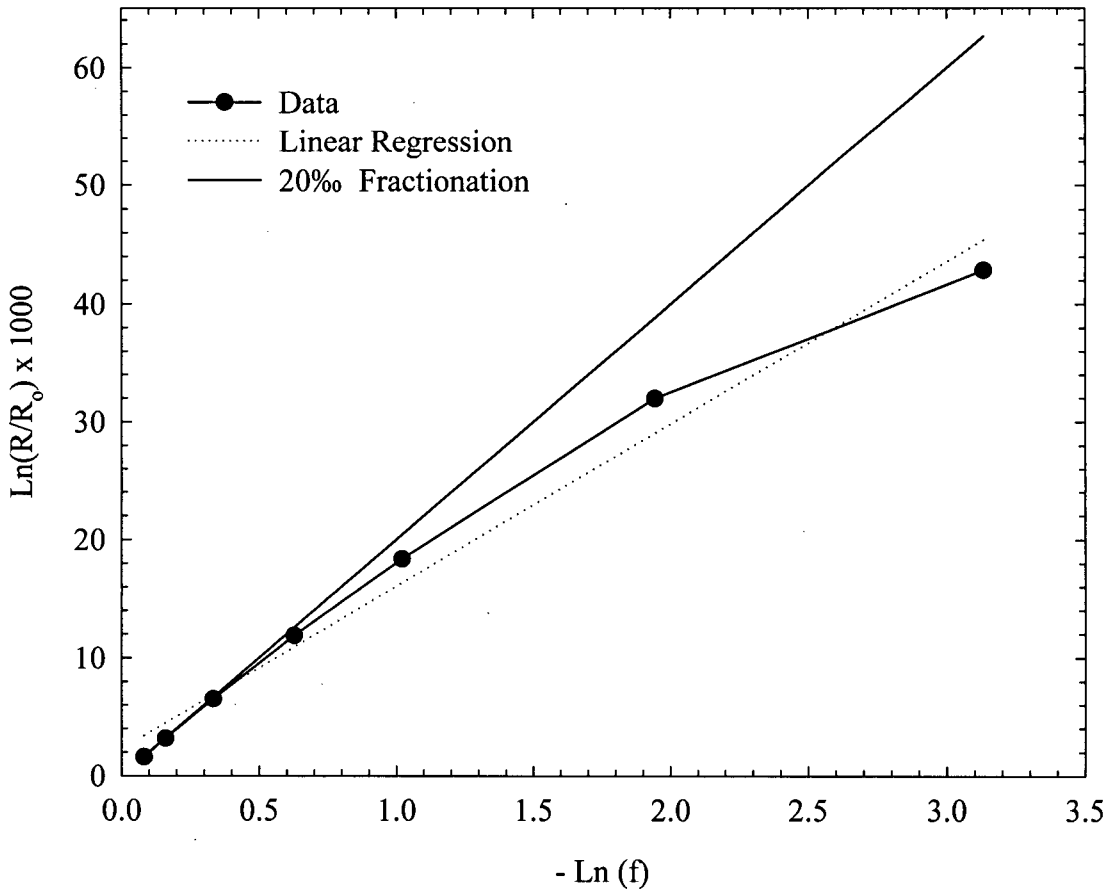

Figure 4.11. Isotope data from the drawdown experiment with buffered medium for *Thalassiosira pseudonana*. Data points represent individual measurements throughout the experiment. Error bars (not visible) represent ± 1 standard deviation of replicates (n=3). The linear regression through the data assumes that fractionation remained constant (no change in slope) during the experiment. The equation for the regression line is Y = 13.78 [-Ln(f)] + 2.26 (r^2 = 0.983, SE slope = 2.26). The 20‰ line assumes that fractionation remained constant at 20‰ throughout the experiment.

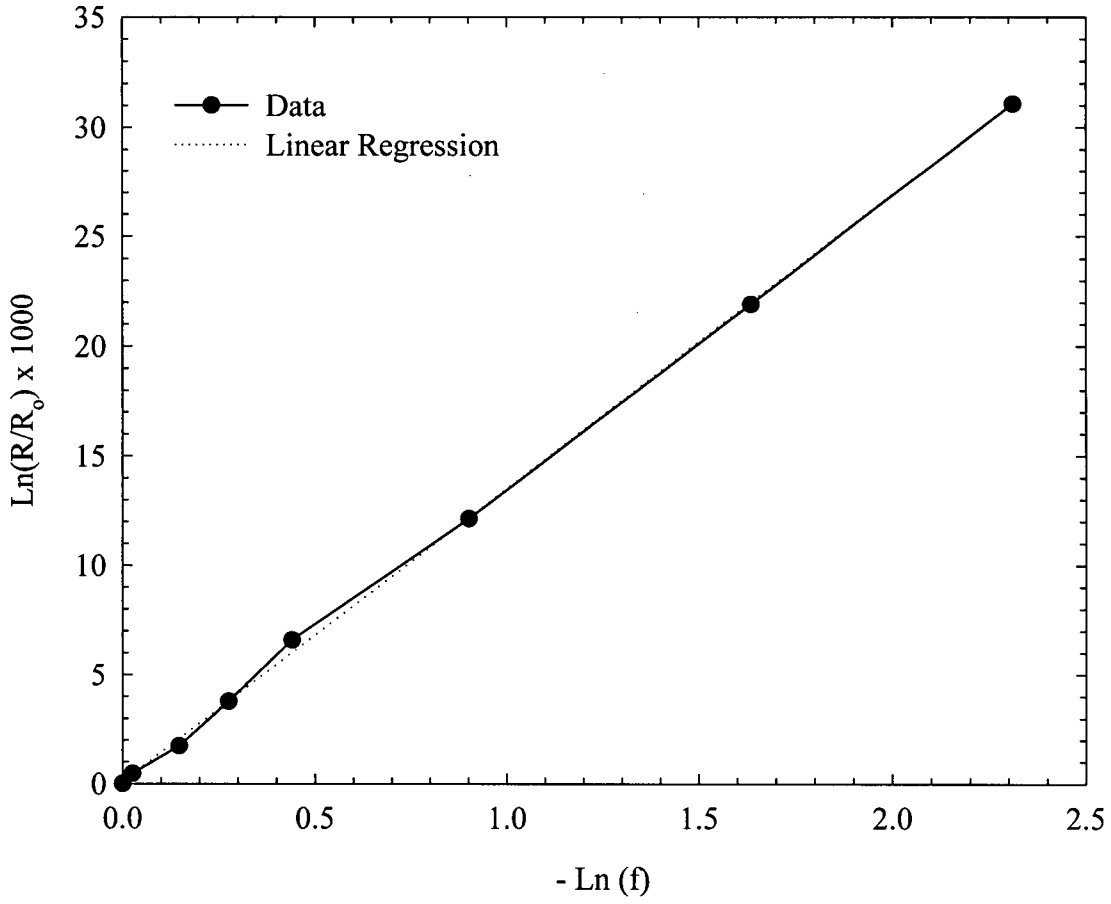

Figure 4.12. Isotope data from the drawdown experiment with buffered medium and no cells. Data points represent individual measurements throughout the experiment. Error bars (not visible) represent ± 1 standard deviation of replicates (n=3). The linear regression through the data assumes that fractionation remained constant (no change in slope) during the experiment. The equation for the regression line is Y = 13.41 [-Ln(f)] + 0.09 (r^2 = 0.999, SE slope = 0.278).

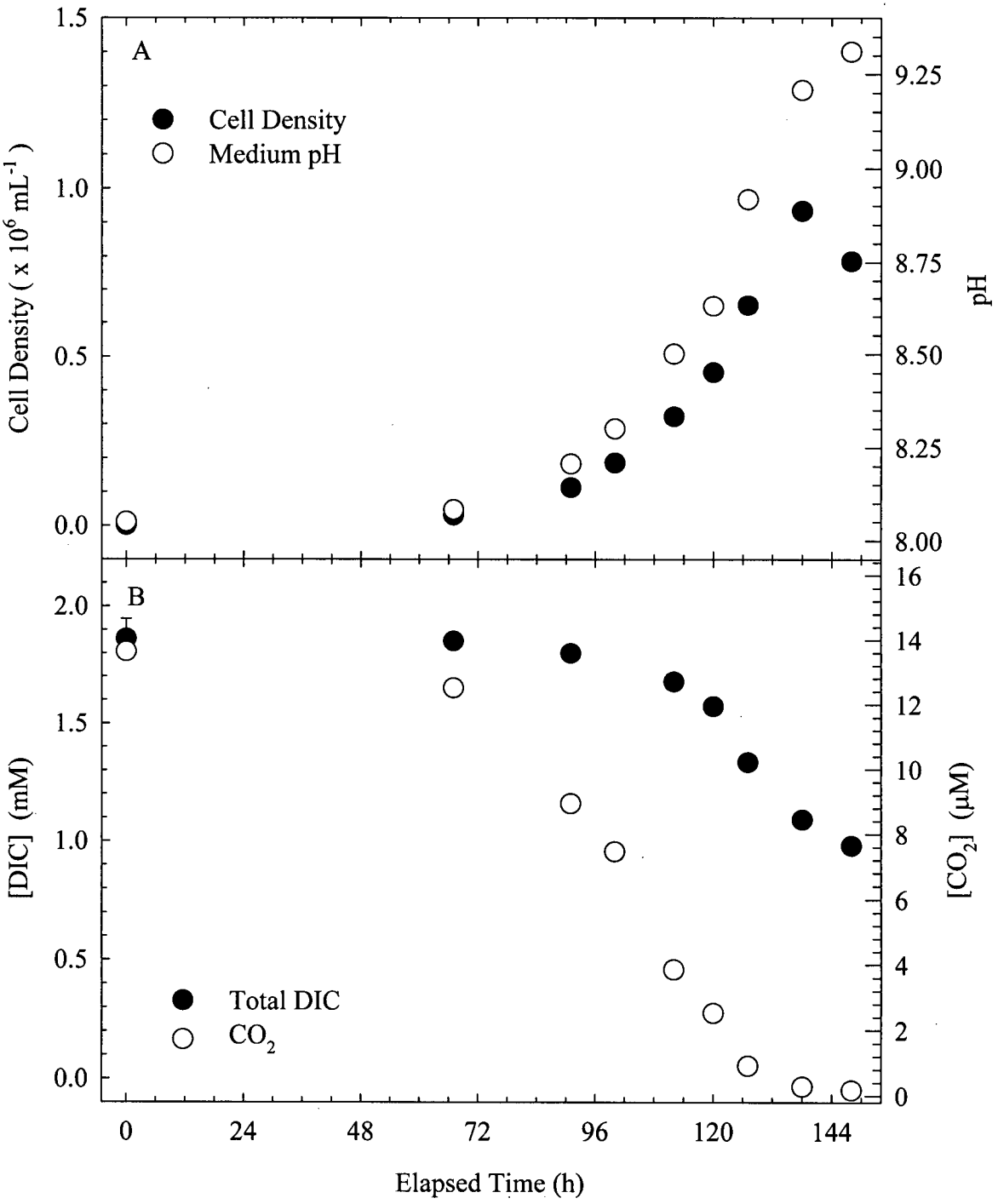

Figure 4.13. Changes in *Thalassiosira pseudonana* cell abundance and medium pH (A), and total DIC and CO_2 concentrations (B), during the closed system drawdown (unbuffered medium) experiment. Error bars represent ± 1 standard deviation ($n \geq 3$). Where error bars are not visible they fit within the symbols.

experiment. Not surprisingly, the DIC concentration decreased only to ca. 1.0 mM (Figure 4.13B). This is about half the drawdown observed in the buffered medium experiment. However, due to changes in the pH, the free CO_2 concentration decreased to near zero which was similar to the buffered experiment. The growth rate of 1.32 ± 0.12 d^{-1} was not significantly different from the growth rate of cells in the buffered experiment.

The $K_{1/2}$DIC decreased throughout the time course of the DIC drawdown (Figure 4.14). Some differences between the buffered and unbuffered experiment were noted. First, the $K_{1/2}$DIC values early in the unbuffered experiment were not as high as in the buffered experiment. Rather, they more closely resembled the $K_{1/2}$DIC values of the high DIC steady state experiments. Secondly, the final data point contained a significant standard error. These cells appeared to exhibit a variable response to DIC concentration. Maximum photosynthetic rates were dramatically lower than cells from previous sampling points during the experiment. Previous experiments (data not shown) for cultures entering nitrogen limited senescence indicated that cells were only capable of a low rate of photosynthesis and that additions of DIC did not increase photosynthetic rates. It is possible that these cells were entering senescence. $K_{1/2}$DIC values as low as ca. 100 μM were not observed for the unbuffered experiment, but might have occurred between the final two sampling points. A $K_{1/2}$DIC of 100 μM appears to be the minimum level for *Thalassiosira pseudonana.*

A trend of decreasing fractionation with lower DIC concentration was observed in the unbuffered culture (Figure 4.15). Although both of the drawdown experiments demonstrated a minimum fractionation of close to 10‰, the highest fractionation values in the unbuffered experiment were slightly higher than those of the buffered drawdown experiment. The decrease to 10‰ fractionation occurred over a smaller range of DIC changes in the unbuffered experiment. This was, of course, also true of the changes in the $K_{1/2}$DIC values.

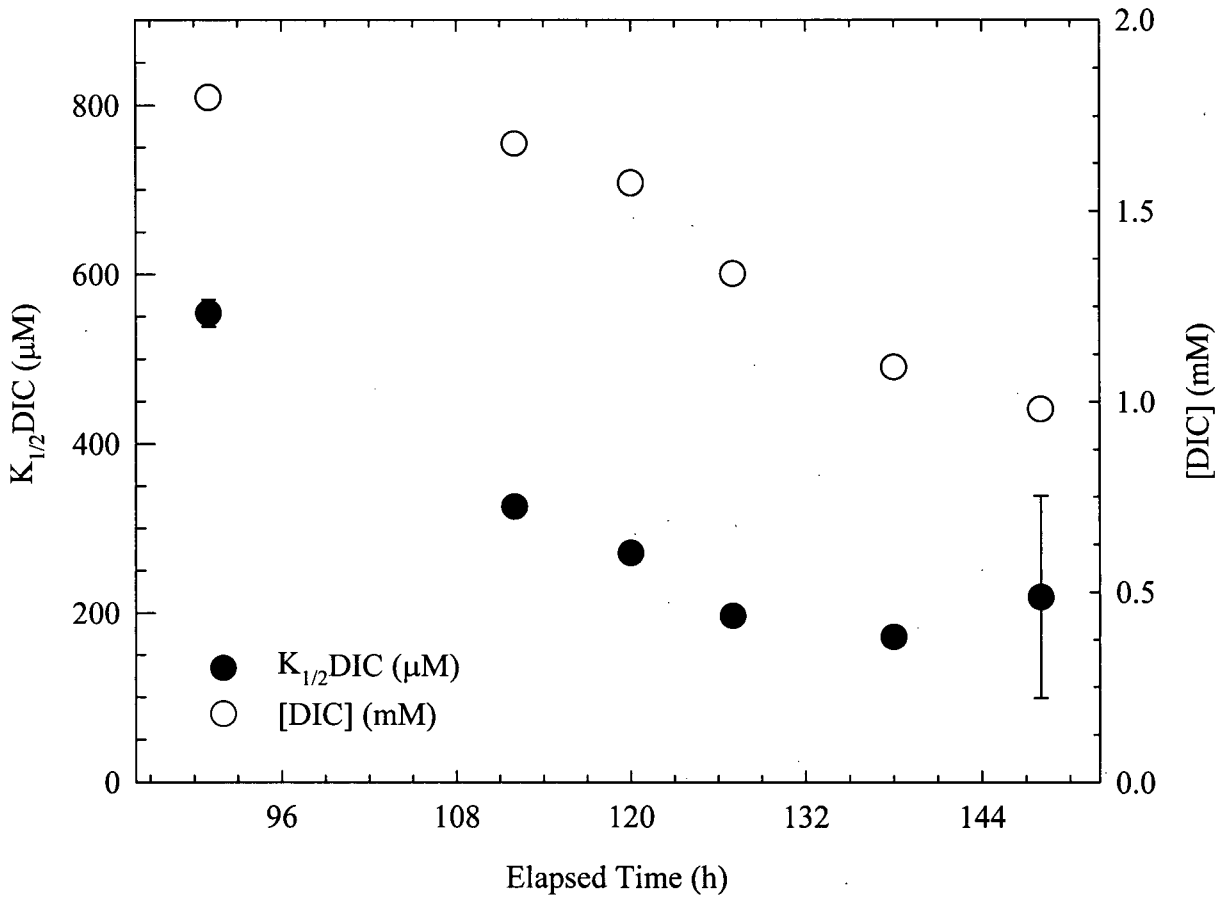

Figure 4.14. Changes in the DIC concentration and $K_{1/2}$DIC values for *Thalassiosira pseudonana* cells during the closed system drawdown (unbuffered medium) experiment. Error bars represent ± 1 standard deviation of DIC measurements (n=3) and ± 1 standard error of the regression through the raw data ($K_{1/2}$DIC). Where error bars are not visible they fall within the symbols.

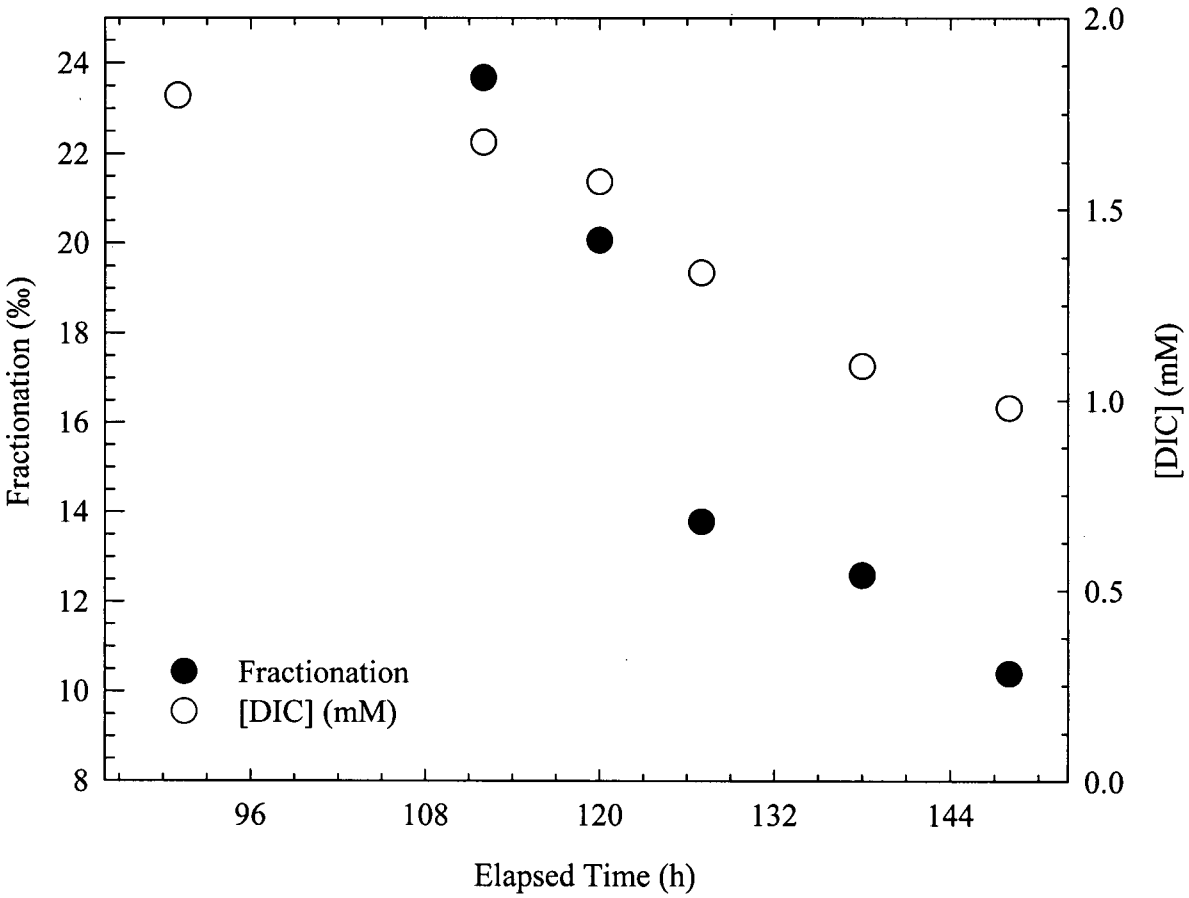

Figure 4.15. Changes in the DIC concentration and fractionation for *Thalassiosira pseudonana* cells during the closed system drawdown (unbuffered medium) experiment. Error bars represent ± 1 standard deviation of DIC measurements (n=3). Where error bars are not visible they fall within the symbols. Standard error was not calculated for fractionation values since only two points were used in the calculation. There is no datum point for fractionation at 88 h since fractionation was only calculated where at least 10% DIC depletion had occurred from the previous sampling time and this did not occur until ca. 116 h.

However, the CO_2 concentration decrease was similar for both experiments (Figures 4.7B and 4.13B).

Figure 4.16 provides further evidence that fractionation was not constant throughout the experiment. Just as in the buffered experiment, there was a significant linear relationship between [$\ln(R/R_o)$x1000] and [$-\ln(f)$] ($p<0.001$, slope = 13.52). The data drift below the 20‰ line, the initial fractionation value, indicating a decrease in fractionation as the experiment progressed. With CO_2 removal from unbuffered medium by N_2 gas stripping, fractionation remained constant at 11.45‰ (Figure 4.17) ($p<0.001$). There was no consistent drift of the data below the regression line.

In the steady state experiments, DIC and CO_2 concentrations were directly proportional since the pH of the culture medium was constant. When pH increases as a result of phytoplankton growth, CO_2 decreases faster than total DIC in a closed system. This adds an extra level of complexity to the interpretation of the drawdown experiments. Figures 4.18A and B present comparisons of the relationship between $K_{1/2}$DIC and either CO_2 or DIC concentration. In all but one case (unbuffered $K_{1/2}$DIC vs [DIC]), linear regressions were significant at the $\alpha=0.05$ level. In all cases, $K_{1/2}$DIC was better correlated with CO_2 than DIC. There were also significant linear relationships between fractionation and either CO_2 or DIC in all cases (Figures 4.19A and B). Fractionation was consistently better correlated with CO_2 than DIC.

The goal of these experiments was to establish a relationship between fractionation and $K_{1/2}$DIC and the results of the steady state experiment confirmed this relationship. There was no significant linear relationship between $K_{1/2}$DIC and fractionation data from the two drawdown experiments when the data were combined. However, a significant linear relationship ($p=0.05$) was observed for the results of the buffered experiment. The data from

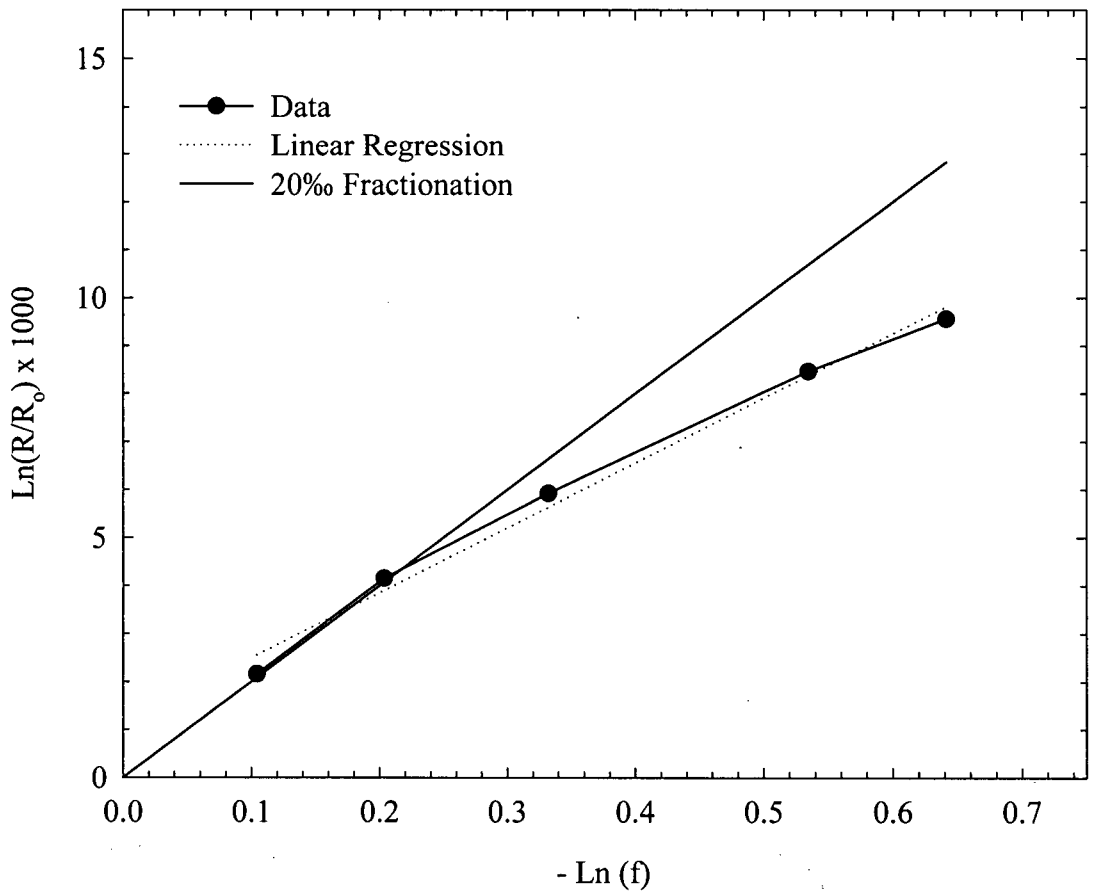

Figure 4.16. Isotope data from the drawdown experiment with unbuffered medium for *Thalassiosira pseudonana*. Data points represent individual measurements throughout the experiment. Error bars (not visible) represent ± 1 standard deviation of replicates (n=3). The linear regression through the data assumes that fractionation remained constant (no change in slope) during the experiment. The equation for the regression line is Y = 13.52 [-Ln(f)] + 1.146 (r^2 = 0.990, SE slope = 0.354). The 20‰ line assumes that fractionation remained constant at 20‰ throughout the experiment.

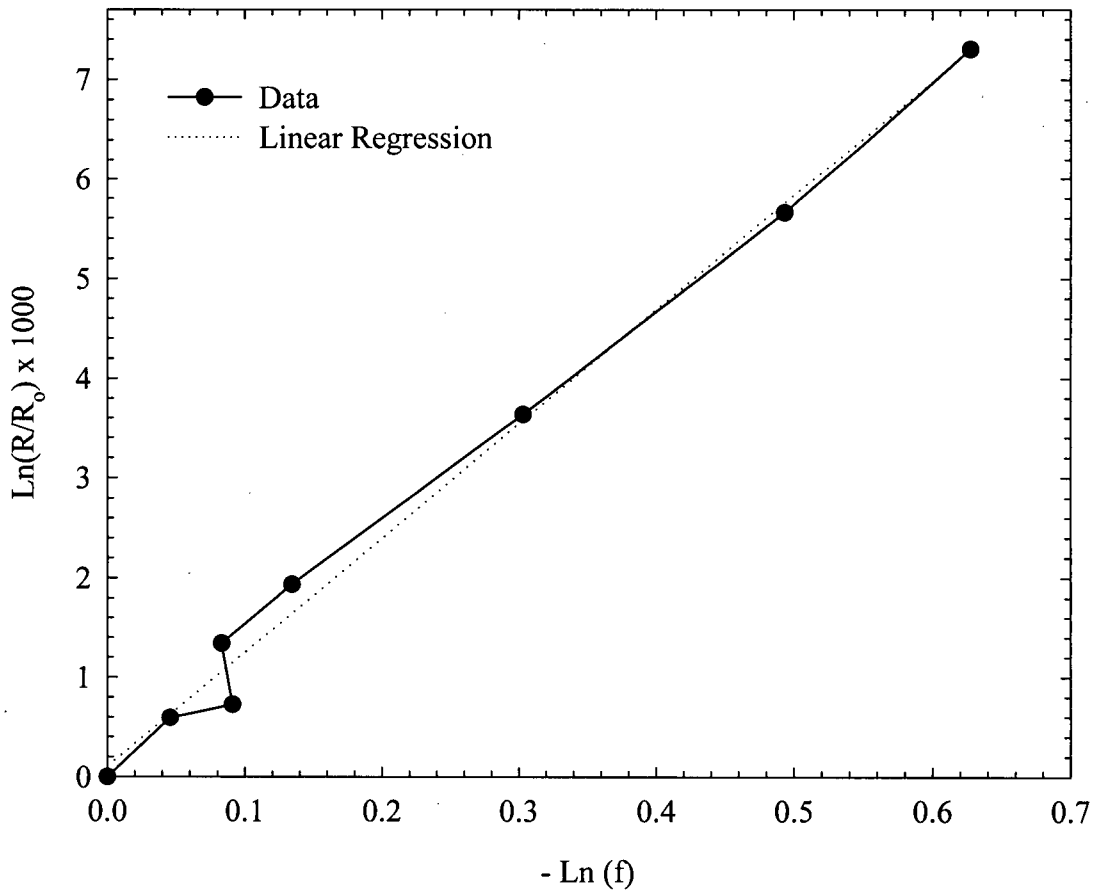

Figure 4.17. Isotope data from the drawdown experiment with unbuffered medium and no cells. Data points represent individual measurements throughout the experiment. Error bars (not visible) represent ± 1 standard deviation of replicates (n=3). The linear regression through the data assumes that fractionation remained constant (no change in slope) during the experiment. The equation for the regression line is Y = 11.46 [-Ln(f)] + 0.101 (r^2 = 0.992, SE slope = 0.249).

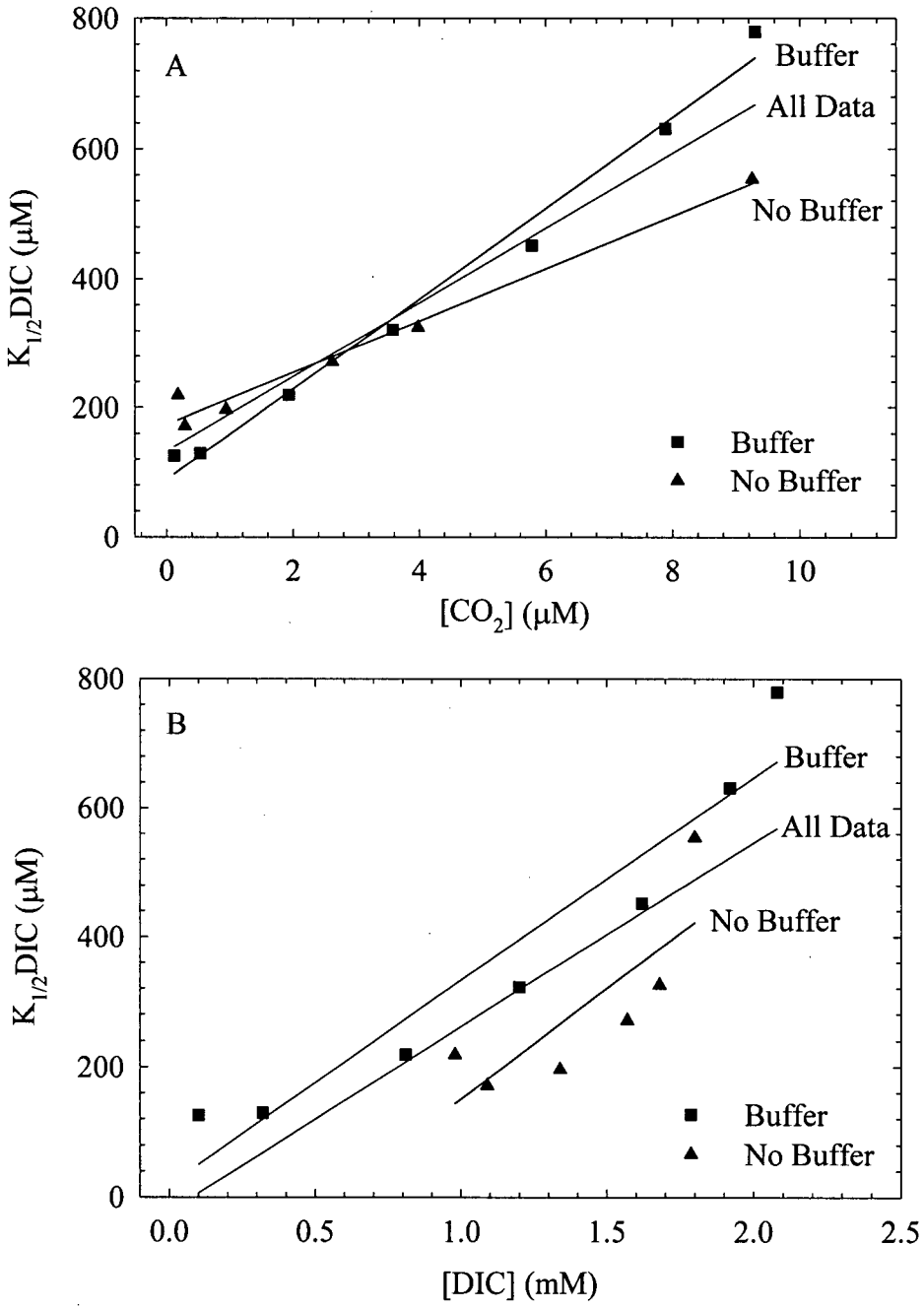

Figure 4.18. Linear regressions showing the relationships between $K_{1/2}$DIC values and carbon concentration for *Thalassiosira pseudonana* cells during the drawdown experiments. A) Relative to CO_2 concentration: All data, $r^2 = 0.928$, $y = 57.59X + 132.58$; Buffered experiment, $r^2 = 0.988$, $Y = 69.93X + 88.64$; Unbuffered experiment, $r^2 = 0.979$, $Y = 40.36X + 173.46$. A) Relative to DIC concentration: All data, $r^2 = 0.687$, $y = 283.93X - 22.52$; Buffered experiment, $r^2 = 0.918$, $Y = 313.83X + 18.75$; Unbuffered experiment, $r^2 = 0.633$, $Y = 339.96X - 189.77$.

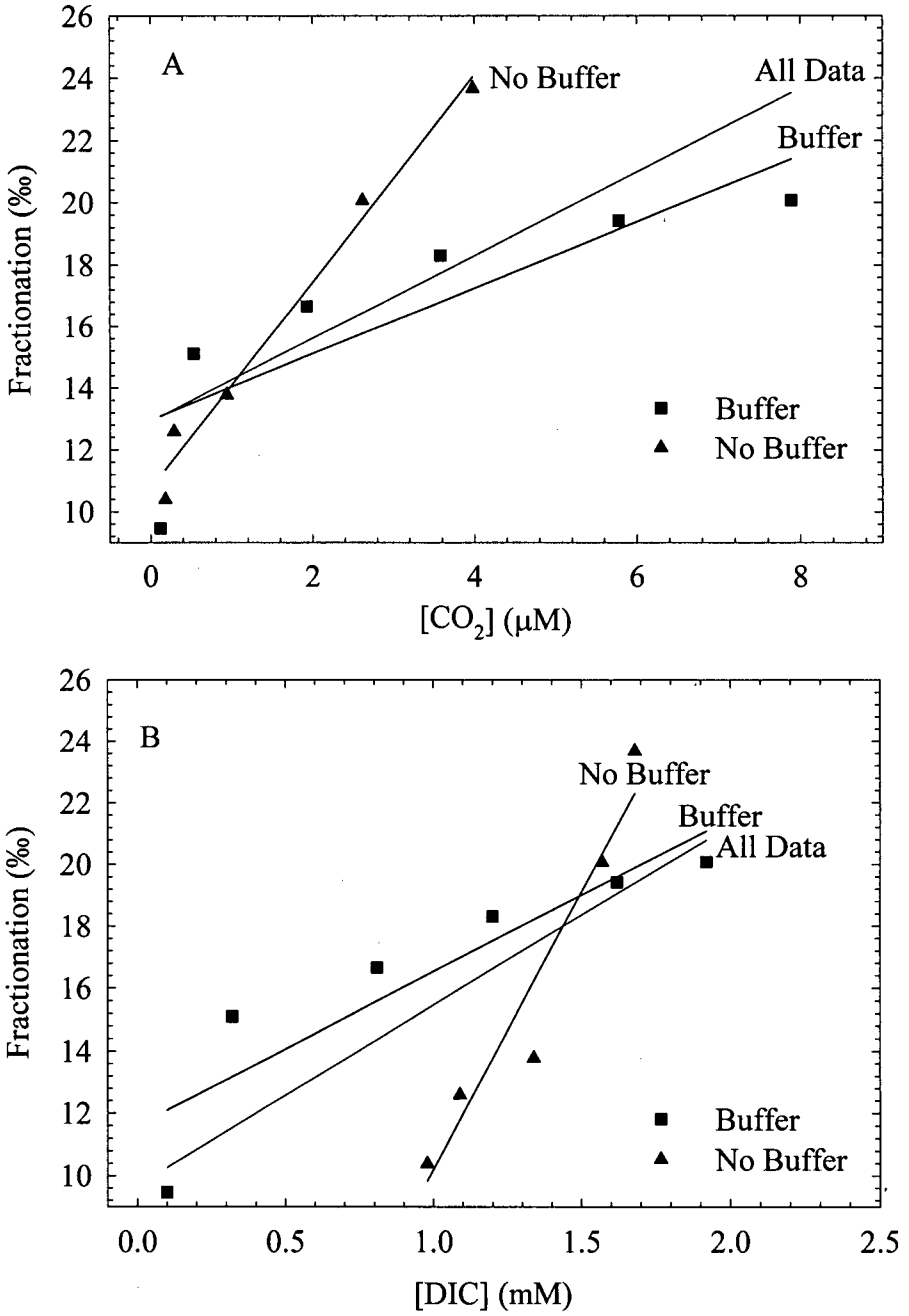

Figure 4.19. Linear regressions showing the relationships between fractionation and carbon concentration for *Thalassiosira pseudonana* cells during the drawdown experiments. A) Relative to CO_2 concentration: All data, $r^2 = 0.595$, $y = 1.34X + 12.92$; Buffered experiment, $r^2 = 0.705$, $Y = 1.07X + 12.97$; Unbuffered experiment, $r^2 = 0.983$, $Y = 3.34X + 10.75$. A) Relative to DIC concentration: All data, $r^2 = 0.542$, $y = 5.78X + 9.69$; Buffered experiment, $r^2 = 0.824$, $Y = 4.93X + 11.60$; Unbuffered experiment, $r^2 = 0.927$, $Y = 17.82X - 7.64$.

the unbuffered experiment falls below the steady state regression line with fractionation being less than expected for a given $K_{1/2}$DIC value (Figure 4.20). Two cautionary notes must be made here. First, the fractionation points were not discrete fractionation values, but rather averages of fractionation over short time periods. They essentially averaged the fractionation over a small range of DIC concentrations. Second, there might have been a delay in changes in fractionation in response to reduced DIC concentration. Third, the $K_{1/2}$DIC values of steady state cultures grown under high DIC and the unbuffered drawdown experiment were not as high as those in the buffered drawdown experiment. This is illustrated by the apparent "stretch" in the $K_{1/2}$DIC axis values in Figure 4.20 for the buffered experiment relative to those of the unbuffered experiment. However, despite these concerns, fractionation appears to be related to CCM induction as shown by the changes in $K_{1/2}$DIC values.

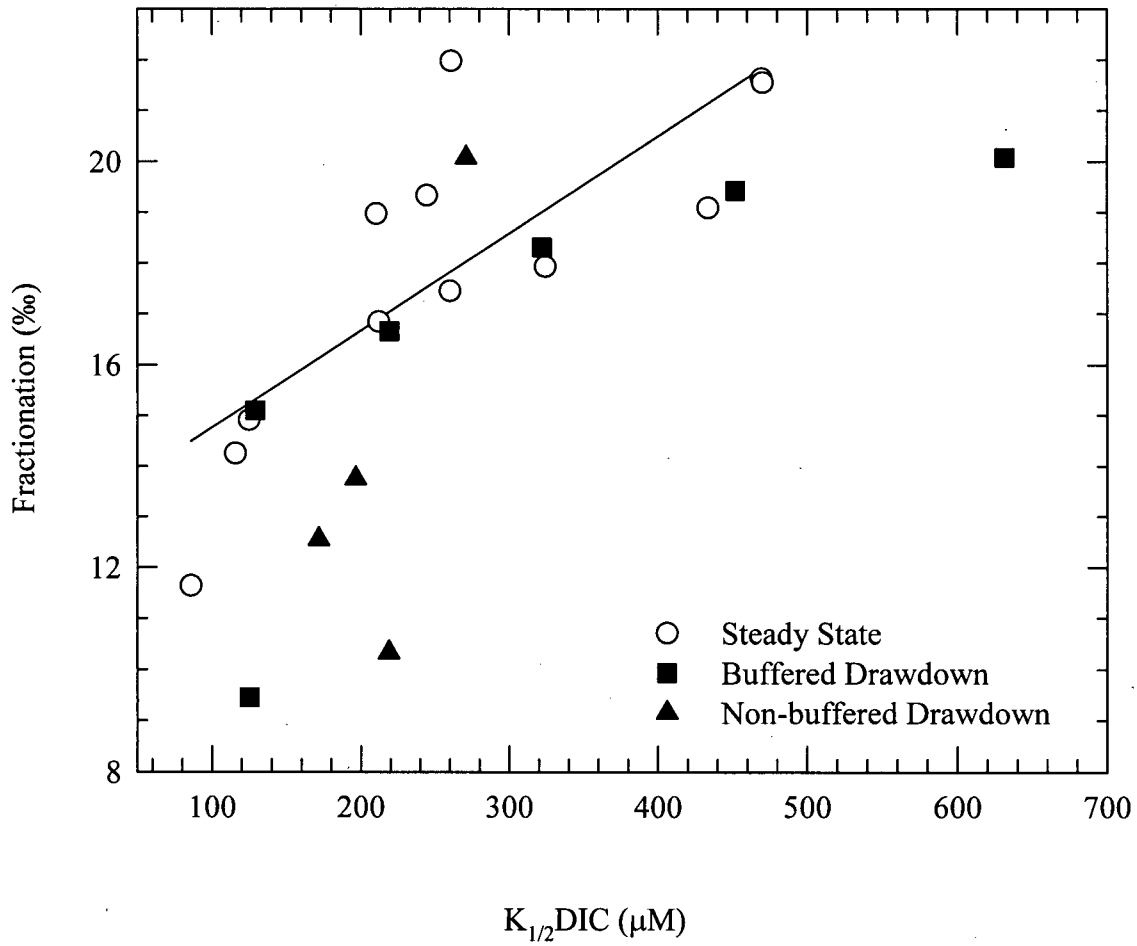

Figure 4.20. Relationship between fractionation and $K_{1/2}$DIC values for *Thalassiosira pseudonana* for both the steady state cultures and the drawdown experiments. The linear regression is for the steady state cultures and is the same as shown in Figure 4.5. The equation is: Fractionation = 0.019 ($K_{1/2}$DIC) + 12.85 (r_2 = 0.6448).

4.4 Discussion

4.4.1 Responses in $K_{1/2}$DIC Values to DIC and CO_2 Concentration

The most direct evidence for the existence of CCM activity in phytoplankton is a higher concentration of CO_2 inside the cells than in the external medium (Raven 1991a). However, the operation of a CCM is also indicated by a change in the affinity of cells for DIC often expressed by $K_{1/2}$DIC values. A $K_{1/2}$DIC value lower than the K_m of RuBisCO indicates enhanced affinity for carbon and suggests that active carbon uptake is occurring (Bloye *et al.* 1992, Raven 1993a, 1993b, Raven and Johnston 1991, Raven *et al.* 1993).

Many studies have demonstrated that phytoplankton grown under a low DIC concentration possess a higher affinity for carbon than those grown under high DIC conditions (See Badger *et al.* 1998 for a review). The results of the steady state experiments described in this chapter extend the evidence from Chapter 3 that CCM induction did occur in *Thalassiosira pseudonana* cultures at low DIC concentrations. Further, this species appears to possess the ability to gradually induce a CCM and maintain it in a state of partial induction (Figures 4.2 and 4.8). This is consistent with data from Mayo *et al.* (1986) where the freshwater cyanobacterium *Synechococcus leopoliensis* was able to maintain states of partial CCM induction. There are few examples of partial induction of a CCM under steady state conditions in the literature and this is the first study to attempt it in *Thalassiosira pseudonana*.

The most likely source of inorganic carbon taken up by phytoplankton is CO_2, given that this is the species fixed by RuBisCO (Raven *et al.* 1993). If this is true, then a reduction in the CO_2 concentration rather than DIC should be responsible for inducing the CCM as

measured by reductions in $K_{1/2}$DIC. Figure 4.3 shows that $K_{1/2}$DIC values were significantly correlated with DIC concentration; however, it is equally likely in this case that they were correlated with CO_2 concentration since, in the steady state experiments, CO_2 and total DIC concentrations were proportional. Although $K_{1/2}$DIC was linearly related to DIC, there should be an upper limit beyond which cells rely solely on diffusion, and thus $K_{1/2}$DIC would not change with further increases in DIC concentration.

However, this was not the case for the drawdown experiments since pH was changing while DIC and CO_2 concentrations were decreasing. As expected, the best indicator for $K_{1/2}$DIC values in the drawdown experiments was CO_2 concentration. This is because DIC was nearly completely consumed in the buffered experiment, but only 50% consumed in the unbuffered drawdown while the CO_2 concentration for both experiments decreased to ca. 0 μM (Figures 4.7 and 4.13). This evidence suggests that CCM induction is controlled by the availability of CO_2 and not total DIC. The complete induction process appears to be responding to depletion of CO_2 rather than DIC. Of course, this does not rule out the possibility that cells are using other forms of inorganic carbon, bicarbonate for example, via their concentrating mechanisms.

A poor relationship between $K_{1/2}$DIC values and both DIC and CO_2 was observed when both steady state and drawdown data were pooled (data not shown). This is not surprising since the photosynthetic physiology of the steady state cultures was static while that of the drawdown cultures was changing. The difficulty is that at a given sampling point, the CCM represents a gradual induction state in response to carbon concentrations higher than at that sample point. Thus, there is a lag between the induction of the CCM and the signal for induction, likely CO_2 concentration. Sharkey and Berry (1985) found that affinity for carbon began to increase within two hours following transfer from high to low CO_2

aeration in *Chlamydomonas reinhardtii*. *Thalassiosira pseudonana* did not change affinity for carbon within two hours during a gradual (20%) drawdown (Figure 2.5) but did change when transferred immediately from a high (2.08 mM) to a low (0.45 mM) DIC concentration (Figure 5.5B). Presumably, CO_2 limitation of photosynthesis results in the synthesis and translocation of carbonic anhydrase or transport proteins associated with CCM activity. Gradual induction of the CCM did occur throughout the drawdown experiments.

It is also possible that other factors such as cell size and shape influence the affinity of cells for external carbon sources. The effect of cell size and surface area to volume ratios on CO_2 supply to cells via diffusion has been considered by Riebesell *et al.* (1993b) though their influence on CCM induction in marine phytoplankton is unknown. Smaller cells relying on CO_2 diffusion would likely have higher affinities for carbon than larger ones given their smaller boundary layers. This is because carbon uptake would be less restricted by diffusion through the boundary layer and thus a smaller concentration gradient would be required to achieve a given rate of photosynthesis. However, the $K_{1/2}$DIC values for *Thalassiosira pseudonana*, and for the other species tested in Chapter 3, if converted to $K_{1/2}CO_2$, are much lower than reported values for the K_m of RuBisCO (Glover 1989, Read and Tabita 1994) (see Badger *et al.* 1998 for a review of various species). Even the highest $K_{1/2}$DIC values found in this study (ca. 800 μM DIC), when converted to $K_{1/2}CO_2$ of ca. 5.8 μM, are much lower than that of RuBisCO. In addition, no changes in cell size were noted in this study (data not shown). It is therefore likely that changes in the $K_{1/2}$DIC represent changes in the induction state of the CCM (Mayo *et al.* 1986, 1989, Raven *et al.* 1993).

4.4.2 Responses in Fractionation to DIC and CO_2 Concentration

The relationship between carbon concentration, most often expressed in terms of CO_2, and fractionation in natural populations has been well studied (Degens *et al.* 1968b, McCabe 1985, Pardue *et al.* 1976, Rau *et al.* 1989, 1992, Sackett 1991). Before any correlation is used to hindcast ancient pCO_2 values from marine sediments, some cautionary notes must be made. Goericke and Fry (1994) suggest that for a relationship between phytoplankton $\delta^{13}C$ (and hence fractionation) and CO_2 concentration to be useful, concentrations of CO_2 in the atmosphere and the surface ocean must be in equilibrium. They also suggest that phytoplankton fractionation must be shown to covary primarily with CO_2 concentrations, a condition they claim is not supported by the literature to date. It has become obvious that numerous factors influence carbon isotope fractionation by marine phytoplankton. Nevertheless, CO_2 concentration does have a strong effect on carbon isotope fractionation.

Laboratory studies have provided mixed evidence for the influence of carbon concentrations on fractionation. Burkhardt *et al.* (1999) showed that there was only a 3‰ difference in fractionation over a range of CO_2 concentrations of 3 to 26 μmol kg^{-1} in both *Skeletonema costatum* and *Thalassiosira weissflogii*. However, they held total DIC constant and thus pH differed by close to one full unit. In addition, they only tested two CO_2 concentrations. Thompson and Calvert (1994) found that there was no strong dependence of fractionation by *Thalassiosira pseudonana* upon the natural range of CO_2 concentrations. However, they allowed pH to change in concert with CO_2 during their experiments and unfortunately this complicates the interpretation of their data.

Hinga *et al.* (1994) found that fractionation increased with increasing CO_2 concentration in both *Skeletonema costatum* and *Emiliania huxleyi*. Korb *et al.* (1998) found a significant negative correlation between POC $\delta^{13}C$ and CO_2 concentration in both *Chaetoceros calcitrans* and *Ditylum brightwellii*, though they did not directly measure $\delta^{13}C$ of the source DIC, and in addition, pH fluctuated throughout their experiment. Fry (1996) summarized the data for *Skeletonema costatum* from several studies and demonstrated a dependence of fractionation upon DIC concentration rather than CO_2, which contradicts the results from this study.

Experiments carried out by Laws *et al.* (1995, 1997) examined the relationship between fractionation and $\mu/[CO_2]$, the latter essentially representing a function of supply (CO_2 concentration) and demand (growth rate). They found a significant linear relationship between μ/CO_2 and fractionation only at CO_2 concentrations above 10 $\mu mol\ kg^{-1}$ and attributed the deviation from linearity below this concentration to the presence of active CO_2 uptake. If one plots ε_p against either CO_2 or DIC concentration (Figure 4.21) from the raw data of Laws *et al.* (1997), a significant linear relationship ($p<0.001$) exists. This suggests that, especially for DIC, lower concentrations result in reduced fractionation. However, pH was not held constant during these experiments, and nitrogen-limited chemostats were used. Beardall *et al.* (1982) found that CCM activity could be induced by nitrogen limitation and that this caused reduced carbon isotope fractionation in *Chlorella emersonii*. The potential induction of a CCM observed by Laws *et al.* (1995, 1997) adds an extra level of complexity to the interpretation of their data.

The results of this thesis support the claim that fractionation does depend strongly on carbon concentration. There was a strong linear relationship between fractionation and DIC

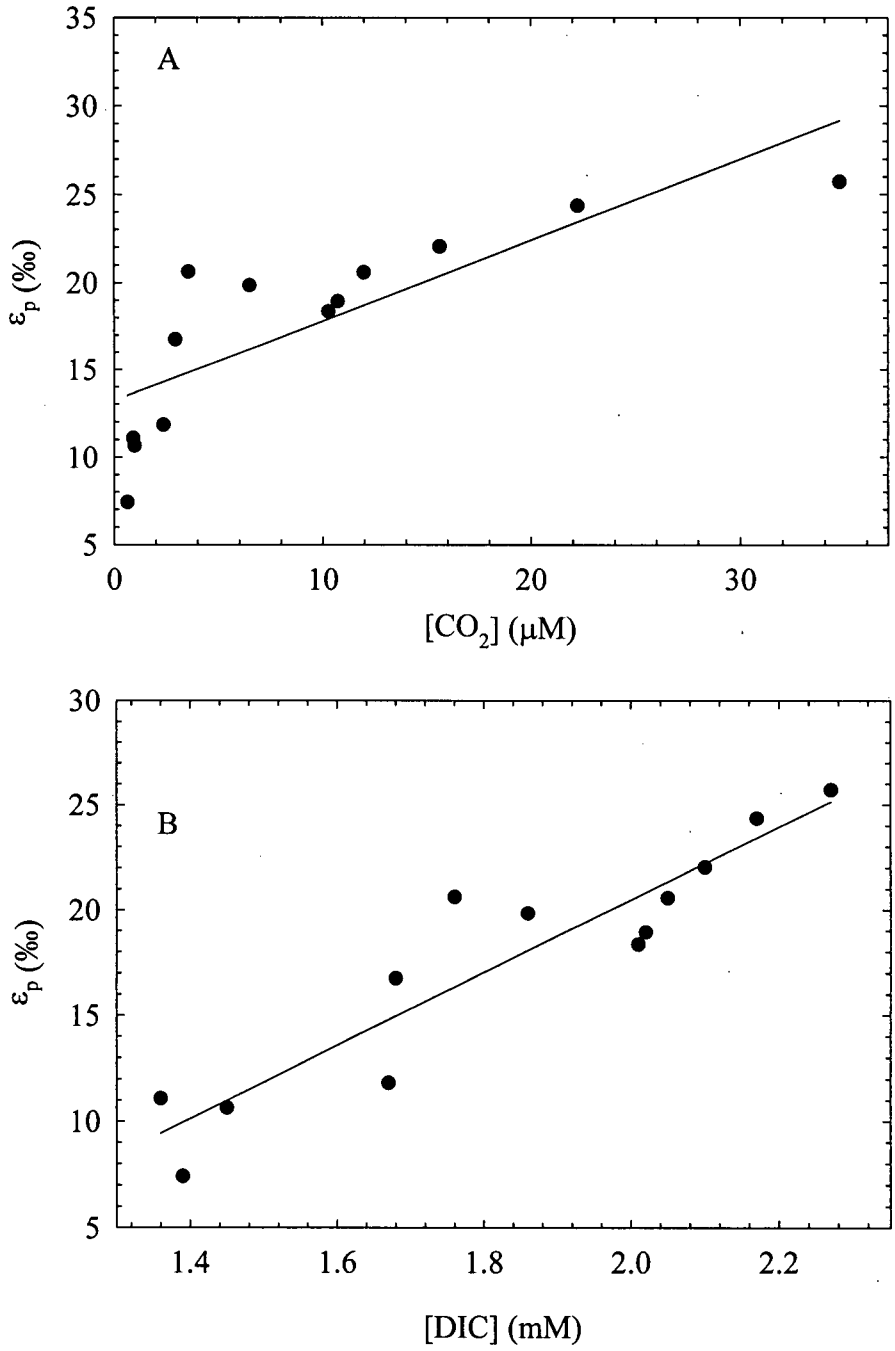

Figure 4.21. Linear regressions showing the relationships between ε_p and either CO_2 (A), or DIC concentration (B) using the raw data for *Phaeodactylum tricornutum* taken from Laws *et al.* (1997). The equations are: CO_2, $\varepsilon_p = 0.46\ [CO_2] + 13.19$, $r^2 = 0.662$; DIC, $\varepsilon_p = 17.27\ [DIC] - 14.05$, $r^2 = 0.861$.

in the steady state cultures. Again, there would be an equally strong relationship between fractionation and CO_2 concentration since, at a constant pH, the CO_2 concentration is proportional to total DIC concentration.

Fractionation also decreased throughout the drawdown experiments (with cells) as expected. The decrease in fractionation appeared to follow the reduction of CO_2 rather than DIC; minimum fractionation was observed after nearly complete DIC consumption in the buffered experiment, but only after 50% depletion in the unbuffered drawdown, although both had near zero levels of CO_2. This is demonstrated in Figure 4.19 A and B where a better correlation was found between fractionation and CO_2 concentration than between fractionation and DIC concentration. The unbuffered culture was only able to remove half the total DIC presumably because the increase in pH either prevented further removal of the DIC predominantly in the form of carbonate at that pH, or because a high pH was detrimental to the physiology of the cells.

When data from both the steady state and the two drawdown experiments were pooled, there was no significant correlation between fractionation and either CO_2 or DIC concentration. This is easily explained when one considers the difference between the two types of experiments. There are two important factors to consider when fractionation is determined throughout the drawdown experiments. First, the measurement of fractionation is based upon changes between two sampling times and is not an instantaneous measurement. Furthermore, even if instantaneous measurement had been possible, changes in CCM induction and the resulting effects on fractionation would likely lag behind the actual change in carbon concentrations. There is no method to overcome this problem in drawdown experiments. However, such experiments are useful to demonstrate that affinity for carbon and fractionation change throughout the time course of a drawdown experiment. They

further emphasize the importance of monitoring and reporting the carbon conditions in laboratory cultures (Fry 1996).

Fractionation values ranged from 9 to 24‰ (relative to DIC) throughout this chapter. As with the $K_{1/2}$DIC values, fractionation should level off at some point beyond which further increases in DIC concentration should not result in higher fractionation. The upper limit was considerably lower than the maximum value of ca. 39‰ expected if a RuBisCO fractionation of 29‰ was fully expressed. This is consistent with other laboratory experiments where fractionation values are frequently lower than those observed in nature (Fry 1996). Low culture biomass was maintained throughout the steady state experiments. Thus, these results are surprising in that high culture biomass has been suggested to lower experimental maximum fractionation values. One possible explanation is that *T. pseudonana* may possess an alternative form of RuBisCO which exhibits a different fractionation (see Guy *et al.* 1993). Alternatively, it is possible that higher fractionation would have been observed if a higher DIC concentration was used. Further work on RuBisCO isolated from this species would shed some light on the maximum fractionation one could expect.

The drawdown experiments without cells represent the equilibrium isotope effect observed between the DIC and CO_2 removed. One would expect a fractionation of ca. 11‰ (Mook *et al.* 1974). The unbuffered drawdown came close to this value (Figure 4.12) while the buffered one was 13.41‰ (Figure 4.17). There was no apparent explanation for this discrepancy. Nevertheless, fractionation was constant throughout the drawdown and lower than that observed when cells were responsible for CO_2 removal.

4.4.3 Relationship Between $K_{1/2}$DIC Values and Fractionation

The suggestion that DIC concentration can have a strong influence on carbon isotope fractionation is not novel although laboratory results are equivocal. However, establishing a relationship between CCM induction and carbon isotope fractionation has been difficult. Beardall *et al.* (1982) found that upon induction of a CCM caused either by carbon or nitrogen limitation, carbon isotope fractionation decreased in the green alga *Chlorella emersonii*. In other words, CCM induction caused by means other than carbon limitation still resulted in decreased fractionation. Thus, even though carbon was not limiting, CCM induction and a decrease in carbon isotope fractionation occurred simultaneously. Though the range in fractionation was close to 20‰, fractionation was measured only in cultures acclimated to either 0.03 or 5% CO_2, the latter being artificially high. Nevertheless, the results from Beardall *et al.* (1982) suggest a potential link between CCM induction and fractionation. However, their study lacked a comprehensive test of the interrelationship between DIC concentration, CCM induction, and fractionation.

The study providing the best evidence for the relationship between carbon affinity and isotope fractionation is that of Sharkey and Berry (1985). By measuring cell affinity for carbon and fractionation simultaneously during a time course study, they were able to demonstrate an apparent link between the two variables. Indeed, their study inspired the experiments described in this thesis. However, they used cells acclimated to an unnaturally high CO_2 concentration (5%) prior to the low CO_2 transfer. A study by Erez *et al.* (1998) for the freshwater cyanobacteria *Synechococcus* also supports the hypothesis that CCM induction results in reduced fractionation. No previous study has sought to measure the induction state of the CCM concurrently with fractionation in marine phytoplankton over a

range of DIC concentrations. The two types of experiments described in this chapter attempted to do just that. While the experimental designs of the steady state and drawdown experiments differed substantially, both experiments provide a different way to establish a relationship between fractionation and CCM induction.

In both cases, induction of the CCM was monitored by changes in the $K_{1/2}$DIC values, and fractionation appeared to change in parallel. The results of the steady state cultures perhaps best illustrate the relationship. The comparison is somewhat less clear for the drawdown experiments. However, the time lag effects of CCM induction and fractionation could be responsible for some of the scatter. Further, the fractionation measure incorporates significant delay since it is based on two points during the time course of the drawdown and is not an instantaneous measurement. Nevertheless, it appears that higher fractionation is associated with cells which have higher $K_{1/2}$DIC values and hence have less CCM activity. These results are in entire agreement with those of Sharkey and Berry (1985) and Erez *et al.* (1998).

When interpreting the link between CO_2 concentration and fractionation, it is tempting to suggest that diffusion models can explain the relationship. This would ignore the strong evidence presented in this chapter that fractionation decreases as CCM activity increases. One can envision CCM induction as a gradual switch from an open system relying on diffusion of CO_2 across the plasmalemma to a semi-closed system where carbon is actively moved across the plasmalemma and its diffusion back out of the cell is restricted. Because of the low fractionation associated with the active uptake (Berry 1989, Raven and Lucas 1985), RuBisCO discrimination is essentially masked. To deny the importance of CCMs in nature ignores the evidence that CCM induction occurs over a range of CO_2 concentrations that have been observed under natural conditions. Further, it ignores the fact

that RuBisCO does not operate at maximum capacity under natural concentrations of CO_2 found in the surface waters of modern oceans. Given the apparent ubiquity of CCM capacity in marine phytoplankton, the results presented in this chapter support the hypothesis that CCM induction influences fractionation in marine phytoplankton.

Chapter 5

Mechanisms and Models of Carbon Isotope Fractionation

5.1 Introduction

The data presented in the previous chapters indicate that CCM induction in response to low DIC (CO_2) concentrations is accompanied by reduced fractionation in *Thalassiosira pseudonana*. However, as already indicated, diffusion models of fractionation also predict reduced fractionation as the CO_2 supply to the cell becomes limiting (Rau *et al.* 1996). Thus, the fractionation data presented so far are consistent with either CO_2 diffusion limitation or CCM induction.

Models of fractionation based on CO_2 diffusion depend on the CO_2 supply rate through the boundary layer of phytoplankton cells relative to the carbon demand by the cell. The latter is often calculated as the product of the growth rate and the cell carbon quota. For instance, Laws *et al.* (1995, 1997) used the ratio of the growth rate to the external CO_2 concentration to represent the demand-supply function. They concluded that deviation from a linear relationship between this parameter and fractionation was the result of active carbon uptake. According to the authors, this model only works when cells are relying on diffusion or active uptake of CO_2 to supply photosynthetic demand. The model presented by Rau *et al.* (1996) is based on the idea that diffusion through the boundary layer of a phytoplankton cell can be the limiting step ultimately resulting in decreased growth rates (Riebesell *et al.* 1993b). However, it is obvious that inducible CCMs can alleviate the potential CO_2 limitation of growth while photosynthetic rates remain limited (see Raven *et al.* 1993).

The fractionation values of cells using active uptake will ultimately be determined by the relative rates of three processes: the rate of carbon uptake (F_1), the rate of carbon fixation (F_2) and the rate of leakage out of the cell (F_3). This simplified model is presented in Figure 3.9. Carbon can be transported either as bicarbonate or CO_2. The form is important since CO_2 is isotopically lighter than bicarbonate by about 10‰ (Mook *et al.* 1974). If CO_2 is produced enzymatically by CA just external to the plasmalemma, the isotopic signature of the resulting CO_2 will be the same as the existing CO_2. This would make it impossible to distinguish between direct transport of CO_2 and external CA-mediated conversion of bicarbonate to CO_2 followed by CO_2 diffusion across the plasmalemma.

Fractionation during active uptake is thought to be zero (Berry 1989, Kerby and Raven 1985). Assuming no leakage, the minimum fractionation expressed by cells would be zero relative to the external source being transported. This occurs because as RuBisCO discriminates against ^{13}C, the latter builds up in the internal pool until it offsets the discrimination of RuBisCO. However, as the leakage rate increases relative to F_1, higher fractionation will be expressed since the unfixed ^{13}C remaining can leak out. The higher the leakage rate, the less ^{13}C is allowed to build up. Presumably, as F_3 approaches F_1, full discrimination of RuBisCO can be expressed.

While the previous chapters did not attempt to determine the nature of the carbon concentrating mechanism, results from this chapter attempt to shed some light on the potential mechanism that operates under low DIC concentrations in *Thalassiosira pseudonana*. The importance placed on growth rates for models of fractionation based on diffusion necessitates an experiment where the effect of growth rate changes on both fractionation and CCM induction is investigated. One way to reduce growth rates is through changes in temperature.

The trend toward heavier $\delta^{13}C$ values of marine particulate organic carbon (POC) (decreased fractionation) at lower latitudes could be caused by reduced CO_2 concentrations resulting from decreased solubility of the gas at higher temperatures. However, the lack of symmetry in the relationship between the northern and southern hemispheres (Goericke and Fry 1994) suggests that the relationship is more complicated. Temperature has a number of direct effects on phytoplankton and the medium in which they grow. Metabolic activity increases at higher temperatures (Beardall *et al.* 1998). This would in turn lead to higher growth rates and thus greater carbon demand. Higher temperatures also cause a shift in the inorganic carbon system from CO_2 to carbonate (Beardall *et al.* 1998) and reduced affinity of RuBisCO for CO_2 (Davison 1987, Descolas-Gros and De Billy 1987).

The combination of temperature effects has led to speculation that the need for CCMs is reduced at low temperatures (Raven 1991b). Assuming that CCM induction in marine phytoplankton results in reduced fractionation, this conclusion is consistent with the observed latitudinal trend in fractionation. However, other factors need to be considered. Oxygen concentration increases as temperature decreases. The competitive effect of oxygen on RuBisCO carboxylation might still necessitate CCM activity at low temperatures. The rate of CO_2 diffusion is lower at lower temperatures (Beardall *et al.* 1998) as is the rate of CO_2 formation from bicarbonate (Raven and Geider 1988).

The problem with interpreting the latitudinal trend on fractionation is that both CO_2 concentration and temperature are changing. In this study, the effect of temperature changes on isotope fractionation was investigated independently of CO_2 concentration effects. This was accomplished by adjusting the pCO_2 level such that medium CO_2 concentration remained constant.

Another way to examine the mechanism that controls fractionation is to acclimate cells to a given DIC concentration and then transfer them to another concentration. If CCM induction and the accompanying reduction in leakage rates (as proposed by Sharkey and Berry 1985) leads to reduced fractionation, then cells transferred from a low DIC concentration to a high one should continue to show reduced fractionation. This hypothesis assumes that CO_2 does not enter via diffusion. If this were the case, then higher fractionation might still occur because cells would be flooded with CO_2 from both the active uptake mechanism and also from diffusion and this CO_2 could also diffuse back out of the cell.

High DIC cells exhibiting large fractionation would be expected to exhibit a low fractionation when transferred to a low DIC concentration since they likely rely on CO_2 diffusion. This assumes that high DIC concentrations suppress active uptake and the induction process is slow. To test these hypotheses, cultures were transferred from a low DIC concentration to a high one and vice versa.

A photosynthetic rate that exceeds the rate of uncatalyzed CO_2 production from bicarbonate is an indication that cells are using active uptake (Raven 1991a). To test if this was the case in my cultures, measured rates of oxygen production in response to external DIC concentration were compared to rates of CO_2 production from bicarbonate (Johnson 1982) for the steady state cultures from Chapter 4. Photosynthetic rates exceeding the rate of CO_2 production would imply that phytoplankton are capable of using bicarbonate as a carbon source.

Finally, the data generated from the steady state experiments of Chapter 4 along with those of the temperature study from this chapter were applied to various models of carbon isotope fractionation. These include the models presented by Raven *et al.* (1993), Hinga *et al.* (1994), Rau *et al.* (1996), Laws *et al.* (1997), Sharkey and Berry (1985) and Keller and

Morel (1999, unpublished). Data from the two drawdown experiments were not used since the fractionation values were not instantaneous measurements and both the fractionation and $K_{1/2}$DIC values as measured incorporate a delayed response. It is difficult to match a given DIC (CO_2) concentration to a given value of fractionation or CCM induction state for this type of experiment. The overall objective of this chapter was to investigate possible mechanisms that control carbon isotope fractionation in the marine diatom *Thalassiosira pseudonana*.

5.2 Methods

5.2.1 Experiments

In all cases, the species used was *Thalassiosira pseudonana* (Clone 3H, NEPCC # 58, Northeast Pacific Culture Collection, University of British Columbia). The experimental design of the temperature response study was similar to that described in Chapter 3 except that cultures were grown at temperatures of 10, 14, 18, and 22°C. The short-term depletion experiments and photosynthetic kinetics were performed at the same temperature to which the cells were acclimated. A concentration of 35 $\mu g\ mL^{-1}$ carbonic anhydrase (Bovine Erythrocyte EC 4.2.1.1, Sigma Chemical Company, St Louis, USA) was added to the depletion medium to ensure that isotopic equilibrium was achieved throughout the depletion experiments.

For the transfer experiments, two separate depletions were performed. In the first experiment, cultures were grown at a specific ambient DIC concentration and the subsequent depletion was carried out at the same DIC concentration. The culture was then re-diluted and grown under identical conditions. Following at least six generations of logarithmic growth, a second depletion was carried out at a different DIC concentration. If cultures had been acclimated to a low DIC concentration, the second depletion experiment was carried out at a high DIC level. Similarly, high DIC acclimated cultures were transferred to a low DIC concentration. The transfer experiments were prepared by transferring the filtered cells to fresh medium of the desired DIC concentration and the depletion was carried out as described in the general methods. A CA concentration of 35 $\mu g\ mL^{-1}$ was added to the depletion medium for the same reason as indicated above. The photosynthetic kinetics of the cells were determined using the same method as was used for the steady state experiments.

No CA was added to the cuvette during the photosynthetic kinetic experiments. Thus, with the possible exception of extracellular CA produced by the cells, CO_2 production from bicarbonate in the medium was uncatalyzed. This was also true of the steady state culture photosynthetic kinetic experiments used to determine the potential use of bicarbonate.

5.2.2 Modeling

Experimental data for the modeling came from Chapter 3 (*Thalassiosira pseudonana* only) and the steady state cultures of Chapter 4 (referred to as "steady state data set"). In some cases, data from the entire thesis (excluding drawdown experiments from chapter 4) as well as that from Lee (1998) were used (referred to as "complete data set"). Fractionation values and growth rates were calculated as described in Chapter 4. DIC concentration was measured as described in the general methods and CO_2 concentration was calculated from these DIC concentrations assuming a constant pH of 8.2, a value confirmed by determination throughout all experiments. Temperature was measured from the water bath in which the cultures were grown. A cell carbon quota of 6 pg $cell^{-1}$ for *Thalassiosira pseudonana* was taken from Montagnes *et al.* (1994). A summary of relevant experimental results and values is included in Appendix B.

The Rau *et al.* (1996) model is based on a spherical cell. When this was not the case, the authors recommended using the surface area equivalent cell radius assuming sphericity. This involves determining the surface area of the species in question and calculating the radius of a spherical cell that would have a similar surface area. *Thalassiosira pseudonana* cells are shaped like a flattened cylinder having a diameter of 4.5 μm and a length of 3.5 μm (NEPCC data). The surface area of a *T. pseudonana* cell was calculated using Equation 13.

This surface area was then used to calculate the appropriate spherical cell radius using Equation 14. Surface area was also used for the models of active uptake.

$$SA = (2 \times \pi \times R \times L) + (2 \times \pi \times R^2) \quad (13)$$

$$R = \sqrt{\frac{SA}{4 \times \pi}} \quad (14)$$

Where

SA = surface area (μm^2)

π = constant (3.141592654)

R = radius (μm)

L = length (μm)

5.3 Results

5.3.1 Temperature Response Study

The major influence of temperature on phytoplankton physiology is its effect on growth rate. Cultures of *Thalassiosira pseudonana* were grown at four different temperatures ranging from 14 to 22°C. Growth rates decreased as temperature decreased as expected (Figure 5.1), resulting in a Q_{10} of ca. 3.06. Growth rate determination at low temperatures was more reliable since the cultures were not diluted as frequently. This allowed for longer periods of undisturbed growth and more sample points. The DIC concentrations used were 0.5 mM (Low) and 2.00 mM (High). The difference between growth rates at the two DIC concentrations was not significant (t-test, α=0.05).

The relationship between $K_{1/2}$DIC and temperature was more complicated (Figure 5.2). With the exception of the 22°C culture, $K_{1/2}$DIC decreased with increasing temperatures in the low DIC cultures. The $K_{1/2}$DIC for the high DIC cultures fell into two groups: high DIC cells grown at higher (18 and 22°C) temperatures had lower $K_{1/2}$DIC values than those grown at lower temperatures. As expected, fractionation decreased for both high and low DIC cells as temperature increased (Figure 5.3).

The results of Chapter 4 indicate the existence of a relationship between fractionation and $K_{1/2}$DIC. To further test this hypothesis, fractionation values were plotted against $K_{1/2}$DIC values for the cultures grown at different temperatures (Figure 5.4). There was a significant linear relationship between fractionation and $K_{1/2}$DIC. Though the trend was similar to the steady state experiments described in Chapter 4, the relationship differed quantitatively.

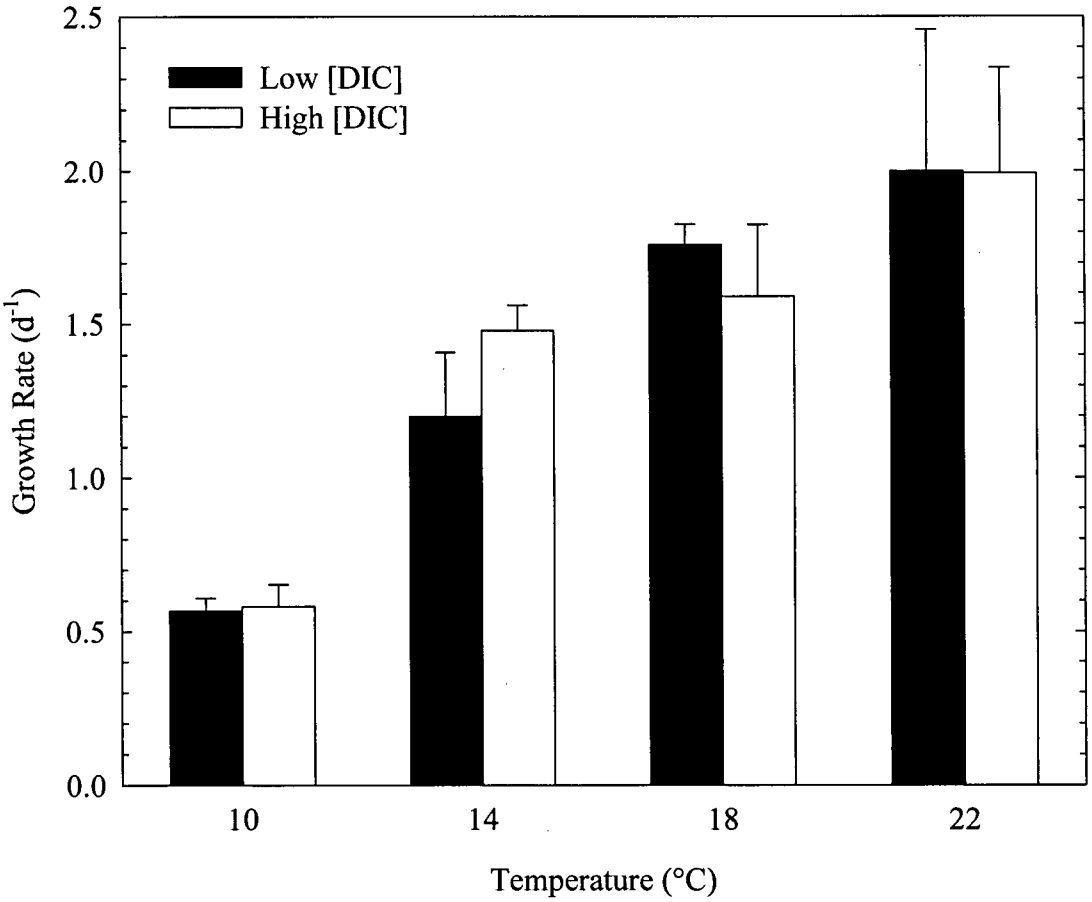

Figure 5.1. Growth rates of *Thalassiosira pseudonana* cultures grown at different temperatures and at either low (0.5 mM) or high (2.0 mM) DIC concentrations. Error bars represent ± 1 standard deviation for at least four growth rate calculations.

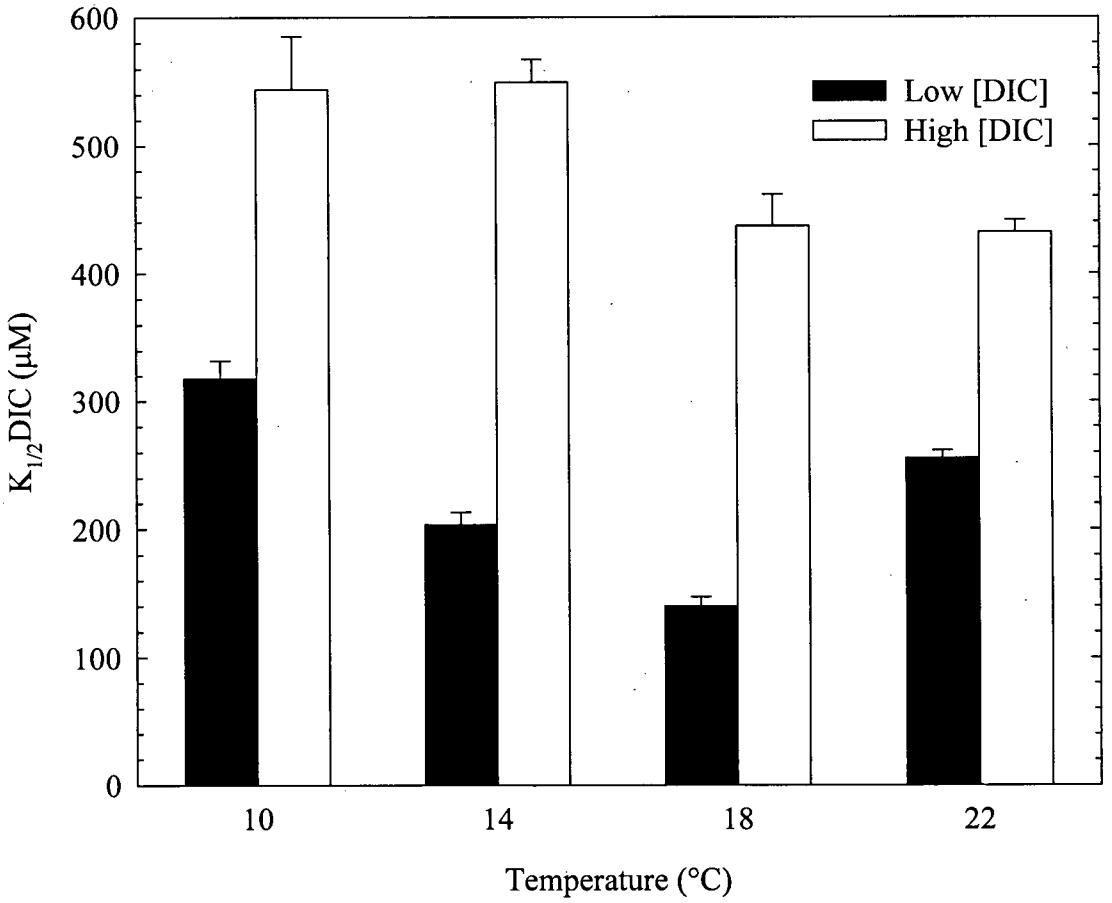

Figure 5.2. $K_{1/2}$DIC values for *Thalassiosira pseudonana* cultures grown at different temperatures and at either low (0.5 mM) or high (2.0 mM) DIC concentrations. Error bars represent ± 1 standard error of the regression through the raw data.

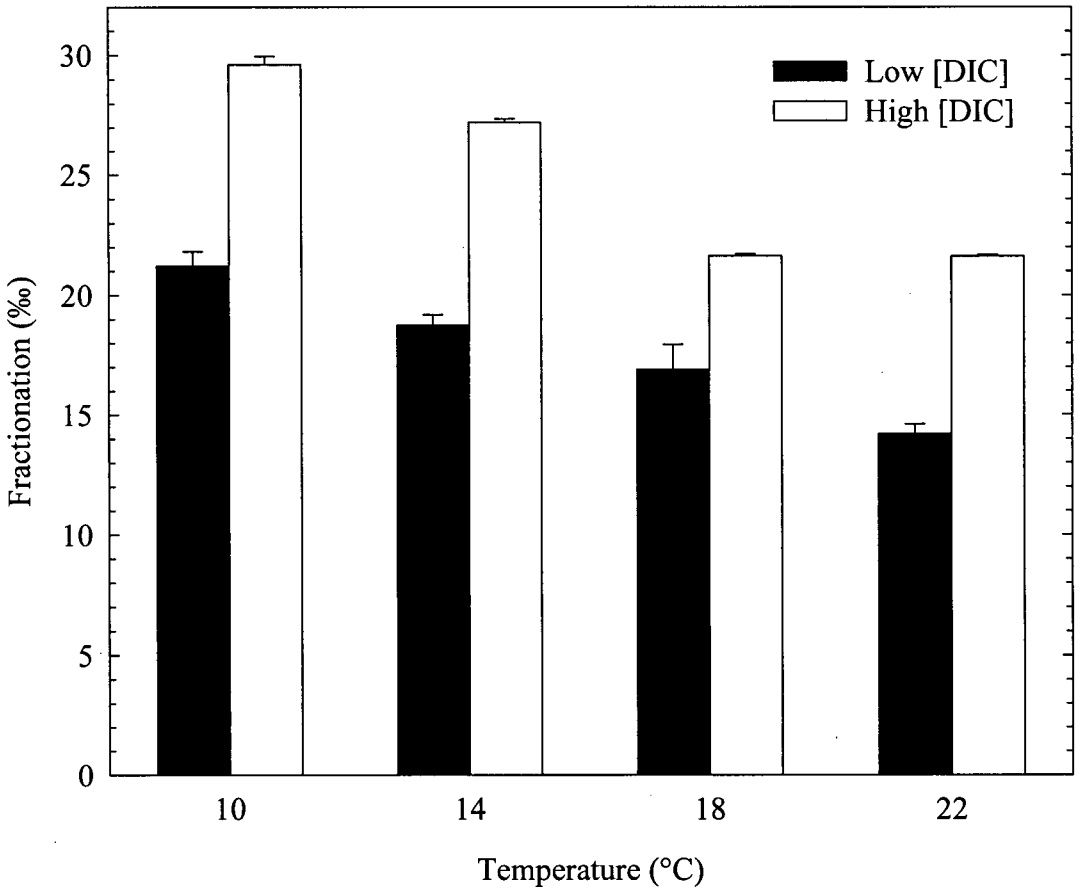

Figure 5.3. Fractionation by *Thalassiosira pseudonana* cultures grown at different temperatures and at either low (0.5 mM) or high (2.0mM) DIC concentrations. Error bars represent ± 1 standard error of the regression through the raw data.

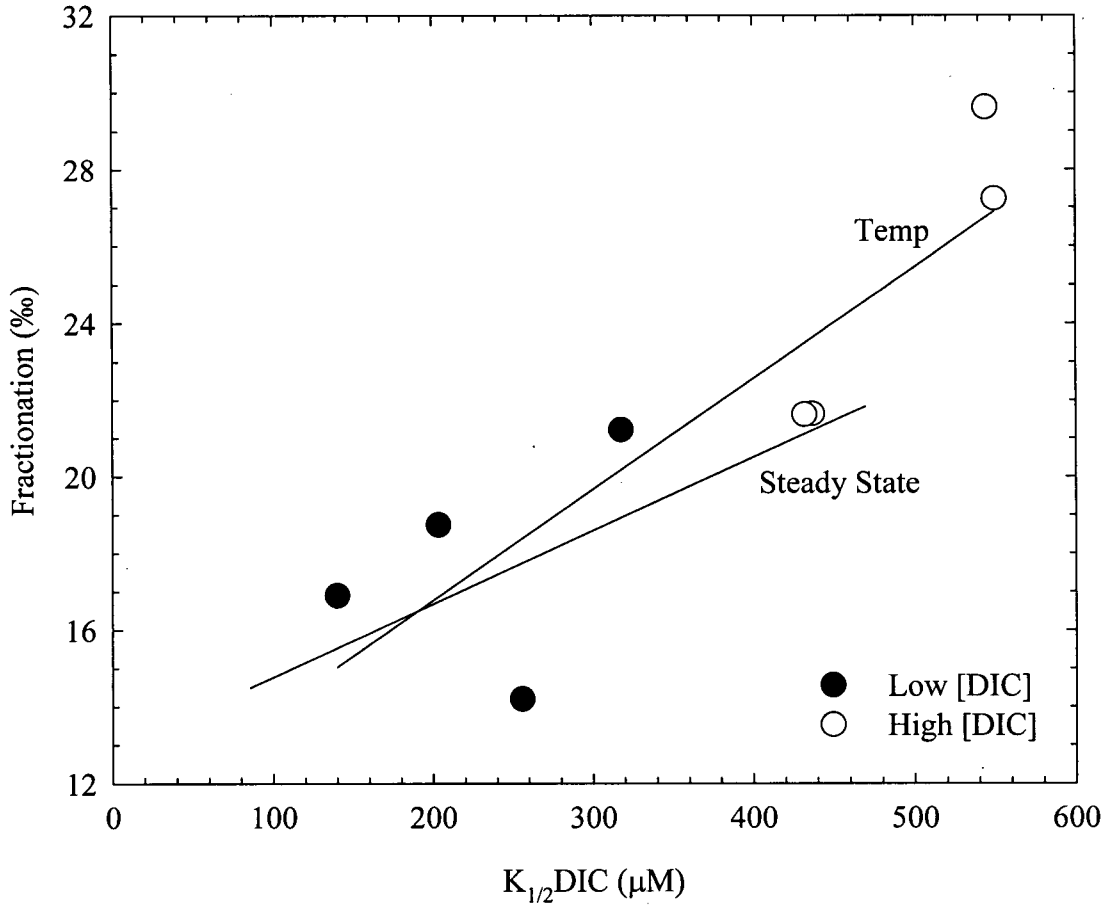

Figure 5.4. Relationship between fractionation and $K_{1/2}$DIC for *Thalassiosira pseudonana* cultures during the temperature experiment. The regression equation for the temperature study is Fractionation = 0.029($K_{1/2}$DIC) + 10.98, (r^2 = 0.771). The regression for the steady state cultures is shown for reference (See Figure 4.5).

5.3.2 Transfer Experiments

The transfer experiments were designed to determine if low DIC-acclimated cells would respond similarly to high DIC-acclimated cultures when transferred to a high DIC concentration. Conversely, high DIC acclimated cultures were transferred to a low DIC concentration and compared to those acclimated to low DIC levels. One concern regarding experiments of this type is that sudden changes in DIC concentrations could influence the physiology of the cells. This might involve the induction or suppression of CCM activity. To more closely examine potential changes in the affinity of cells for carbon, photosynthetic kinetics were monitored during the time course of the depletion experiment. Figure 5.5 shows the $K_{1/2}$DIC values during the experiments. When low (0.4 mM) DIC-acclimated cells were transferred to a high (2.0 mM) DIC concentration, there was no significant adjustment in their photosynthetic kinetics (Figure 5.5A). However, there was a decrease in the $K_{1/2}$DIC within approximately 2h following transfer of high (2.08 mM) DIC-acclimated cultures to low (0.45 mM) DIC concentrations (Figure 5.5B). The decrease was as much as 25% although ± 2 SE overlap does occur. Similar trends were observed for all three high-low DIC transfer experiments. Maximum photosynthetic rates did not change within 2h following transfer (data not shown).

Figure 5.6A illustrates the $K_{1/2}$DIC values for cultures transferred from low to high DIC concentration. Cultures were also grown and depletion experiments were conducted at a constant high or low DIC concentration. These are included in Figure 5.6 and 5.7 for comparison. The ambient and depletion DIC concentrations are summarized in Table 5.1. Cells transferred from a low to a high DIC concentration for the depletion experiment did not exhibit a significant change in $K_{1/2}$DIC (Figure 5.6A) with the exception of the second

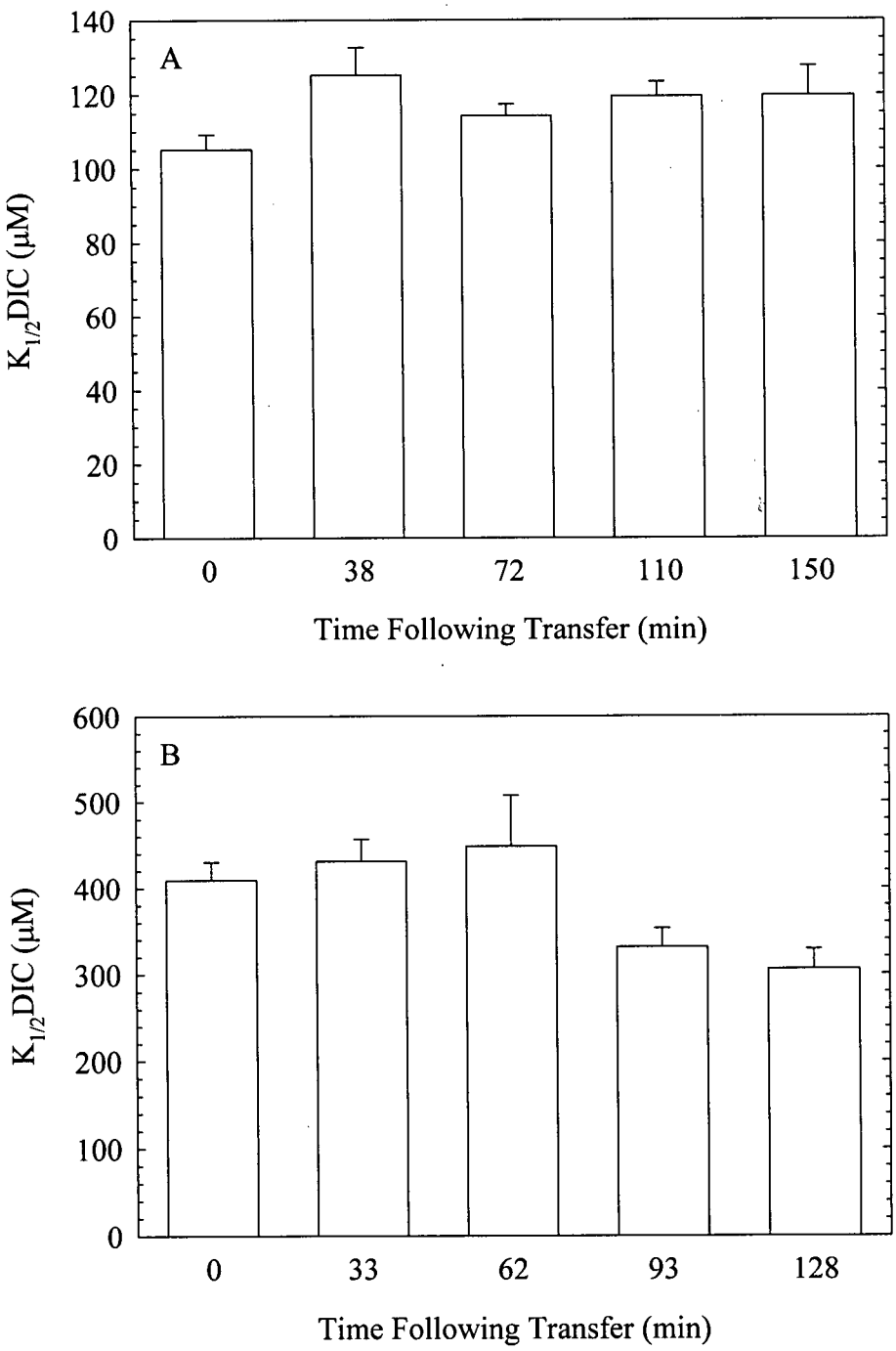

Figure 5.5. Changes in $K_{1/2}$DIC values for *Thalassiosira pseudonana* cultures following transfer from a low (0.4 mM) to a high (2.0 mM) DIC concentration (A), or from a high (2.08 mM) to a low (0.45 mM) DIC concentration (B). Each bar represents a single curve (photosynthesis vs [DIC]) and error bars represent ± 1 standard error of the regression through the raw data.

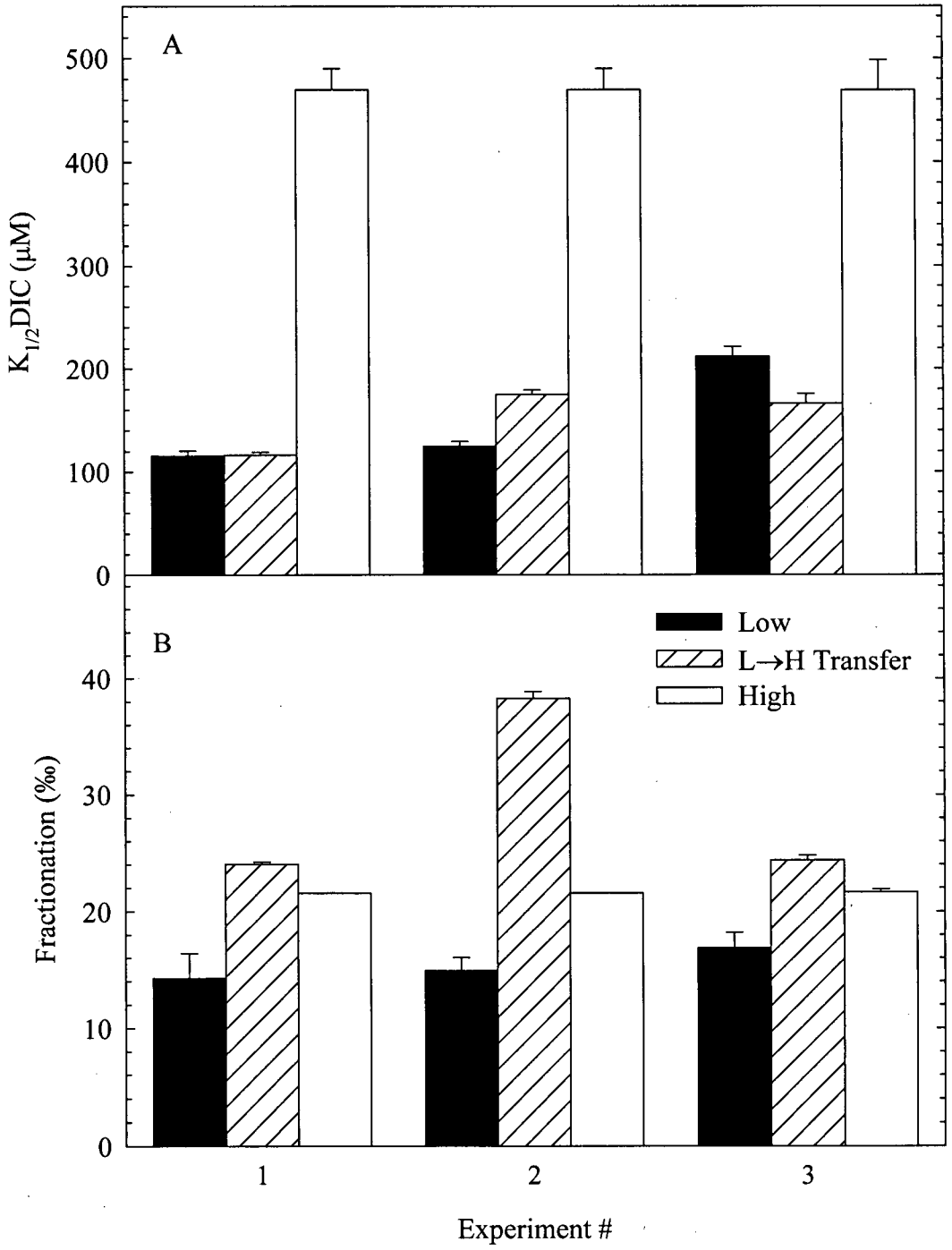

Figure 5.6. $K_{1/2}$DIC (A) and fractionation (B) for *Thalassiosira pseudonana* cultures from the low→high transfer experiments. Comparative values are included for both high and low DIC cultures where the depletion was performed at the same DIC concentration under which the cultures were acclimated. Error bars represent ± 1 standard error of the regression through the raw data.

Table 5.1. Ambient DIC concentrations and the corresponding DIC concentrations under which the source depletion experiments were carried out for the transfer experiments. H→L indicates that cultures were acclimated to a high DIC concentration with the depletion experiment being performed at low DIC concentrations (Figure 5.6). L→H indicates the opposite of the H→L experiments (Figure 5.7). For each transfer experiment, comparative depletion experiments (both high and low [DIC]) were performed where the acclimation and source depletion DIC concentration were the same.

Manipulation (Experiment #)	Reference	Ambient [DIC] (mM)	Depletion [DIC] (mM)
Low → High (1)	Low	0.45	0.45
	Transfer	0.45	2.00
	High	2.00	2.00
Low → High (2)	Low	0.67	0.67
	Transfer	0.67	2.00
	High	2.00	2.00
Low → High (3)	Low	1.00	1.00
	Transfer	1.00	3.00
	High	2.75	2.75
High → Low (1)	High	2.75	2.75
	Transfer	2.75	0.60
	Low	0.67	0.67
High → Low (2)	High	1.90	1.90
	Transfer	1.90	0.55
	Low	0.67	0.67
High → Low (3)	High	2.00	2.00
	Transfer	2.00	0.45
	Low	0.45	0.45

experiment. In all three trials, fractionation for the transferred cultures was significantly higher than either that of the low and high DIC-acclimated cultures (Figure 5.6B). This effect was most pronounced in the second experiment.

Figures 5.7A and B summarize experiments similar to those described by Figure 5.6; but in this case, the transfers were from a high to a low DIC concentration. Low and high DIC cultures where the depletion experiments were carried out at the same DIC concentrations as ambient are included for comparison. In two of the three trials, $K_{1/2}$DIC decreased following transfer, although only one was significant (Figure 5.7A). In all three experiments, $K_{1/2}$DIC values were significantly higher than that of the low DIC-acclimated cultures. Fractionation was lower than during the high DIC depletion experiments in two out of the three experiments, though this difference was only significantly different for the third experiment (Figure 5.7B). In all three cases, fractionation was not significantly different from the low DIC-acclimated depletion experiments (Figure 5.7B).

5.3.3 Modeling

There are numerous models of carbon isotope fractionation. They all involve diffusion, and a few incorporate the possible effects of active uptake. The assumption that phytoplankton rely on diffusion to meet their carbon requirements necessitates the consideration of both the rate of CO_2 production from bicarbonate and the diffusion to and across the plasmalemma. To determine whether the rate of CO_2 production from bicarbonate was sufficient to supply the observed photosynthetic rates during the photosynthetic kinetics (DIC curve) experiments, rate constants were used from Johnson (1982). Figures 5.8A-J demonstrate that low (below 1.22 mM) DIC-acclimated cultures were capable of

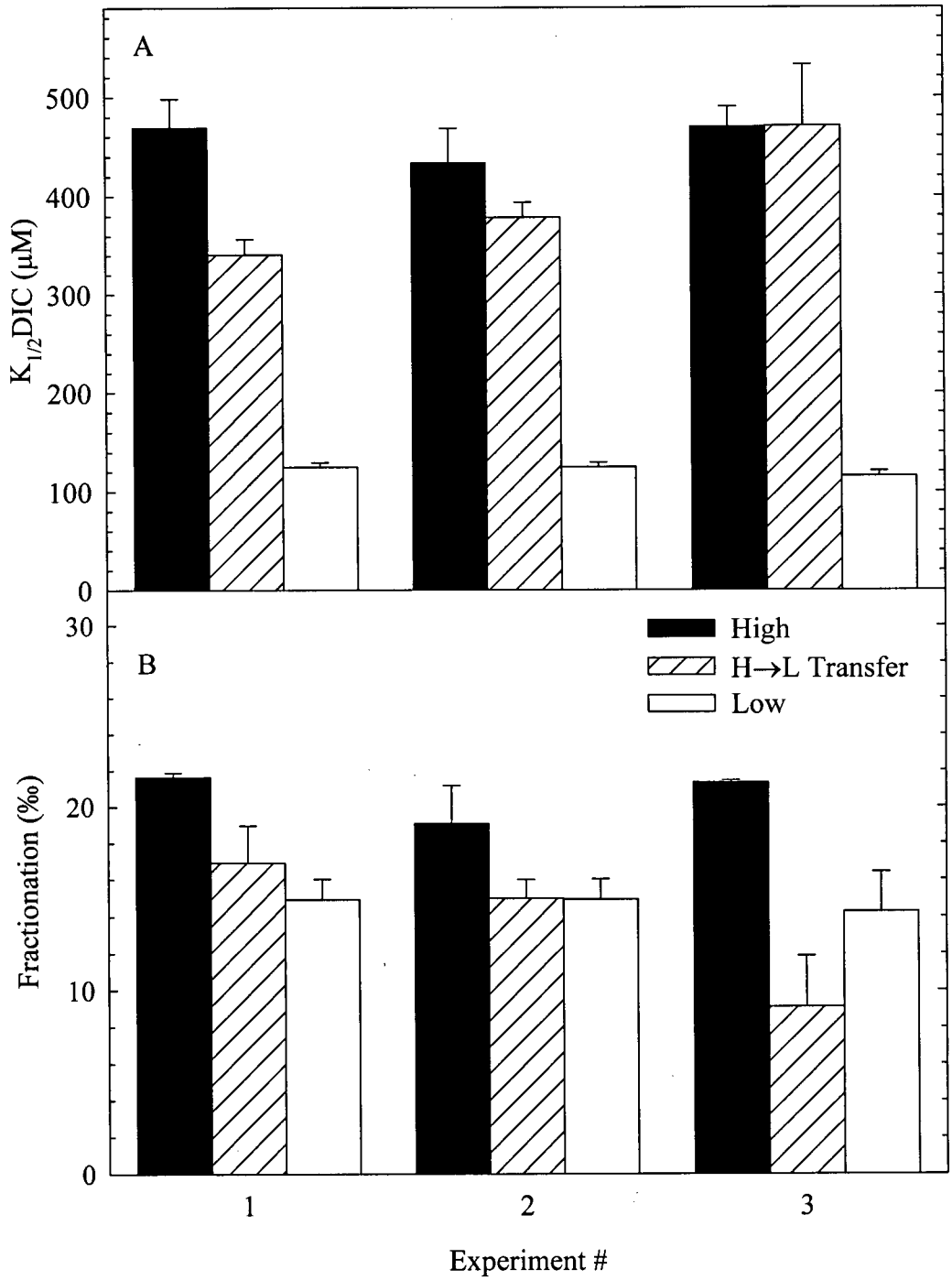

Figure 5.7. $K_{1/2}$DIC (A), and fractionation (B), for *Thalassiosira pseudonana* cultures from the high→low transfer experiments. Comparative values are included for both high and low DIC cultures where the depletion was performed at the same DIC concentration under which the cultures were acclimated. Error bars represent ± 1 standard error of the regression through the raw data.

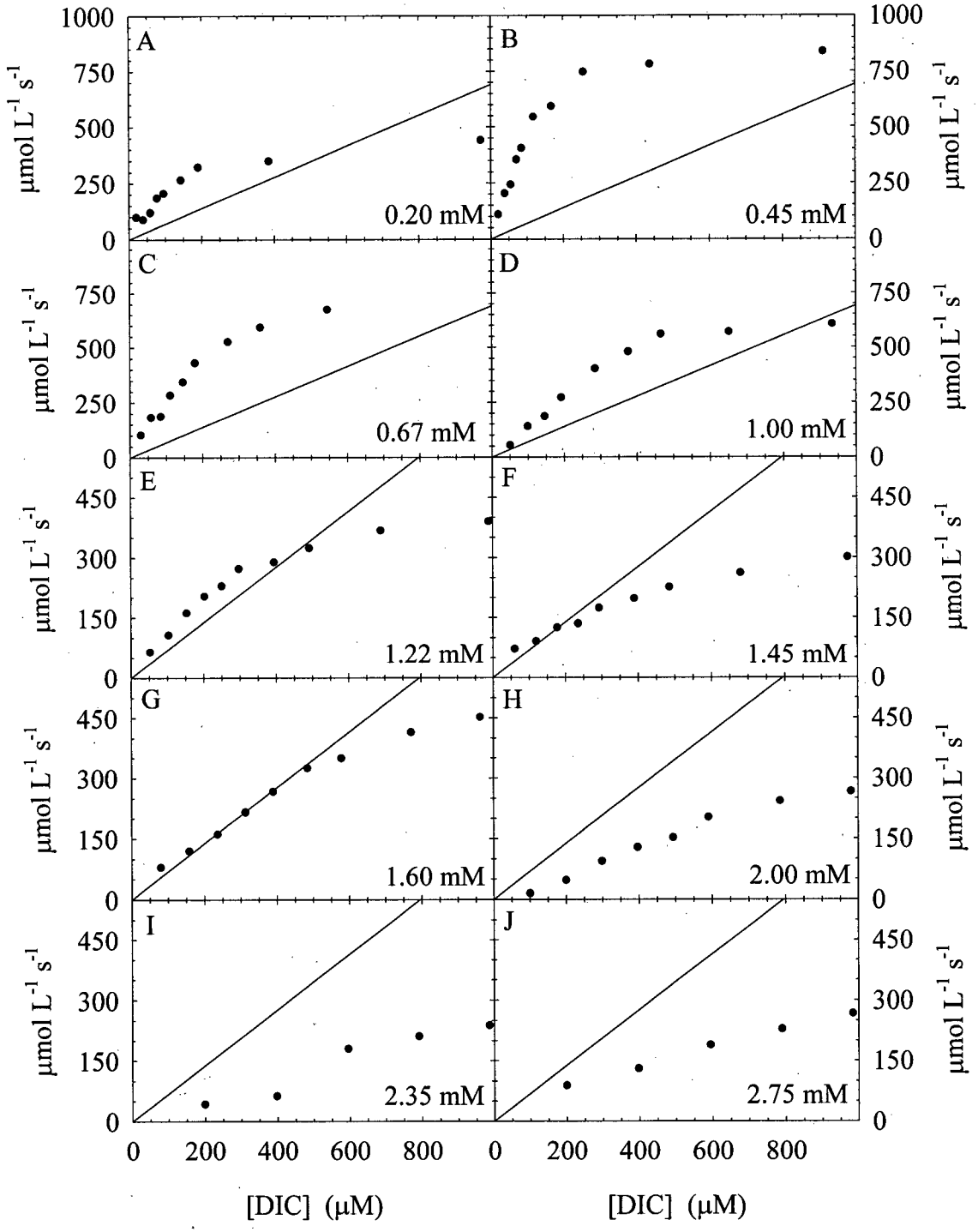

Figure 5.8. Photosynthetic oxygen evolution rates in response to external DIC concentration for *Thalassiosira pseudonana* cultures acclimated to ambient DIC concentrations ranging from 0.20 mM (A), to 2.75 mM (J). The corresponding rate of uncatalyzed CO_2 formation from bicarbonate is included for comparison.

photosynthetic rates exceeding the uncatalyzed rate of CO_2 production from bicarbonate. This ability diminishes as cultures were acclimated to higher ambient DIC levels. To insure that photosynthetic rates did not exceed the CO_2 supply rate during depletion experiments, lower cell densities were used and carbonic anhydrase was added. The implications of photosynthetic rates exceeding uncatalyzed CO_2 production will be discussed further.

The models used in this section were all taken from the literature and are described in Appendices C through I. The data used for the modeling are presented in Appendix B. The key aspect of many of these models is the fractionation associated with carbon fixation. Estimates used by various authors range from 25 to 29‰. The range is justified by the potential reduction if fractionation during carbon fixation caused by the enzyme PEPCase. This enzyme is believed to exhibit a fractionation of only 4.7‰ (O'Leary *et al.* 1992). Furthermore, the estimate of 29‰ for RuBisCO is based on a higher plant form (Guy *et al.* 1987, 1993). Due to the uncertainty regarding the estimated fractionation of carbon fixation in *T. pseudonana*, the values used by the authors of the models were used in this thesis.

Models of fractionation based on diffusion have some common characteristics. They all assume that the species of carbon diffusing passively across the plasmalemma is CO_2. This is logical since the charged bicarbonate ion would tend not to cross the lipid membrane. The second feature is that, since CO_2 is taken up, fractionation is expressed relative to the $\delta^{13}C$ of the CO_2. This value can be determined, if not independently measured, from the equations of Mook *et al.* (1974) and the $\delta^{13}C$ of the total DIC. This method of calculating the $\delta^{13}C$ of CO_2 from the $\delta^{13}C$ of the DIC assumes that there is isotopic equilibrium between CO_2 and bicarbonate. A second assumption here is that the $\delta^{13}C$ of the bicarbonate is similar

to that of the total DIC pool. At a pH of 8.2, this assumption is reasonable since most of the DIC is in the form of bicarbonate. Fractionation relative to CO_2 is often referred to as ε_p.

Diffusion-based fractionation models range from the relatively simple to highly complex. Three models of fractionation based on passive carbon uptake are presented in Figures 5.9 to 5.11. Perhaps the easiest way to predict fractionation is to determine the relative concentrations of CO_2 inside and outside the cell. Figure 5.9, derived from Raven *et al.* (1993), is presented conceptually since the internal CO_2 concentration was not measured during the experiments described in this thesis and thus data fits were not possible. In theory, a low CO_2 concentration inside the cell relative to outside the cell indicates a diffusional limitation of photosynthesis. As diffusion becomes less limiting, fractionation is predicted to increase based on this model (Figure 5.9).

The model presented in Figure 5.10, taken from Hinga *et al.* (1994), is essentially another presentation of the model described in Figure 5.9. The model is independent of growth rate although growth rate would influence the difference between internal and external CO_2 concentrations. As a result, only the steady state data set was superimposed on the model predictions of ε_p. These cultures all had a similar growth rate of ca. 1.4 d^{-1}. This model assumes that the combined discrimination by RuBisCO and other carboxylase enzymes is 27‰ and hence the maximum predicted ε_p values should be 27‰ when the internal and external CO_2 concentrations are equal ($C_e - C_i = 0$). The data did not fit any given trend line indicating that the difference between the internal and external CO_2 concentration depends on the ambient external CO_2 concentration. As the external CO_2 concentration increased, the difference between the two concentrations ($C_e - C_i$) increased.

The model presented in Figure 5.11 (Rau *et al.* 1996) is a more complex one that considers diffusion through the cell's boundary layer and its plasmalemma. The

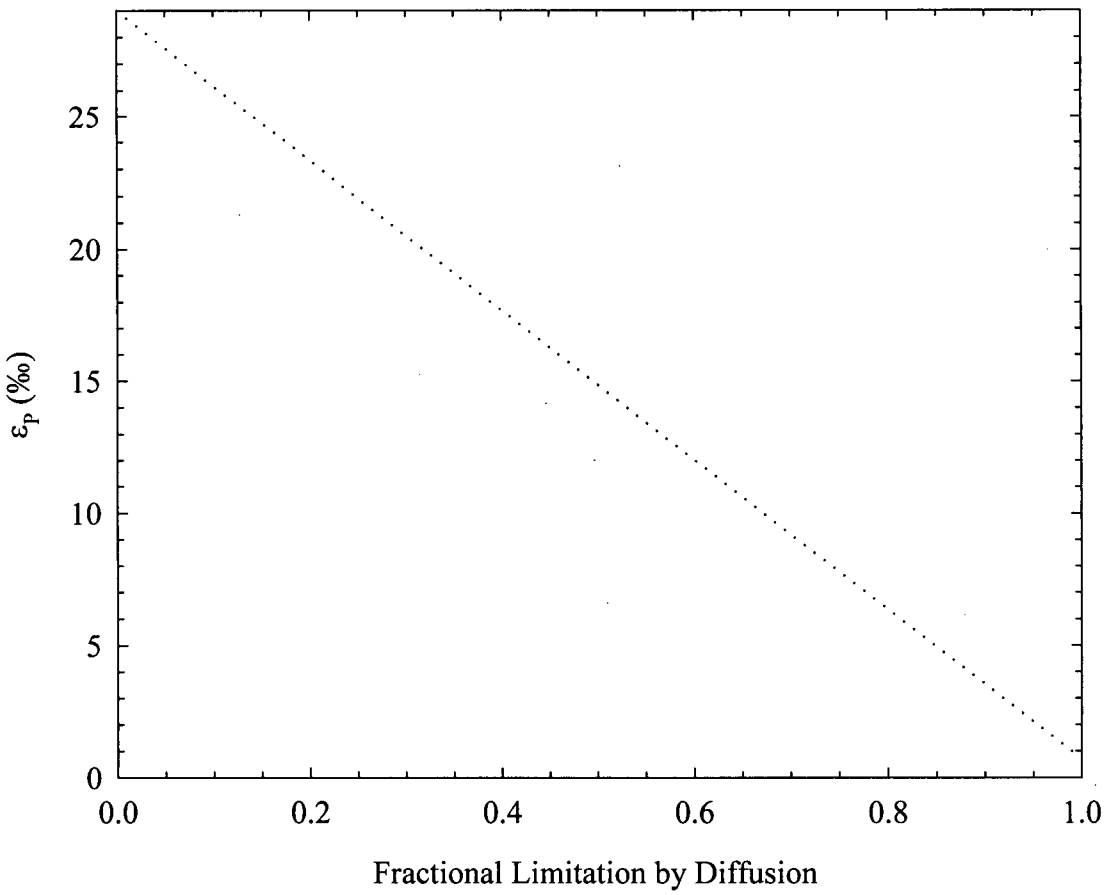

Figure 5.9. First diffusion model. Conceptual relationship between the fractionational limitation of carbon fixation by diffusion and ε_p values for phytoplankton relying on CO_2 diffusion (Raven *et al.* 1993).

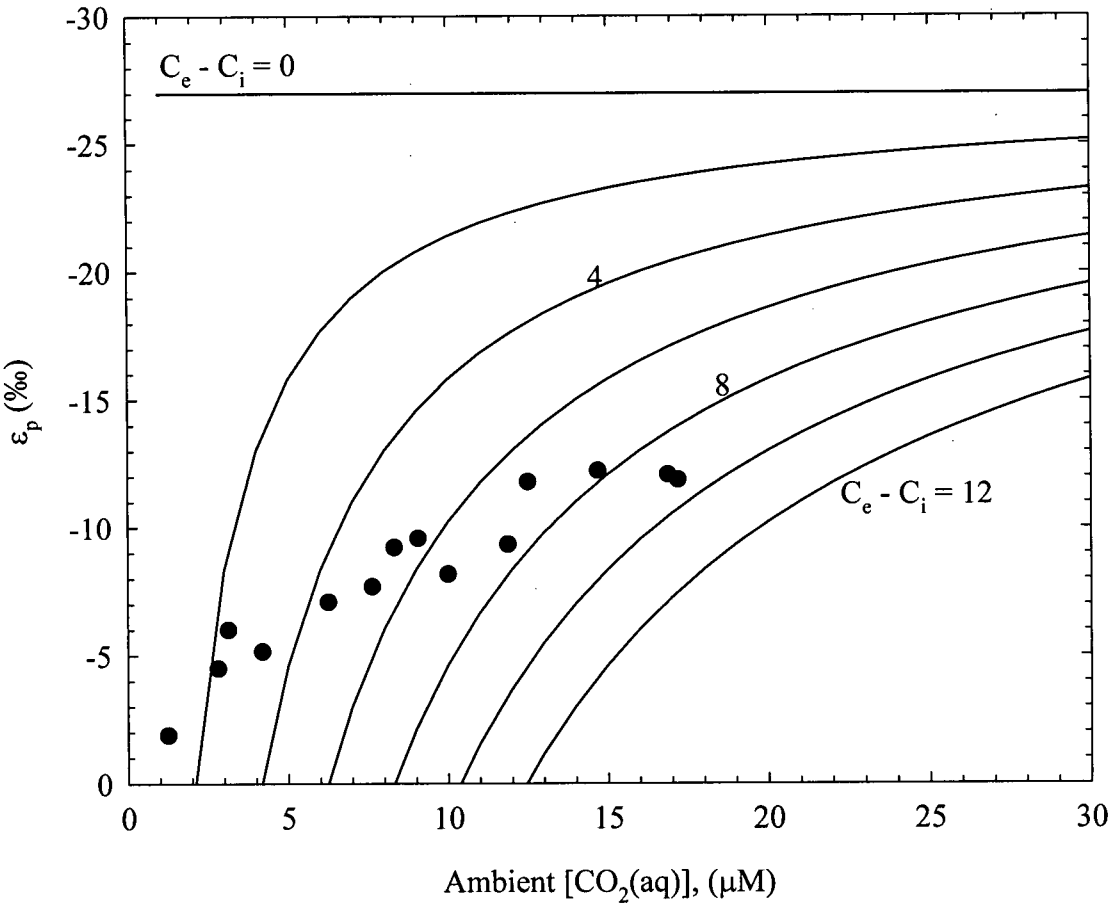

Figure 5.10. Second diffusion model. Comparison of measured ε_p values for *Thalassiosira pseudonana* cultures (Steady state data set) grown at various ambient external CO_2 concentrations with model trend lines based on the CO_2 concentration gradient across the cell plasmalemma. The model assumes passive CO_2 entry into cells. The model was taken from Hinga *et al.* (1994) though it was first proposed by Farquhar *et al.* (1982).

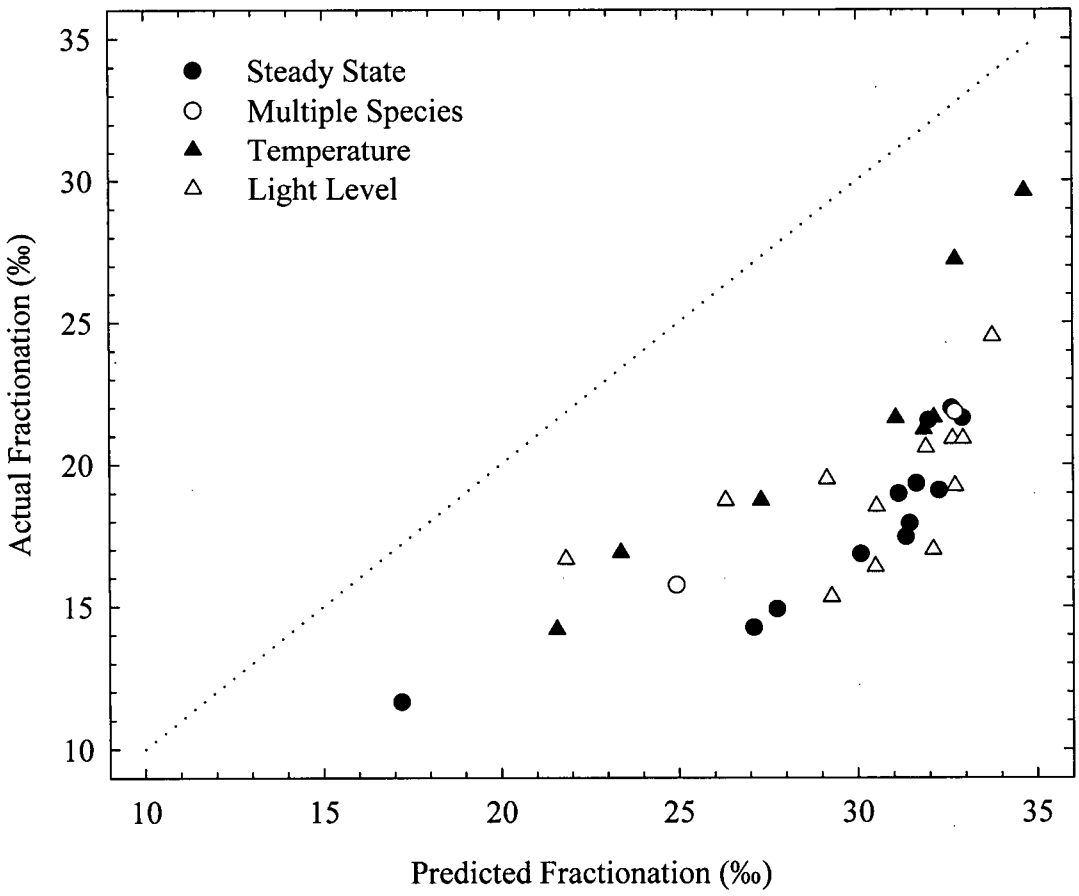

Figure 5.11. Third diffusion model. Comparison of measured fractionation values for *Thalassiosira pseudonana* cultures (complete data set) grown under various conditions to predicted values generated from the model proposed by Rau *et al.* (1996). The model assumes passive CO_2 entry into cells and considers the concept of a boundary layer surrounding cells. The dashed line is the 1:1 line that would indicate a perfect correlation between actual and predicted fractionation values.

fractionation associated with carbon fixation (various carboxylase enzymes) in this model was assumed to be 25‰. Fractionation was plotted relative to total DIC and the complete data set was used. In all cases, the cells exhibited lower fractionation than predicted by the model.

The preceding models all ignore the possible effects of active uptake on carbon isotope fractionation. Laws *et al.* (1995) found a linear relationship between the ratio of growth rate to external CO_2 concentration (μ/C_e) and fractionation (ε_p). However, at low (less than 10 μM) external CO_2 concentrations, the relationship ceased to be linear for *Phaeodactylum tricornutum* (Laws *et al.* 1997). The curvature of their revised model was interpreted to represent active uptake. The linear regression shown in Figure 5.12 was fitted through experimental data where the external CO_2 concentration was greater than 10 μM and represents the diffusion only version of the model found to be applicable only at high CO_2 concentrations. The relationship between μ/C_e and ε_p was significant ($p=0.05$) for the linear portion of the full data set (Figure 5.12A); however, this was not the case for the reduced data set (Figure 5.12B). When the nonlinear model (Laws *et al.* 1997) was used, the regression was significant for both data sets ($p<0.001$). The parameters estimated with the non-linear model are the minimum and maximum fractionation expressed by cells (Table 5.2). The maximum fractionation parameter estimates were well below the expected value of ca. 27 – 29‰ based on the discrimination by RuBisCO.

The model used by Sharkey and Berry (1985) is based on the ratio of carbon efflux (F_3) to carbon influx (F_1). This model is similar to the fractional limitation model involving only diffusion. The higher the F_3/F_1 ratio, the more leakage is occurring and fractionation should increase. The carbon influx and efflux rates were not measured during the

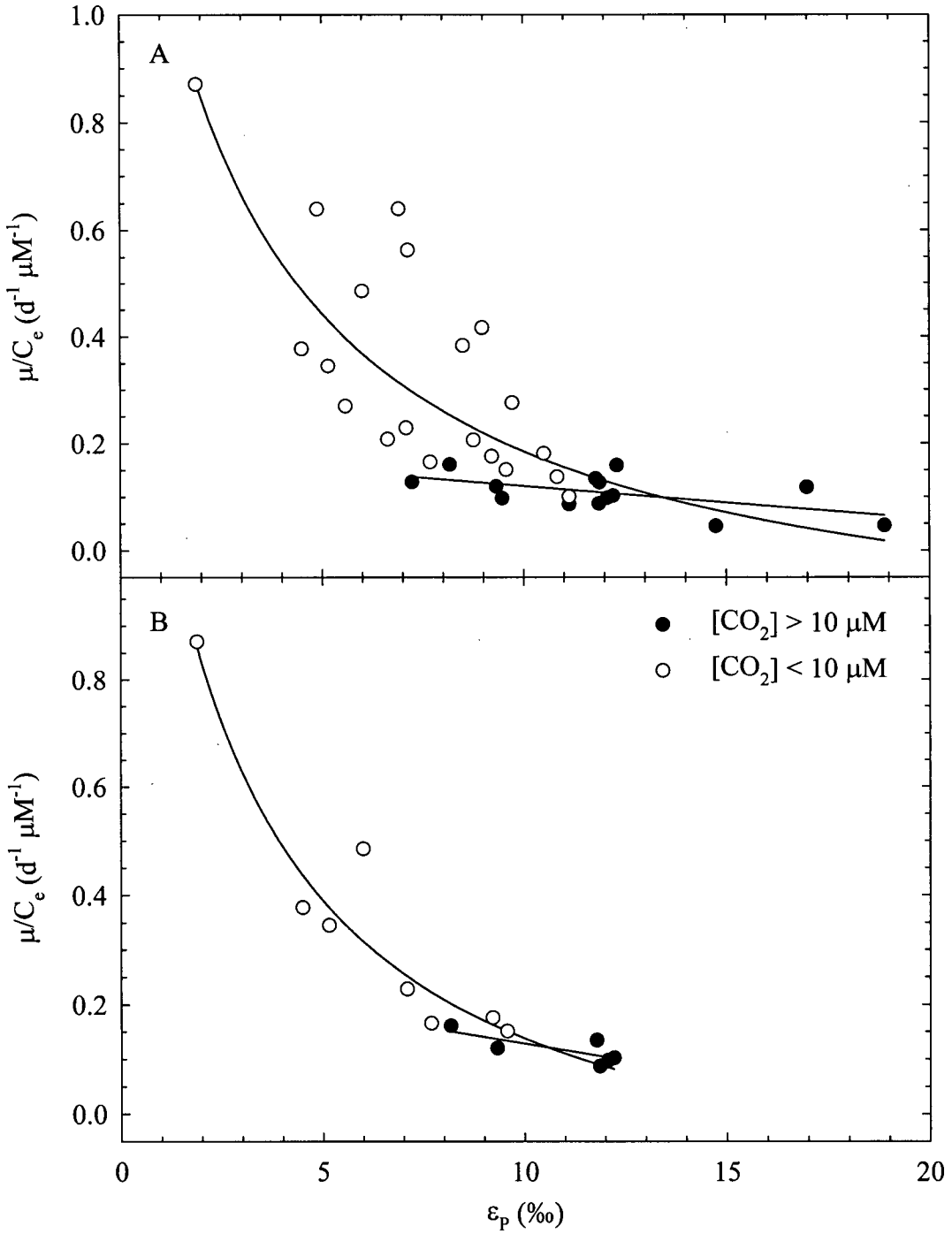

Figure 5.12. First model of active uptake. Model regression through measured ε_p values for *Thalassiosira pseudonana* cultures grown under various conditions for the complete data set (A), and the steady state data set (B). The model assumes that above an external CO_2 concentration of 10 μM, cells rely on passive CO_2 entry and that active uptake occurs below this concentration. Fitted parameter values are included in Table 5.2. The model was taken from Laws *et al.* (1997).

Table 5.2. Values for the parameters ± 1 SE (regression fits) from the first active uptake model representing the minimum possible ε_p value presumably due to uptake fractionation (ε_1') and maximum possible ε_p value presumably due to fixation fractionation (ε_2'). Values are for regressions through the entire data set and the steady state only data set.

Data Set	ε_1' ± SE (‰)	ε_2' ± SE (‰)
All Data	-2.95 ± 0.90	20.66 ± 1.76
Steady State Only	-2.18 ± 0.46	17.45 ± 1.11

experiments presented in this thesis. However, the ratio can be predicted from the fractionation data obtained here. Figure 5.13 suggests that low DIC cells lose approximately 15% of the carbon taken up while high DIC cells lose three times this amount. Since carbon efflux was not measured, the F_3/F_1 ratios are theoretical values based on the observed fractionation.

Despite their consideration of active uptake, the two preceding models are relatively simple. Figure 5.14 presents the results of fitting both the complete and steady state data sets to the model presented by Keller and Morel (1999). This model predicts that phytoplankton maintain CCM activity proportional to the photosynthetic rate and can incorporate active uptake of either bicarbonate or CO_2 with the balance of carbon supplied by CO_2 diffusion. The model fit was identical for either CO_2 or bicarbonate active uptake and the regression was significant for both the complete and reduced data sets ($p<0.001$). Using this model, regression estimates of γ (ratio of active carbon uptake to photosynthesis) and p (cell wall permeability) can be obtained. The parameter estimates differed depending on the species of carbon used by the CCM (Table 5.3) although they always fell within the tolerable range suggested by Keller and Morel (1999). The fractionation expressed by RuBisCO was set to 29‰ and active uptake fractionation was set to 0‰. As previously mentioned, there is considerably uncertainty over the maximum expected fractionation during carbon fixation and active uptake.

Alternatively, one can assume that phytoplankton only use active uptake at low DIC concentrations. This assumes that cells maintain a minimum internal CO_2 concentration ($CO_{2\ i,critical}$). The models presented in figure 5.15 are for active uptake of bicarbonate or CO_2. The pure diffusion model is also included for comparison. Calculations for *Thalassiosira pseudonana* (see Appendix I) suggest that at external CO_2 concentrations

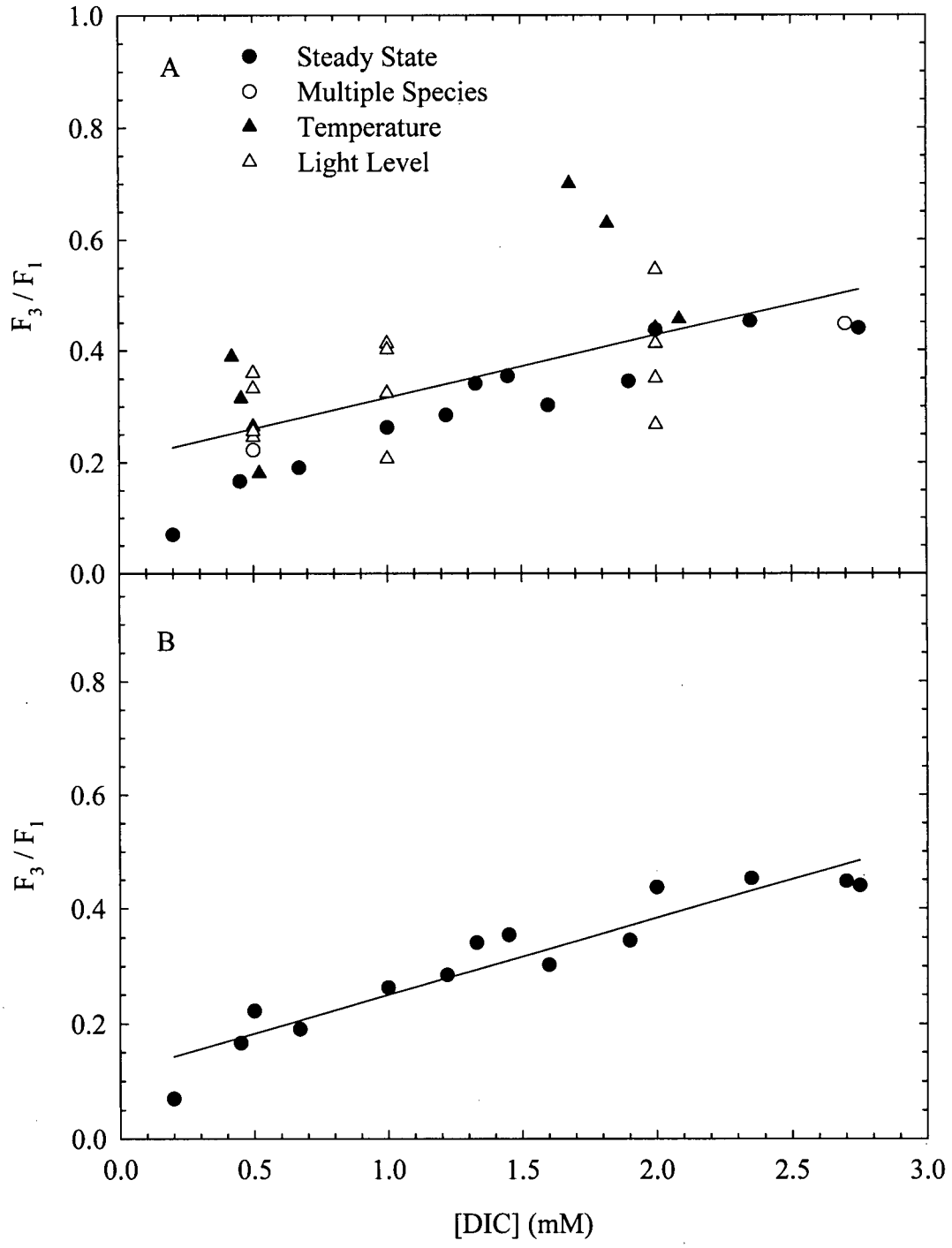

Figure 5.13. Second model of active uptake. Predicted values of fractionation limitation of photosynthesis in cultures of *Thalassiosira pseudonana* grown under various conditions for the complete data set (A) and the steady state data set (B). The r^2 values were 0.41 and 0.89 respectively. The model was taken from Sharkey and Berry (1985).

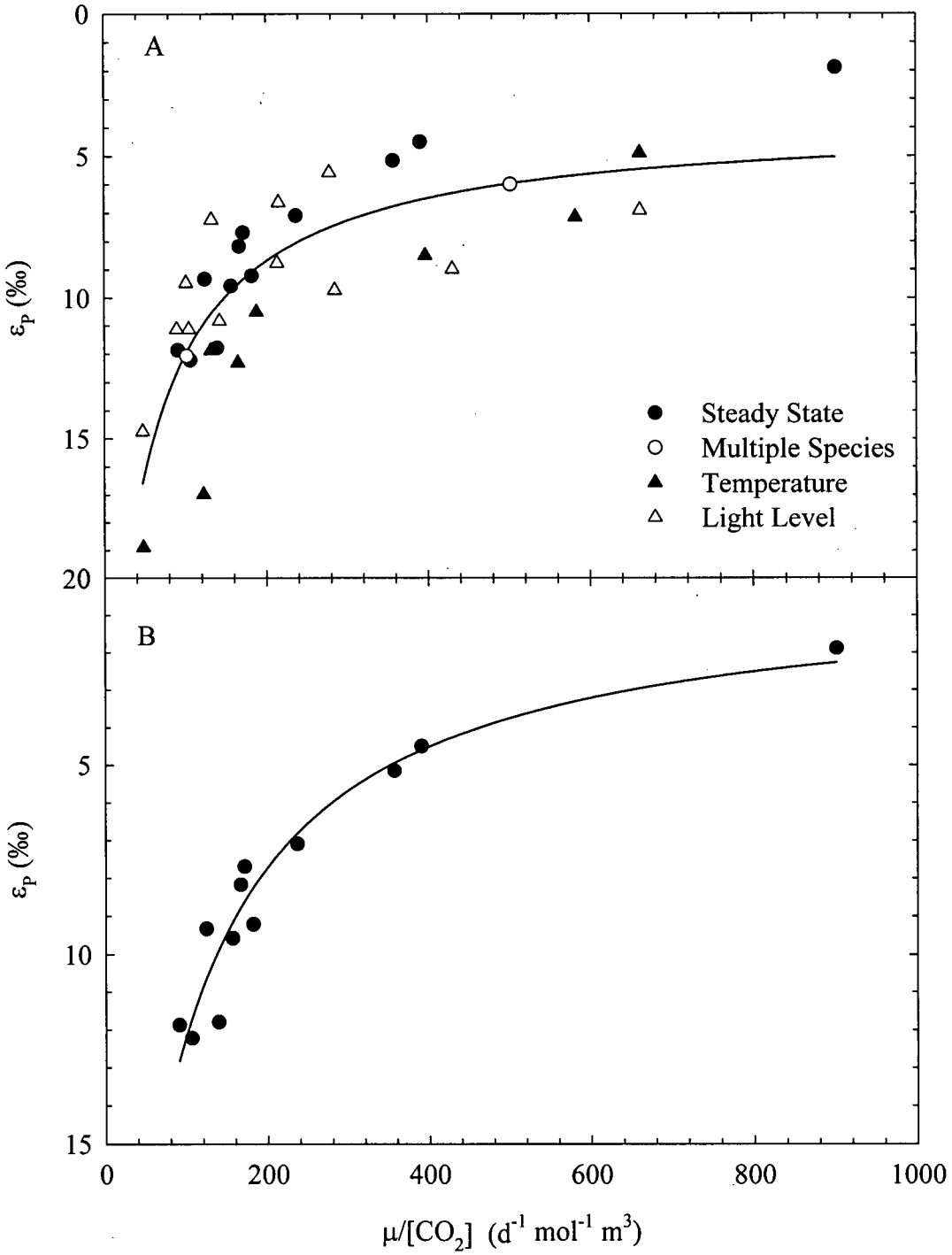

Figure 5.14. Third model of active uptake. Model regression through measured ε_p values for *Thalassiosira pseudonana* cultures grown under various conditions for the complete data set (A), and the steady state data set (B). The r^2 values were 0.67 and 0.92 respectively. The regression fit is independent of the source of carbon used during active transport. The model was taken from Keller and Morel (1999).

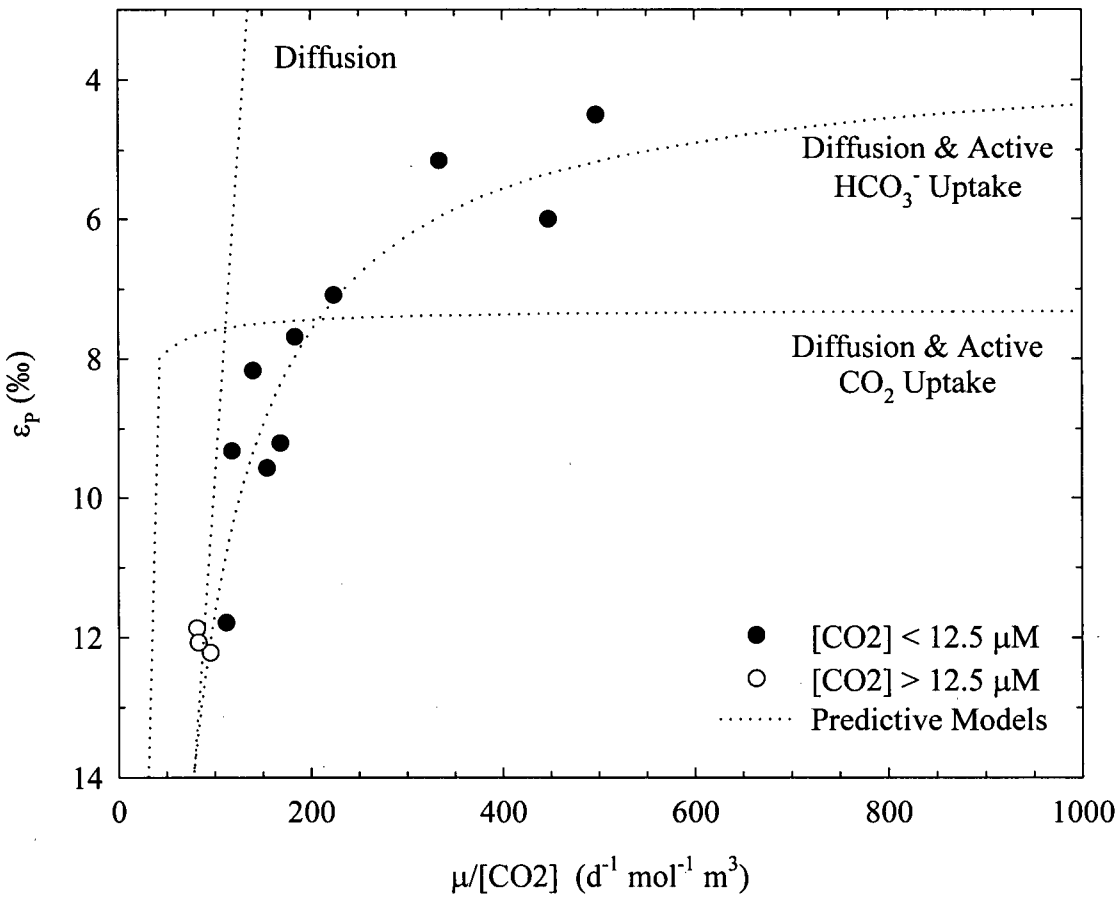

Figure 5.15. Fourth model of active uptake. Model regression through measured ε_p values for *Thalassiosira pseudonana* cultures grown under various conditions for the steady state data set. Regression r^2 values were 0.77 (bicarbonate uptake) and 0.001 (CO_2 uptake). The model was developed by Keller and Morel (unpublished).

Table 5.3. Values for the parameters ± 1 SE (regression fits) from the third active uptake model representing the active carbon uptake: photosynthetic rate ratio (γ) and membrane permeability to CO_2 (P). Values are for regressions through the entire data set and the steady state only data set. The form of carbon actively transported was either CO_2 or bicarbonate.

Data Set	Source	$\gamma \pm$ SE (unitless)	P ± SE ($m\ s^{-1}$)
All Data	CO_2	1.12 ± 0.04	$3.89 \times 10^{-7} \pm 5.55 \times 10^{-7}$
Steady State Only	CO_2	0.98 ± 0.03	$4.95 \times 10^{-6} \pm 4.65 \times 10^{-7}$
All Data	HCO_3^-	1.74 ± 0.10	$6.05 \times 10^{-6} \pm 7.62 \times 10^{-7}$
Steady State Only	HCO_3^-	1.43 ± 0.01	$7.20 \times 10^{-7} \pm 5.84 \times 10^{-7}$

below 12.5 μM, cells require active uptake to supplement CO_2 diffusion to maintain growth rates that were observed for the steady state data set cultures. Above this concentration, diffusion is sufficient to meet cellular demand. The regression was significant assuming bicarbonate was actively taken up ($p<0.001$); however, the model fit assuming active CO_2 uptake was not significant at the 95% confidence level. The data clearly did not fit the pure diffusion model. The membrane permeability parameter estimates resulting from fitting the steady state data to this model are included in Table 5.4.

Table 5.4. Values for the membrane permeability to CO_2 (P) ± 1 SE (regression fits) for the fourth active uptake model. Values are for the steady state data set only and assume either bicarbonate or CO_2 uptake.

Carbon Source	P ± SE ($m\ s^{-1}$)
CO_2	$4.15 \times 10^{-6} \pm 6.41 \times 10^{-7}$
HCO_3^-	$1.05 \times 10^{-5} \pm 3.86 \times 10^{-7}$

5.4 Discussion

5.4.1 Temperature Response Study

Changes in temperature have a strong influence on phytoplankton growth rates. Other factors influenced by temperature include CO_2 solubility and diffusion rates (Raven 1991a). Raven (1991a) suggested that the increased CO_2 concentration at lower temperatures is offset by the reduced rate of diffusion through seawater. However, the more important impact of lower temperatures is a reduced growth rate. As a result, cells growing at lower temperatures should be less limited by CO_2 diffusion and low temperature cells are also less likely to require a CCM (Raven 1991a) though cold water species may still possess CCM activity (Mitchell and Beardall 1996). Both reduced diffusion limitation of photosynthesis and decreased CCM activity would result in higher fractionation when cells are grown at lower temperatures. An increase in CCM activity as temperatures increase would suggest that active carbon uptake might be at least partially responsible for any observed changes in fractionation.

The results of the temperature response study support the hypothesis that fractionation is influenced by CCM activity. That is to say, growth rate increased with temperature. Growth rate was more than three times faster at 22°C than at 10°C ($Q_{10} = 3.06$). Lower growth rates appeared to be accompanied by reduced affinity for carbon, as indicated by higher $K_{1/2}$DIC values and increased fractionation, as predicted. At lower temperatures, phytoplankton photosynthesis would be less limited by carbon, thus reducing the necessity for CCM activity. Reduced CCM activity would in turn result in higher fractionation.

Ignoring the changes in CCM activity, these results are also in accord with diffusion models of fractionation. At lower growth rates (lower temperatures), cells are less limited by

CO_2 diffusion. Diffusion of CO_2 in seawater is only ca. 30% faster at 22°C relative to 10°C (Raven 1991a) whereas growth rate increases by more than three fold. Fractionation should increase as diffusion becomes less limiting. This is exactly what was observed in this experiment. However, changes in the $K_{1/2}$DIC value indicate that the photosynthetic physiology changed as temperature changed.

Although this is the first study to simultaneously examine changes in both fractionation and CCM activity in response to varying temperature, responses in fractionation to temperature changes have been documented. Johnston (1996) found that decreased growth rates in response to lower temperatures resulted in increased fractionation in both *Phaeodactylum tricornutum* and *Emiliania huxleyi*. In contrast, reduced growth rates caused by light limitation were accompanied by reduced fractionation in *E. huxleyi*, but not *P. tricornutum*. It is possible that under reduced light levels, *E. huxleyi* cells used active carbon uptake to prevent photorespiration, thus enabling more efficient use of the limited light energy. Active uptake would result in reduced fractionation. This theory might also explain why CCM activity increased and fractionation decreased in nitrogen stressed *Chlorella emersonii* cultures (Beardall *et al.* 1982). The non-uniform fractionation response to growth rate changes brought about by different means in *P. tricornutum* and *E. huxleyi*, highlights the importance of species variability when interpreting phytoplankton fractionation experiments.

Hinga *et al.* (1994) found that fractionation actually increased with higher temperatures in the diatom *Skeletonema costatum*. This is the opposite to what one might expect and from the results of this study. They attributed the effects to increased CO_2 diffusion rates at the higher temperatures. Though they did not measure growth rates at all three temperatures tested, the diffusion rate effect must have exceeded any growth rate effect

on fractionation. They did compare growth rate changes for cultures grown at 15°C and found no correlation between fractionation and growth rate. This agrees with the data of Korb *et al.* (1996) who found that growth rate changes in light-limited chemostats did not result in changes in fractionation in two species of marine diatoms.

Data on the diatom *Thalassiosira pseudonana* are limited to the effects of light-limited growth rate changes (Lee 1998). The decrease in growth rate was accompanied by increased fractionation. However, $K_{1/2}$DIC values actually decreased with decreasing growth rate when one would expect them to increase. The apparent increase in cell affinity for carbon at lower light levels (lower growth rates) was attributed to cell size changes, since low light cells were smaller. This could result in an apparent increase in affinity even if cells were relying on diffusion since the boundary layer is thinner for smaller cells (Falkowski and Raven 1998). No changes in cell size were noted in the temperature study, thus avoiding this complication. Another possibility is that, like the *E. huxleyi* cultures from Johnston (1996), low light cultures might use active uptake to reduce photorespiration. Higher fractionation could still occur if efflux rates remained high.

Clearly, the data on the influence of growth rate changes on fractionation are not consistent. Of considerable concern is the fact that the effects of growth rate can vary depending on the limiting factor. Nitrogen often limits phytoplankton growth in marine environments. Nitrogen stress has been shown to cause increased CCM activity (Beardall *et al.* 1982) which in turn influences fractionation. This is the opposite of what one might expect if reduced growth rates simply resulted in less demand for carbon and hence CCM activity. As a result, both the cause of growth rate limitation and species variability must be considered when interpreting the influence of growth rate changes on isotope fractionation.

5.4.2 Transfer Experiments

The ability of phytoplankton to actively take up carbon is widespread (Falkowski and Raven 1998) and the mechanisms involved in active uptake are thought to be diverse (Badger *et al.* 1998). Most physiological models of active uptake are based on the photosynthetic characteristics and physiology of freshwater *Synechococcus* species and *Chlamydomonas reinhardtii*. This is likely due to the ease of culturing, the lack of bulky cell walls, and the well characterized genome of these species. Nonetheless, one can extrapolate such models to marine phytoplankton species.

The transfer experiments were designed to shed further light on the mechanism involved in active uptake in *Thalassiosira pseudonana*. Sharkey and Berry (1985) proposed that reduced fractionation occurring simultaneously with increased CCM activity and was the result of reduced plasmalemma permeability to diffusive CO_2 efflux. If this were the case, one would expect that low DIC-acclimated cells possessing CCM activity would continue to express a low fractionation even when transferred to high DIC concentrations. Thus, continued low fractionation would serve as strong evidence that CCM activity was regulating fractionation. However, if plasmalemma permeability to CO_2 did not change, the results would be inconclusive. One could not distinguish between the reduced CO_2 diffusion limitation of photosynthesis from simple flooding of the cell with CO_2 caused by CCM activity and the subsequent efflux. Both situations would result in increased fractionation.

In the experiments where *Thalassiosira pseudonana* cells were grown at low DIC concentrations and fractionation was subsequently measured at high DIC concentrations, fractionation was higher than if the cells had been acclimated to the high DIC concentrations

prior to the depletion experiment. The elevated fractionation would appear to rule out an active uptake mechanism that involves a reduced permeability of the plasmalemma to CO_2 efflux. However, the $K_{1/2}$DIC values did not change during the experiment, indicating that the cells still possessed CCM activity. These data are in accord with the hypothesis that the cells were flooded with carbon that exceeded the amount that could be fixed or sequestered internally. The excess CO_2 was allowed to diffuse back out across the plasmalemma and thus the cell more closely resembles an open system.

The experiments where cells were acclimated to high DIC concentrations and fractionation was subsequently measured at low DIC concentrations were in accord with the hypothesis that cells rely on CO_2 diffusion when grown at high DIC concentrations. Such cells should possess a low level of CCM activity since diffusion rates would be higher. This is not to say that CCM activity is completely suppressed under these conditions. Fractionation decreased and was statistically indistinguishable from the cells acclimated to low DIC concentrations. Though $K_{1/2}$DIC values began to decrease during the depletion experiment, they remained at levels well above those of the low DIC cells.

The results of the experiments described above neither support or refute the hypothesis that CCM induction state is the primary mechanism behind changes in fractionation. It is possible that carbon is sequestered within an internal organelle in *T. pseudonana*. Photosynthetic carbon fixation by RuBisCO takes place in the chloroplast stroma (Falkowski and Raven 1998). In diatoms, there are four membranes separating the chloroplast stroma from the cytosol. It has been suggested that carbon is actively transported into the chloroplast (Badger *et al.* 1998, Falkowski and Raven 1998). Additionally, pyrenoids have been found within the chloroplast for many species, including the marine diatom *Phaeodactylum tricornutum* (Falkowski and Raven 1998). Cells may maintain low

cytoplasmic carbon concentrations to reduce loss via efflux while elevating the concentration of CO_2 around RuBisCO. Such a mechanism would be consistent with the data obtained in the transfer experiments. Perhaps the rate of active carbon transport exceeded the rate that carbon could be sequestered when low DIC cells were transferred to high DIC resulting in efflux. This would in turn result in increased fractionation.

A great deal of diversity has been found to exist across taxonomic groups of phytoplankton with respect to the nature of the CCM (Badger *et al.* 1998). The active uptake mechanisms of marine phytoplankton have been poorly characterized to date. Given the results presented thus far, it is likely that reduced permeability of the outer membrane to CO_2 efflux does not occur in *T. pseudonana*. The results are insufficient to determine the features of the CCM possessed by *T. pseudonana*, but are consistent with some form of internal sequestering of carbon. My data support a mixed model in that under high DIC concentrations, *T. pseudonana* cultures rely on CO_2 diffusion but use active carbon uptake when CO_2 becomes limiting.

5.4.3 Form of Inorganic Carbon Transported

Although a number of possible mechanisms have been proposed, the form of inorganic carbon actively transported by marine phytoplankton remains largely unresolved. Carbon can pass through the plasmalemma by several means (Figure 3.9). The most likely method under high CO_2 concentrations is simple diffusion of CO_2. Under reduced carbon concentrations, external CO_2 concentrations could become limiting to phytoplankton photosynthesis. This limitation could be alleviated by accelerated production of CO_2 from bicarbonate mediated by the enzyme carbonic anhydrase (CA). The CO_2 generated could

then either be actively taken up or simply diffuse across the plasmalemma. Either way, CO_2 could still become depleted within the boundary layer (Riebesell *et al.* 1993b) though external CA would reduce this potential limitation. Without the use of external CA, one might conclude that active transport of CO_2 is unlikely since its production from bicarbonate is slow.

Alternatively, bicarbonate could be actively transported across the plasmalemma and later converted to CO_2 internally. This method would reduce the potential loss of carbon through efflux since bicarbonate would tend not to leak out across the plasmalemma due to its negative charge (Korb *et al.* 1997). It is difficult to definitively prove that phytoplankton can use bicarbonate either directly or indirectly using external CA due to the CO_2 – bicarbonate interconversion.

One method of determining whether cells rely on passive CO_2 diffusion is to compare observed photosynthetic rates to the theoretical rate of uncatalyzed CO_2 production from bicarbonate (Laws *et al.* 1998). This approach was first used by Briggs (1959) to support the theory of bicarbonate use by microalgae. The results presented in Figure 5.8 indicate that *Thalassiosira pseudonana* cells acclimated to ambient DIC concentrations at or below 1.22 mM were capable of sustaining photosynthetic rates greater than the rate of uncatalyzed CO_2 production from bicarbonate. This suggests that the cells were using bicarbonate. Similar evidence has been found for a number of other species of marine phytoplankton. These include the diatoms *Phaeodactylum tricornutum* (Burns and Beardall 1987, Coleman and Rotatore 1995), *Chaetoceros calcitrans* (Korb *et al.* 1997), *Cosinodiscus* sp. (Goldman 1999), *Cyclotella* sp. (Coleman and Rotatore 1995), *Ditylum brightwellii* (Goldman 1999, Korb *et al.* 1997), and *Skeletonema costatum* (Korb *et al.* 1997). Active uptake of

bicarbonate has also been found for mixed natural phytoplankton assemblages (Tortell *et al.* 1997).

A photosynthetic rate exceeding uncatalyzed conversion of bicarbonate to CO_2 is consistent with either the use of external CA to accelerate the conversion rate or the direct transport of bicarbonate during active carbon uptake. There is conflicting evidence that marine phytoplankton produce extracellular CA. Extracellular CA has been observed for *Phaeodactylum tricornutum* by Burns and Beardall (1985), although Iglesias-Rodrigues and Merrett (1997) found that external CA was only produced by this species when DIC was significantly depleted. Merrett (1991) did not find external CA in cultures of *Skeletonema costatum*.

There is evidence that bicarbonate is directly taken up by marine microalgae (Merrett *et al.* 1996, Colman and Rotatore 1995, Tortell *et al.* 1997). The nature of active bicarbonate uptake is largely unknown, although some hypotheses have been proposed. One possibility is an anion antiport system using chloride ions (Drechsler *et al.* 1993, 1994). Alternatively, hydroxide, sulphate, or nitrate ions could function as the anion for the antiport system, although nitrate is typically limiting in marine environments. Another possible mechanism is a proton co-transport system (Lucas 1983). However, given its abundance, the co-transport of sodium ions is more plausible for marine phytoplankton (Dixon and Merrett 1988) though few co-transport mechanisms have been identified (Ritchie 1998).

The mechanism by which *Thalassiosira pseudonana* actively transports carbon remains unknown. The high rates of photosynthesis observed in the low DIC experiments relative to rates of CO_2 production from bicarbonate strongly suggest bicarbonate use. The results are consistent with either direct bicarbonate transport or the use of external CA. Since photosynthetic rates of high DIC cells did not exceed the uncatalyzed rate of CO_2 production

from bicarbonate, one cannot conclude that these cells were using bicarbonate. High DIC cells could potentially rely on CO_2 diffusion though the restriction by the boundary layer has not been considered in this discussion.

A more plausible conclusion is that the ability to use bicarbonate is gradually induced as CO_2 becomes limiting. This is supported by the gradual change in $K_{1/2}$DIC values of *Thalassiosira pseudonana* in the steady state experiments. The exact nature of the signal leading to CCM induction in phytoplankton might involve the total DIC concentration, CO_2 concentration, or CO_2 : O_2 ratio (Kaplan *et al.* 1998). However, evidence from the drawdown experiments indicates that CO_2 concentration rather than that of DIC is involved.

The isotopic content of phytoplankton provides further evidence for bicarbonate uptake. Fractionation values relative to total DIC exceeding 29‰ (the fractionation associated with RuBisCO) have been taken as evidence that CO_2 is used. This is because CO_2 is ca. 10‰ more negative than DIC at 18°C. Though fractionation values falling below 29‰ relative to DIC do not rule out diffusive CO_2 entry, they are not inconsistent with bicarbonate use (Korb *et al.* 1997). However, fractionation values relative to DIC below ca. 10‰ would strongly suggest direct bicarbonate transport. If, on the other hand, external CA was used to accelerate CO_2 formation from bicarbonate with the resulting CO_2 entering the cells, fractionation should not drop below 10‰ relative to the DIC.

With the exception of the transfer experiment where low DIC cells were transferred to a high DIC concentration, fractionation values relative to DIC for experiments described in this thesis were consistently below 29‰. Although there is no proof that bicarbonate is used, the results are compatible with this hypothesis. The lowest fractionation relative to DIC observed was ca. 9.1‰ (ca. 0‰ relative to CO_2). These cells were acclimated to high DIC and then transferred to a low DIC concentration. As a result, they were most likely relying

on CO_2 diffusion. The fractionation value obtained is consistent with the theoretical minimum fractionation value possible if CO_2 diffusion was used exclusively. However, even low DIC acclimated cultures possessing CCM activity did not exhibit fractionation below 10‰. This, in itself, supports the idea that *T. pseudonana* uses bicarbonate by means of external CA. While fractionation data can shed some light on the possible mechanism of carbon uptake, it is not sufficient to definitively prove that bicarbonate uptake is occurring (Korb *et al.* 1997).

5.4.4 Models of Phytoplankton Isotope Fractionation

Although the results presented here are not sufficient to prove that changes in fractionation are the direct result of changes in the induction state of the CCM, there is a strong indication that this is the case. An increase in CCM activity appears to result in reduced fractionation. However, models of carbon isotope fractionation based solely on CO_2 diffusive uptake also predict a decrease in fractionation as CO_2 concentration decreases. It is interesting to examine various hypothetical models of isotope fractionation in phytoplankton and compare experimental data with predicted results from these models. To that end, several models of isotope fractionation by phytoplankton were included in this chapter.

The first diffusion model was included mostly for conceptual purposes. This is the traditional model where fractionation relative to CO_2 falls between two extremes depending on the degree of limitation imposed by diffusion. When carbon fixation is completely limited by the rate of carboxylation by RuBisCO, fractionation should approach the theoretical maximum value of 29‰ (Raven *et al.* 1993). Conversely, when diffusion is the limiting step, fractionation approaches 0.7‰. The model is based on measurements of both

the internal and external CO_2 concentrations. The internal CO_2 concentration was not measured in these experiments and thus it is not possible to determine if the data fit this model.

The second diffusion model is that of Hinga *et al.* (1994), although it was originally proposed by Farquhar *et al.* (1982). This model uses fractionation relative to CO_2 (ε_p) with the upper limit of fractionation assumed to be 27‰ as a result of the fractionation expressed during carbon fixation by both RuBisCO and the other carboxylase enzymes. The fractionation values that I obtained under high external CO_2 concentrations were well below the maximum predicted by the model (Figure 5.10). One would expect cells grown at high CO_2 concentrations to have a smaller difference between external and internal CO_2 concentrations than those grown at low DIC. This is because diffusion becomes less limiting as external CO_2 concentrations increase.

Similar conclusions were reached by Hinga *et al.* (1994) for *Skeletonema costatum* fractionation. Interestingly, the trend in their data parallels my own data. They concluded that varying degrees of β-carboxylation and pH effects might have influenced their results. I did not conduct experiments under extremely high carbon concentrations (> 20 mM CO_2), and hence I was not able to determine the upper limit of fractionation. However, a fractionation of 38.3‰ was obtained for low DIC acclimated cells upon transfer to a high DIC concentration. This would correspond to an ε_p value of ca. 28.5‰, which approaches the maximum value of higher plant RuBisCO (Guy *et al.* 1993).

The third diffusion model (Rau *et al.* 1996) perhaps best illustrates that active uptake has a strong influence on carbon isotope fractionation. This model is by far the most comprehensive model of fractionation based on CO_2 diffusion. The foundation of the model is based on the idea that CO_2 must first diffuse to the outer edge of the boundary layer

surrounding a phytoplankton cell and then across the boundary layer where it passively crosses the plasmalemma. The data from this thesis consistently fall below the values predicted by the model (Figure 5.11), a result that would be expected if active carbon uptake was occurring.

There are many issues that the Rau *et al.* (1996) model does not address. The first and most important is the potential ability of phytoplankton to actively take up bicarbonate (Raven 1993b). The direct transport of bicarbonate would presumably reduce the fractionation expressed by phytoplankton since it is ca. 10‰ heavier than CO_2. The model also fails to consider the possibility of external CA activity. The existence of both bicarbonate uptake and external CA activity is not in doubt (Turpin 1993) and they ultimately cast uncertainty on the adequacy of this model to explain the range in $\delta^{13}C$ values found in nature. Another concern with this model is the considerable range in permeability estimates of phytoplankton membranes (see Keller and Morel 1999). However, adjusting the permeability value does not significantly improve the fit of my experimental data to this model.

The potential involvement of active carbon uptake by phytoplankton was recognized by Laws *et al.* (1997). As one would expect, higher values of μ/CO_2 resulted in reduced fractionation. The model assumes that passive CO_2 diffusion was sufficient to supply a cell's carbon demand when external CO_2 concentrations were greater than 10 $\mu mol\ kg^{-1}$. Below this concentration, active uptake of CO_2 was suggested to account for the deviation from a linear relationship between μ/CO_2 and ε_p, although the interpretation that CO_2 was transported and not bicarbonate is controversial. Keller and Morel (1999) show that the data of Laws *et al.* (1997) are consistent with active uptake of both bicarbonate and CO_2.

There is a good fit of the data that I obtained to the non-linear model of Laws *et al.* (1997) (Figure 5.12). This fit may be consistent with the idea that phytoplankton grown at a low external CO_2 concentration rely to some extent on a CCM since the data do not fit the linear relationship between μ/CO_2 and ε_p predicted if cells rely solely on diffusion. It is interesting to note that the lower ε_p limit parameters (Table 5.2) obtained from the regressions were below 0‰ (ca. 10‰ relative to DIC) and well below the 5.5‰ obtained by Laws *et al.* (1997) suggesting that bicarbonate might be the inorganic species of carbon actively transported. Definitive evidence that bicarbonate was transported would manifest itself in negative ε_p values (*ie.* fractionation relative to DIC approaches 0‰) when CO_2 concentrations are low (Laws *et al.* 1997). One must note that no actual negative ε_p values were measured during my experiments. This could be due to an efflux of CO_2 produced internally from the transported bicarbonate. Alternatively, it suggests that CO_2, produced by external CA, is the form of inorganic carbon that crosses the plasmalemma.

The model proposed by Sharkey and Berry (1985) is based on the concept of cell membrane leakiness. They propose that high CO_2 cells rely on diffusion to meet cell carbon requirements. They observed ε_p values of 28‰, close to the theoretical maximum value resulting from the discrimination by RuBisCO. However, this value decreased significantly when cells possessed CCM activity as inferred by increased affinity for carbon. The model they proposed predicts that the relative rates of influx and efflux are responsible for the measured fractionation values. Although the influx and efflux rates were not measured in this thesis, one can calculate the ratio of efflux to influx. When the data are applied to this model (Figure 5.13), it appears that the rate of efflux relative to influx is three times higher for cells acclimated to high DIC concentrations compared to low DIC cells; high DIC cells

loose approximately half of all carbon taken up. It would be advantageous for carbon limited cells to reduce the rate of efflux by either reduced membrane permeability to CO_2 (Sharkey and Berry 1985) or sequestering of carbon within the cell (Badger 1998). The mechanism of carbon sequestration is still being debated.

CO_2 efflux rates exceeding those of CO_2 uptake (net CO_2 efflux) during photosynthesis have been documented for a marine *Synechococcus* species (Tchernov *et al.* 1998). The authors suggest that actively transported bicarbonate was converted to CO_2 within the cell, perhaps by means of internal CA, and the resulting CO_2 was free to leak back out of the cell. The apparent waste of energy expended during active bicarbonate uptake could be explained by the need for cells to dissipate excess light energy (Kaplan *et al.* 1998). Although these experiments were carried out on a marine *Synechococcus* species, it is possible that such mechanisms are widespread among other classes of marine phytoplankton.

There are two comprehensive models of phytoplankton carbon isotope fractionation that acknowledge the ability of cells to actively transport carbon. The first of these models (Keller and Morel 1999) assumes that phytoplankton adjust their active carbon uptake in a constant ratio (γ) to their carbon fixation rate (Keller and Morel 1999). Whether this form of CCM regulation is applicable remains to be tested. Nonetheless, the data from this thesis fit the model well (Figure 5.14). This is especially the case for the steady state experimental data. The model can be set up to assume active uptake of either CO_2 or bicarbonate. In both cases, the fits are identical, although the fitted parameters are different (Table 5.3). According to the model, if cells are actively transporting bicarbonate, they must maintain higher rates of active transport relative to photosynthetic rates. In both cases, the membrane permeability is within the range suggested by Keller and Morel (1999).

Instead of maintaining active uptake rates in constant proportion to photosynthesis, phytoplankton cells are more likely to maintain a critical internal CO_2 level. This is the premise behind the fourth model of fractionation based on active uptake (Keller and Morel unpublished). If the diffusive uptake of external CO_2 is insufficient to maintain the critical internal CO_2 concentration, active uptake would be induced. An important parameter of this model is the critical CO_2 concentration required to support a given growth rate.

The critical internal CO_2 concentration depends on a number of factors, including the quantity and K_m of RuBisCO, growth rate and cell carbon quota. In this case, the maximum photosynthetic rate per cell under logarithmic growth for my cultures was used in order to eliminate the need to use chlorophyll and RuBisCO concentrations. The maximum photosynthetic rate was used as V_{max} and the K_m was assumed to be 40 μM, a value similar to that for RuBisCO isolated from the marine diatom *Phaeodactylum tricornutum* (Badger 1998), in the Michaelis-Menten equation. A growth rate of 1.4 d^{-1} was assumed since this was the average value of the steady state experiment. Cell carbon quota was estimated to be 6 pg carbon per cell (Montagnes *et al.* 1994). With these values, a critical internal CO_2 concentration of 8.33 μM was calculated (see Appendix I).

Using this value for the critical internal CO_2 concentration, the data from the steady state experiments were found to fit very well if cells were assumed to supplement CO_2 diffusion with active transport of bicarbonate (Figure 5.15). However, the data did not fit the model if CO_2 was used as the carbon source for the CCM (Figure 5.15). These results support the hypothesis that the CCM in *Thalassiosira pseudonana* actively transports bicarbonate rather than CO_2. However, the evidence provided by models must be taken as circumstantial at best. Until direct evidence of bicarbonate use by *T. pseudonana* is obtained, one can only speculate on the source of inorganic carbon actively transported by this species.

Of the models presented above, the ones that consider active uptake are most likely to be representative of actual phytoplankton physiology since there is overwhelming evidence that phytoplankton do use active uptake. It is unlikely that, given the variability in strategies employed by marine phytoplankton to accumulate inorganic carbon, one model will be capable of accurately predicting the isotopic fractionation of a given species. The potential effect of species variability on the $\delta^{13}C$ values of natural phytoplankton assemblages is profound because even separate isolates of a single species can have different CCM characteristics (Colman and Rotatore 1995). Nevertheless, simplified models of carbon isotope fractionation are useful in that they have stimulated interest and occasional controversy (Turpin 1993) regarding the factors that influence $\delta^{13}C$ of marine phytoplankton.

Summary

The main objective of this thesis was to gain a better understanding of how the induction of the carbon concentrating mechanism influences carbon isotope fractionation in marine phytoplankton. Given the potential use of the isotopic content of phytoplankton preserved in marine sediments as a proxy for past atmospheric CO_2 concentrations, an understanding of how CCM activity influences fractionation is very important. In the past, models of carbon isotope fractionation have largely ignored the potential influence of CCM activity on fractionation. The results of this thesis suggest that CCM induction must be considered.

Six species of marine phytoplankton, including four diatoms, a chlorophyte, and a cyanobacterium, all showed reduced fractionation when grown at lower DIC levels. This reduced fractionation was accompanied by a reduction in the $K_{1/2}$DIC value. Reduced $K_{1/2}$DIC values indicate a higher affinity of the cell for carbon. This has traditionally been viewed as strong evidence for CCM activity. No significant relationship was found between fractionation and either growth rate or cell volume. The results suggest that reduced fractionation occurs under low DIC concentrations and this could at least be partially due to CCM induction.

A more detailed examination of the interaction between fractionation and CCM induction was carried out on the marine diatom *Thalassiosira pseudonana*. This species was chosen mainly because it was easy to culture and withstood the manipulations required for the experiments. It also demonstrated a substantial range in $K_{1/2}$DIC values. Two types of experiments were carried out. The first involved growing cultures at steady state DIC (CO_2)

concentrations while maintaining a constant pH and temperature. The results indicate that CCM induction is a gradual process and that it occurs over an ecologically relevant range of CO_2 concentrations. A decrease in fractionation was correlated with CCM induction. Growth rates were relatively constant throughout the entire range of DIC concentrations tested. The second type of experiment used a closed system DIC drawdown approach. Two experiments were carried out; one with buffered medium and the other with unbuffered medium. In both cases, reduced fractionation and increased CCM induction occurred as the medium DIC concentration decreased. Fractionation and CCM induction appeared to respond to changes in CO_2 concentration rather than those of DIC.

The final section of the thesis attempted to gain insight into the possible nature of the CCM in *Thalassiosira pseudonana*. The effect of growth rate changes in response to culture temperature on both fractionation and CCM induction was investigated. At lower growth rates, both fractionation and $K_{1/2}$DIC values were higher. This result strengthens the hypothesis that CCM induction results in reduced fractionation. Experiments where cultures were acclimated to one DIC concentration and where fractionation was subsequently measured at a different DIC concentration (transfer experiments) indicated that CCM induction by *T. pseudonana* does not involve reduced outer membrane permeability to CO_2 as has been suggested for other species.

The final aspect of the thesis was to apply various models of isotope fractionation to the data from the thesis. The results suggest, not surprisingly, that fractionation is not well described by models that fail to consider active carbon uptake. The results of the modeling and the transfer experiments suggest that bicarbonate can be used as a carbon source by *T. pseudonana*. The data suggest that external CA is used to accelerate CO_2 formation from

bicarbonate and that the CO_2 is subsequently taken up by the cells. The carbon transported might be sequestered within the cell to avoid diffusive efflux.

Given the results of this thesis, one must consider the influence of CCM induction on carbon isotope fractionation when interpreting the relationship between CO_2 concentration and phytoplankton isotope content. CCM induction occurred over an ecologically relevant range of CO_2 concentrations. Although all species tested exhibited reduced fractionation simultaneously with increased CCM induction, considerable species variability was observed. This is potentially due to the different forms of CCM possessed by these species.

Implications and Future Studies

Primary productivity in the marine environment has traditionally been assumed to be limited by nitrogen. Only in the past few years has the importance of trace metal limitation been considered. Even less likely was the prospect of carbon limitation of phytoplankton growth. While there is ample dissolved inorganic carbon to support phytoplankton growth, only a small portion of this carbon pool is in the form of CO_2. It is this form of carbon that is ultimately fixed by RuBisCO, the major carbon fixation enzyme used in photosynthesis. This has led some authors to suggest that phytoplankton growth could be limited by CO_2 supply.

While CO_2 concentration could be limiting to photosynthesis, most species of marine phytoplankton possess the ability to actively transport carbon. Thus, while photosynthesis is limited by CO_2 supply, growth rate is maintained as a result of active carbon transport. An interesting finding is that nitrogen limitation resulted in CCM induction in the freshwater alga *Chlorella emersonii* (Beardall *et al.* 1982). Induction of active uptake is thought to result in the suppression of oxygenase activity of RuBisCO, and this would increase nitrogen use efficiency. It would be interesting to determine if nitrogen limitation in marine phytoplankton also results in CCM induction. If so, CCM induction could reduce fractionation below that expected based on the availability of CO_2.

Carbonic anhydrase has been linked to the active uptake mechanism in several algal species. This enzyme requires zinc and hence zinc limitation has important implications for CCM activity (Morel *et al.* 1994). Zinc and carbon might co-limit primary productivity in some marine environments where cells require CCM activity to maintain high growth rates. The potential for trace metal limitation of primary productivity has already been

demonstrated for iron (Martin *et al.* 1991). The influence of nitrogen on CCM induction suggests that iron limitation might also influence active carbon uptake since iron is required for enzymes involved in nitrate assimilation. The physiology of phytoplankton cells is undoubtedly complex and the potential involvement of both macro- and micronutrients must be considered. In addition, different species might respond to nutrient limitation in different ways and possess different mechanisms of active carbon uptake. Changes in the CO_2 concentration associated with global warming will undoubtedly influence the dynamics of phytoplankton assemblages as a result of their different nutrient use efficiencies.

Future research should examine the influence of nitrogen and trace metal limitation on both CCM induction and fractionation. The focus should be on bloom forming species since they are more likely to be present in marine sediments. Recent work has focused on biomarkers since they are uniquely representative of specific algal groups. With the complexity alluded to above, it is unlikely that a simple correlation between CO_2 concentration and carbon isotope fractionation will be established. If this is indeed the case, the use of carbon isotopic content of phytoplankton preserved in the sediments as a paleobarometer will not be possible.

Literature Cited

Arnelle, D.R., O'Leary, M.H. (1992) Binding of carbon dioxide to phosphoenolpyruvate carboxykinase deducted from carbon kinetic isotope effects. Biochem. **31**, 4363-4368.

Badger, M.R., Andrews, T.J., Whitney, S.M., Ludwig, M., Yellowlees, D.C., Leggat, W., Price, G.D. (1998) The diversity and coevolution of Rubisco, plastids, pyrenoids, and chloroplast-based CO_2-concentrating mechanisms in algae. Can. J. Bot. **76**, 1052-1071.

Badger, M.R., Price, G.D. (1992) The CO_2 concentrating mechanism in cyanobacteria and microalgae. Physiol. Plant. **84**, 606-615.

Beardall, J., Griffiths, H., Raven, J.A. (1982) Carbon isotope discrimination and the CO_2 accumulating mechanism in *Chlorella emersonii*. J. Exp. Bot. **33**, 729-737.

Beardall, J., Johnston, A., Raven, J.A. (1998) Environmental regulation of CO_2-concentrating mechanisms in microalgae. Can. J. Bot. **76**, 1010-1017.

Beardall, J., Mukerji, D., Glover, H.E., Morris, I. (1976) The path of carbon in photosynthesis by marine phytoplankton. J. Phycol. **12**, 409-417.

Berry, J.A. (1989) Studies of mechanisms affecting the fractionation of carbon isotopes in photosynthesis. In: Stable isotopes in ecological research. pp. 82-94, Rundel, P.W., Ehleringer, J.R., Nagy, K.A., eds, Springer Verlag, Berlin.

Bidigare, R.R., Fluegge, A., Freeman, K.H., Hanson, K.L., Hayes, J.M., Hollander, D., Jasper, J.P., King, L.L., Laws, E.A., Milder, J., Millero, F.J., Pancost, R., Popp, B.N., Steinberg, P.A., Wakeham, S.G. (1997) Consistent fractionation of ^{13}C in nature and in the laboratory: Growth-rate effects in some haptophyte algae. Global Biogeochem. Cycles **11**, 279-292.

Bloye, S.A., Karangouni, A.D., Carr, N.G. (1992) A continuous-culture approach to the question of inorganic carbon concentration by *Synechococcus* species. F.E.M.S. Lett. **99**, 79-84.

Briggs, G.E. (1959) Bicarbonate ion as a source of carbon dioxide in photosynthesis. J. Exp. Bot. **10**, 90-92.

Broecker, W.S., Peng, T. (1982). Tracers in the Sea. Columbia University Press, New York. 690 p.

Burkhardt, S., Riebesell, U., Zondervan, I. (1999) Stable carbon isotope fractionation by marine phytoplankton in response to daylength, growth rate, and CO_2 availability. Marine Ecology Progress Series **In Press**,

Burns, B.D., Beardall, J. (1987) Utilization of inorganic carbon by marine microalgae. J. Exp. Mar. Biol. Ecol. **107**, 75-86.

Chisholm, S.W. (1992) Phytoplankton size. In: Primary productivity and biogeochemical cycles in the sea. pp. 213-237, Falkowski, P.G., Woodhead, A.D. , eds, Plenum Press, New York.

Codispoti, L.A., Friederich, G.E., Hood, D.W. (1986) Variability in the inorganic carbon system over the southeastern Bering Sea shelf during spring 1980 and spring-summer 1981. Cont. Shelf Res. **5**, 133-160.

Codispoti, L.A., Friederich, G.E., Iverson, R.L., Hood, D.W. (1982) Temporal changes in the inorganic carbon system in the south-eastern Bering Sea during Spring. Nature **296**, 242-245.

Colman, B., Rotatore, C. (1995) Photosynthetic inorganic carbon uptake and accumulation in two marine diatoms. Plant Cell Environ. **18**, 919-924.

Cooper, D.J., Watson, A.J., Ling, R.D. (1998) Variation of PCO_2 along a North Atlantic shipping route (U.K. to the Caribbean): a year of automated observations. Mar. Chem. **60**, 147-164.

Crawford, D.W., Harrison, P.J. (1997) Direct measurement of PCO_2 in cultures of marine phytoplankton : how good is the estimate from pH_{NBS} and single point alkalinity titration? Mar. Ecol. Prog. Ser. **158**, 61-74.

Davison, I. (1987) Adaptation of photosynthesis in *Laminaria saccharina* (Phaeophyta) to changes in growth temperature. J. Phycol. **23**, 273-283.

Degens, E.T., Behrendt, M., Gotthardt, B., Reppmann, E. (1968a) Metabolic fractionation of carbon isotopes in marine plankton - II. Data on samples collected off the coast of Peru and Ecuador. Deep Sea Res. **15**, 11-20.

Degens, E.T., Guillard, R.R.L., Sackett, W.M., Hellebust, J.A. (1968b) Metabolite fractionation of carbon isotopes in marine plankton - I. Temperature and respiration experiments. Deep Sea Res. **15**, 1-9.

Descolas-Gros, C., De Billy, G. (1987) Temperature adaptation of RUBP carboxylase: kinetic properties in marine Antarctic diatoms. J. Exp. Mar. Biol. Ecol. **108**, 147-158.

Descolas-Gros, C., Fontugne, M.R. (1985) Carbon fixation in marine phytoplankton: carboxylase activities and stable carbon-isotope ratios; physiological and paleoclimatological aspects. Mar. Biol. **87**, 1-6

Descolas-Gros, C., Fontugne, M. (1990) Stable carbon isotope fractionation by marine phytoplankton during photosynthesis. Plant Cell Environ. **13**, 207-218.

Deuser, W.G., Degens, E.T., Guillard, R.R.L. (1968) Carbon isotope relationships between plankton and seawater. Geochim. Cosmochim. Acta **32**, 657-660.

Dixon, G.K., Merrett, M.J. (1988) Bicarbonate utilization by the marine diatom *Phaeodactylum tricornutum* Bohlin. New Phytol. **109**, 47-51.

Drechsler, Z., Sharkia, R., Cabantchik, Z.I., Beer, Z. (1993) Bicarbonate uptake in the marine macroalgae *Ulva* sp. is inhibited by classical probes of anion exchange in red blood cells. Planta **191**, 34-40.

Drechsler, Z., Sharkia, R., Cabantchik, Z.I., Beer, Z. (1994) The relationship of arginine groups to photosynthetic HCO_3^- uptake in *Ulva* sp. mediated by a putative anion exchanger. Planta **194**, 250-255.

Erez, J., Bouevitch, A., Kaplan, A. (1998) Carbon isotope fractionation by photosynthetic aquatic microorganisms: experiments with *Synechococcus* PCC7942, and a simple carbon flux model. Can. J. Bot. **76**, 1109-1118.

Falkowski, P.G. (1991) Species variability in the fractionation of ^{13}C and ^{12}C by marine phytoplankton. J. Plank. Res. **13 Supp**, 21-28.

Falkowski, P.G. (1994) The role of phytoplankton photosynthesis in global biogeochemical cycles. Photosynth. Res. **39**, 235-258.

Falkowski, P.G., Raven, J.A. (1998) Aquatic Photosynthesis. Blackwell Science, Malden, USA. 375 p.

Farquhar, G.D., O'Leary, M.H.O., Berry, J.A. (1982) On the relationship between carbon isotope discrimination and the intercellular carbon dioxide concentration in leaves. Aust. J. of Plant Physiol. **9**, 121-137.

France, F.L. (1995) Carbon-13 enrichment in benthic compared to planktonic algae: foodweb implications. Mar. Ecol. Prog. Ser. **124**, 307-312.

Freeman, K.H., Hayes, J.M. (1992) Fractionation of carbon isotopes by phytoplankton and estimates of ancient CO_2 levels. Global Biochem. Cycles **6**, 185-198.

Fry, B. (1996) $^{13}C/^{12}C$ fractionation by marine phytoplankton. Mar. Ecol. Prog. Ser. **134**, 283-294.

Fry, B., Wainright, S.C. (1991) Diatom sources of ^{13}C-rich carbon in marine food webs. Mar. Ecol. Prog. Ser. **76**, 149-157.

Glover, H.E. (1989) Ribulosebisphosphate carboxylase/oxygenase in marine organisms. Int. Rev. Cytol. **115**, 67-138.

Goericke, R., Fry, B. (1994) Variations of marine plankton $\delta^{13}C$ with latitude, temperature, and dissolved CO_2 in the world ocean. Global. Biogeochem. Cycles **8**, 85-90.

Goericke, R., Montoya, J.P., Fry, B. (1994) Physiology of isotope fractionation in algae and cyanobacteria. In. Stable Isotopes in Ecology. pp. 187-221, Lajtha, K., Michener, B., eds, Blackwell Scientific, Boston.

Goldman, J.C. (1999) Inorganic carbon availability and the growth of large marine diatoms. Mar. Ecol. Prog. Ser. **180**, 81-91.

Goldman, J.C., Carpenter, E.J. (1974) A kinetic approach to the effect of temperature on algal growth. Limnol. Oceanogr. **19**, 756-766.

Guy, R.D., Berry, J.A., Fogel, M.L., Turpin, D.H., Weger, H.G. (1992) Fractionation of the stable isotopes of oxygen during respiration by plants - the basis of a new technique to estimate partitioning to the alternative path. In: Molecular, Biochemical and Physiological Aspects of Plant Respiration. pp. 443-453, Lambers, H., van der Plas, L.H.W., eds, SPB Academic Publishing, The Hague.

Guy, R.D., Fogel, M.L., Berry, J.A. (1993) Photosynthetic fractionation of the stable isotopes of oxygen and carbon. Plant Physiol. **101**, 37-47.

Guy, R.D., Fogel, M.L., Berry, J.A., Hoering, T.C. (1987) Isotope fractionation during oxygen production and consumption by plants. Prog. Photosynth. Res. **3**, 597-600.

Guy, R.D., Vanlerberghe, G.C., Turpin, D.H. (1989) Significance of phospho*enol*pyruvate carboxylase during ammonium assimilation. Plant Physiol. **89**, 1150-1157.

Harrison, P.J., Waters, R.E., Taylor, F.J.R. (1980) A broad spectrum artificial seawater medium for coastal and open ocean phytoplankton. J. Phycol. **16**, 28-35.

Hayes, J.M., Freeman, K.H., Popp, B.N., Hoham, C.H. (1990) Compound-specific isotopic analyses : A novel tool for reconstruction of ancient biogeochemical processes. Organic Geochem. **16**, 1115-1128.

Hayes, J.M., Popp, B.N., Takigiku, R., Johnson, M.W. (1989) An isotopic study of biogeochemical relationships between carbonates and organic carbon in the Greenhorn Formation. Geochim. Cosmochim. Acta **53**, 2961-2972.

Hayes, J.M., Takigiku, R., Ocampo, R., Callot, H.J., Albrecht, P. (1987) Isotopic compositions and probable origins of organic molecules in the Eocene Messel shale. Nature **329**, 48-51.

Hinga, K.R., Arthur, M.A., Pilson, M.E.Q., Whitaker, D. (1994) Carbon isotope fractionation by marine phytoplankton in culture: the effects of CO_2 concentration, pH, temperature, and species. Global Biogeochem. Cycles **8**, 91-102.

Iglesias-Rodriguez, M.D., Merrett, M.J. (1997) Dissolved inorganic carbon utilization and the development of extracellular carbonic anhydrase by the marine diatom *Phaeodactylum tricornutum*. New Phytol. **135**, 163-168.

Jahne, B., Heinz, G., Dietrich, W. (1987) Measurement of the diffusion coefficients of sparingly soluble gases in water. J. Geophys. Res **92**, 10767-10776.

Jasper, J.P., Hayes, J.M. (1990) A carbon isotope record of CO_2 levels during the late Quaternary. Nature **347**, 462-464.

Johnson, K.S. (1982) Carbon dioxide hydration and dehydration kinetics in seawater. Limnol. Oceanogr. **27**, 849-855.

Johnston, A.M. (1996) The effect of environmental variables on ^{13}C discrimination by two marine phytoplankton. Mar. Ecol. Prog. Ser. **132**, 257-263.

Johnston, A.M., Raven, J.A. (1992) Effect of aeration rates on growth rates and natural abundance $^{13}C/^{12}C$ ratio of *Phaeodactylum tricornutum*. Mar. Ecol. Prog. Ser. **87**, 295-300.

Kaplan, A., Ronen-Tarazi, M., Zer, H., Schwarz, R., Tchernov, D., Bonfil, D.J., Schatz, D., Vardi, A., Hassidim, M., Reinhold, L. (1998) The inorganic carbon-concentrating mechanism in cyanobacteria: induction and ecological significance. Can. J. Bot. **76**, 917-924.

Keller, K., Morel, F.M.M. (1999) A model of carbon isotope fractionation and active carbon uptake in phytoplankton. Mar. Ecol. Prog. Ser. **182**, 295-298.

Kerby, N.W., Raven, J.A. (1985) Transport and fixation of inorganic carbon by marine algae. Adv. Bot. Res. **11**, 71-123.

Korb, R.E., Raven, J.A., Johnston, A.M. (1998) Relationship between aqueous CO_2 concentrations and stable carbon isotope discrimination in the diatoms *Chaetoceros calcitrans* and *Ditylum brightwellii*. Mar. Ecol. Prog. Ser. **171**, 303-305.

Korb, R.E., Raven, J.A., Johnston, A.M., Leftley, J.W. (1996) Effects of cell size and specific growth rate on stable carbon isotope discrimination by two species of marine diatom. Mar. Ecol. Prog. Ser. **143**, 283-288.

Korb, R.E., Saville, P.J., Johnston, A.M., Raven, J.A. (1997) Sources of inorganic carbon for photosynthesis by three species of marine phytoplankton. J. Phycol. **33**, 433-440.

Laws, E.A., Bidigare, R.R., Popp, B.N. (1997) Effect of growth rate and CO_2 concentration on carbon isotope fractionation by the marine diatom *Phaeodactylum tricornutum*. Limnol. Oceanogr. **42**, 1552-1560.

Laws, E.A., Popp, B.N., Bidigare, R.R., Kennicutt, M.C., Macko, S.A. (1995) Dependence of phytoplankton carbon isotope composition on growth rate and $[CO_2]$aq : theoretical considerations and experimental results. Geochim. Cosmochim. Acta **59**, 1131-1138.

Laws, E.A., Thompson, P.A., Popp, B.N., Bidigare, R.R. (1998) Sources of inorganic carbon for marine microalgal photosynthesis: A reassessment of $\delta^{13}C$ data from batch culture studies of *Thalassiosira pseudonana* and *Emiliania huxleyi*. Limnol. Oceanogr. **43**, 136-142.

Li, Y.H., Gregory, S. (1974) Diffusion of ions in sea water and deep-sea sediments. Geochim. Cosmochim. Acta **38**, 703-714.

Lee, L. (1998) The effects of light limited growth rate on carbon isotope fractionation by the marine diatom *Thalassiosira pseudonana*. Honours Thesis, University of British Columbia, Canada.

Lucas, W.J. (1983) Photosynthetic assimilation of exogenous HCO_3^- by aquatic plants. Ann. Rev. Plant Physiol. **34**, 71-104.

Maberly, S.C., Raven, J.A., Johnston, A.M. (1992) Discrimination between ^{12}C and ^{13}C by marine plants. Oecologia **91**, 481-492

Mariotti, A., Germon, J.C., Hubert, P., Kaiser, P., Letolle, R., Tardieux, A., Tardieux, P. (1981) Experimental determination of nitrogen kinetic isotope fractionation: some principles; illustration for the denitrification and nitrification processes. Plant Soil **62**, 413-430.

Martin, J.H., Gordon, R.M., Fitzwater, S.E. (1991) The case for iron. Limnol. Oceanogr. **36**, 1793-1802.

Mayo, W.P., Williams, T.G., Birch, D.G., Turpin, D.H. (1986) Photosynthetic adaptation by *Synechococcus leopoliensis* in response to exogenous dissolved inorganic carbon. Plant Physiol. **80**, 1038-1040.

Mayo, W.P., Elrifi, I.R., Turpin, D.H. (1989) The relationship between ribulose bisphosphate concentration, dissolved inorganic carbon (DIC) transport and DIC-limited photosynthesis in the cyanobacterium *Synechococcus leopoliensis* grown at different concentrations of inorganic carbon. Plant Physiol. **90**, 720-727.

McCabe, B. (1985) The dynamics of ^{13}C in several New Zealand lakes. Ph.D. Thesis, University of Waikato, New Zealand.

Merrett, M.J., Nimer, N.A., Dong, L.F. (1996) The utilization of bicarbonate ions by the marine microalga *Nannochloropsis oculata* (Droop) Hibberd. Plant Cell Environ. **19**, 478-484.

Mitchell, C., Beardall, J. (1996) Inorganic carbon uptake by an Antarctic sea-ice diatom, *Nitzschia frigida*. Polar Biol. **16**, 95-99.

Mizutani, H., Wada, E. (1982) Effect of high atmospheric CO_2 concentration on $\delta^{13}C$ of algae. Origins of Life **12**, 377-390.

Montagnes, D.J.S., Berges, J.A., Harrison, P.J., Taylor, F.J.R. (1994) Estimating carbon, nitrogen, protein, and chlorophyll a from volume in marine phytoplankton. Limnol. Oceanogr. **39**, 1044-1060.

Mook, W.G., Bommerson, J.C., Staverman, W.H. (1974) Carbon isotope fractionation between dissolved bicarbonate and gaseous carbon dioxide. Earth Planet. Sci. Lett. **22**, 169-176.

Morel, F.M.M. (1987) Kinetics of nutrient uptake and growth in phytoplankton. J. Phycol **23**, 137-150.

Morel, F.M.M., Reinfelder, J.R., Roberts, S.B., Chamberlain, C.P., Lee, J.G., Yee, D. (1994) Zinc and carbon co-limitation of marine phytoplankton. Nature **369**, 740-742.

Morse, D., Salois, P., Markovic, P., Hastings, J.W. (1995) A nuclear-encoded form II RuBisCO in dinoflagellates. Science **268**, 1622-1624.

O'Leary, M.H. (1981) Carbon isotope fractionation in plants. Phytochem. **20**, 553-567.

O'Leary, M.H. (1984) Measurement of the isotope fractionation associated with diffusion of carbon dioxide in aqueous solution. J. Phys. Chem. **88**, 823-825.

O'Leary, M.H. (1988) Carbon isotopes in photosynthesis: fractionation techniques may reveal new aspects of carbon dynamics in plants. BioScience **38**, 328-336.

O'Leary, M.H., Mandavan, S., Paneth, P. (1992) Physical and chemical basis of carbon isotope fractionation in plants. Plant Cell Environ. **15**, 1099-1104.

Pardue, J.W., Scalan, R.S., Van Baalen, C., Parker, P.L. (1976) Maximum carbon isotope fractionation in photosynthesis by blue-green algae and a green alga. Geochim. Cosmochim. Acta **40**, 309-312.

Park, R., Epstein, S. (1961) Metabolic fractionation of ^{13}C and ^{12}C in plants. Plant Physiol. **36**, 133-138.

Parsons, T.T., Maita, Y., Lalli, C.M. (1984) A manual of chemical and biological methods for seawater analysis. Pergamon Press, Oxford. 173 p.

Platt, T., Gallegos, C.L. (1980) Modelling primary production. In: Primary productivity in the sea. pp. 339-362, Falkowski, P.G., ed, Plenum Press, New York.

Popp, B.N., Laws, E.A., Bidigare, R.R., Dore, J.E., Hanson, K.L., Wakeham, S.G. (1998) Effect of phytoplankton cell geometry on carbon isotope fractionation. Geochim. Cosmochim. Acta **62**, 69-77.

Rau, G.H., Riebesell, U., Wolf-Gladrow, D. (1996) A model of photosynthetic ^{13}C fractionation by marine phytoplankton based on diffusive molecular CO_2 uptake. Mar. Ecol. Prog. Ser. **133**, 275-285.

Rau, G.H., Sweeney, R.E., Kaplan, I.R. (1982) Plankton ^{13}C : ^{12}C ratio changes with latitude: differences between northern and southern oceans. Deep Sea Res. **29**, 1035-1039.

Rau, G.H., Takahashi, T., Des Marais, D.J. (1989) Latitudinal variations in plankton $\delta^{13}C$: implications for CO_2 and productivity in past oceans. Nature **341**, 516-518.

Rau, G.H., Takahashi, T., Des Marais, D.J., Repeta, D.J., Martin, J.H. (1992) The relationship between $\delta^{13}C$ of organic matter and $[CO_2(aq)]$ in ocean surface water: Data from a JGOFS site in the northeast Atlantic Ocean and a model. Geochem. Cosmochim. Acta **56**, 1413-1419.

Raven, J.A. (1991a) Implications of inorganic carbon utilization: ecology, evolution, and geochemistry. Can. J. Bot. **69**, 908-924.

Raven, J.A. (1991b) Physiology in inorganic carbon acquisition and implications for resource use efficiency by marine phytoplankton: relation to increased CO_2 and temperature. Plant Cell Environ. **14**, 779-794.

Raven, J.A. (1993a) Carbon : a phycocentric view. In: Towards a Model of Ocean Biogeochemical Processes, Vol 1. pp. 123-152, Evans, G.T., Fasham, M.J.R., eds, Springer Verlag, Berlin.

Raven, J.A. (1993b) Limits on growth rates. Nature **361**, 209-210.

Raven, J.A. (1994) Why are there no picoplankton O_2 evolvers with volumes less than $10^{-19}m^3$? J. Plank. Res. **16**, 565-580.

Raven, J.A., Farquhar, G.D. (1990) The influence of N metabolism and organic acid synthesis on the natural abundance of C isotopes in plants. New Phytol. **116**, 505-529.

Raven, J.A., Geider, R.J. (1988) Temperature and algal growth. Nw Phytol. **110**, 441-461.

Raven, J.A., Johnston, A.M. (1991) Mechanisms of inorganic-carbon acquisition in marine phytoplankton and their implications for the use of other resources. Limnol. Oceanogr. **36**, 1701-1714.

Raven, J.A., Johnston, A.M., Turpin, D.H. (1993) Influence of changes in CO_2 concentration and temperature on marine phytoplankton $^{13}C/^{12}C$ ratios: an analysis of possible mechanisms. Glob. Planet. Change **8**, 1-12.

Raven, J.A., Lucas, W.J. (1985) Energy costs of carbon acquisition. In: Inorganic Carbon Uptake by Aquatic Photosynthetic Organisms. pp. 305-324, Lucas, W.J., Berry, J.A., eds. Waverly Press, Baltimore.

Read, B.A., Tabita, F.R. (1994) High substrate specificity factor ribulose bisphosphate carboxylase/oxygenase from eukaryotic marine algae and properties of recombinant cyanobacterial Rubisco containing "algal" residue modifications. Arch. Biochem. Biophys. **312**, 210-218.

Riebesell, U., Wolf-Gladrow, D.A., Smetacek, V. (1993a) Phytoplankton growth and CO_2. Nature **363**, 678-679.

Riebesell, U., Wolf-Gladrow, D.A., Smatacek, V. (1993b) Carbon dioxide limitation of marine phytoplankton growth rates. Nature **361**, 249-251.

Ritchie, R.J. (1998) Bioenergetics of membrane transport in *Synechococcus R-2* (*Anacystis nidulans*, *S. leopoliensis*) PCC7942. Can. J. Bot. **76**, 1127-1145.

Robertson, J.E., Robinson, C., Turner, D.R., Holligan, P., Watson, A.J., Boyd, P., Fernandez, E., Finch, M. (1994) The impact of a coccolithophore bloom on ocean carbon uptake in the northeast Atlantic during summer 1991. Deep Sea Res. **41**, 297-314.

Roeske, C.A., O'Leary, M.H.O. (1984) Carbon isotope effects on the enzyme-catalyzed carboxylation of rubulose bisphosphate. Biochemistry **23**, 6275-6284.

Roeske, C.A., O'Leary, M.H.O. (1985) Carbon isotope effect on carboxylation of ribulose bisphosphate catalyzed by ribulose bisphosphate carboxylase from *Rhodospirillum rubrum*. Biochemistry **24**, 1603-1607.

Sackett, W.M. (1991) A history of the $\delta^{13}C$ composition of oceanic plankton. Mar. Chem. **34**, 153-156.

Sackett, W.M., Eckelmann, W.R., Bender, M.L., Be, A.W.H. (1965) Temperature dependence of carbon isotope composition in marine plankton and sediments. Science **148**, 235-237.

Sharkey, T.D., Berry, J.A. (1985) Carbon isotope fractionation of algae as influenced by an inducible CO_2 concentrating mechanism. In: Inorganic Carbon Uptake by Aquatic Photosynthetic Organisms. pp. 389-401, Lucas, W.J., Berry, J.A., eds. Waverly Press, Baltimore.

Smith, F.R., Walker, N.A. (1980) Photosynthesis by aquatic plants: effects of unstirred layer in relation to assimilation of CO_2 and HCO_3^- to carbon isotope discrimination. New Phytol. **86**, 245-259.

Strathmann, R.R. (1967) Estimating the organic carbon content of phytoplankton from cell volume or plasma volume. Limnol. Oceanogr. **12**, 411-418.

Tchernov, D., Hassidim, M., Vardi, A., Luz, B., Sukenik, A., Reinhold, L., Kaplan, A. (1998) Photosynthesizing marine microorganisms can constitute a source of CO_2 rather than a sink. Can. J. Bot. **76**, 949-953.

Thompson, P.A., Calvert, S.E. (1994) Carbon-isotope fractionation by a marine diatom : The influence of irradiance, daylength, pH, and nitrogen source. Limnol. Oceanogr. **39**, 1835-1844.

Thompson, P.A., Harrison, P.J., Parslow, J.S. (1991) Influence of irradiance on cell volume and carbon quota for ten species of marine phytoplankton. J. Phycol. **27**, 351-360.

Tortell, O.D., Reinfelder, J.R., Morel, F.M.M. (1997) Active uptake of bicarbonate by diatoms. Nature **390**, 243-244.

Turpin, D.H. (1993) Phytoplankton growth and CO_2. Nature **363**, 678.

Turpin, D.H., Elrifi, I.R., Birch, D.W., Weger, H.G., Holmes, J.J. (1988) Interactions between photosynthesis, respiration and nitrogen assimilation in microalgae. Can. J. Bot. **66**, 2083-2097.

Wada, E., Terazaki, M., Kabaya, Y., Nemoto, T. (1987) ^{15}N and ^{13}C abundances in the Antarctic Ocean with emphasis on the biogeochemical structure of the food web. Deep Sea Res. **34**, 829-841.

Wanninkhof, R., Feely, R.A. (1998) f CO_2 dynamics in the Atlantic, South Pacific, and South Indian oceans. Mar. Chem. **60**, 15-31.

Wolf-Gladrow, D., Riebesell, U. (1997) Diffusion and reactions in the vicinity of microalgae: a refined model for inorganic transport. Mar. Chem. **59**, 17-34.

Wong, W.W. (1976) Carbon isotope fractionation by marine phytoplankton. Ph.D. Thesis, Texas A & M University, College Station.

Wong, W.W., Sackett, W.M. (1978) Fractionation of stable carbon isotopes by marine phytoplankton. Geochim. Cosmochim. Acta **42**, 1809-1815.

Appendix A

Cell Volume Determination

Table A.1. Various size measurements of the six phytoplankton species tested. Cylindrical cell volume calculated using $v = \pi \cdot r^2 \cdot l$; spherical cell volume calculated using $v = {}^4/_3 \cdot \pi \cdot r^3$; oblong cell volume calculated using $v = l \cdot t \cdot w$ (t and w are average across length of cell). Data are from Northeast Pacific Culture Collection (NEPCC) or from the reference cited.

Species	Shape	Radius (μm)	Length (μm)	Thickness (μm)	Width (μm)	Volume (μm^3)	Reference
T. pseudonana	Cylinder	2.25	3.50	n/a	n/a	55.67	NEPCC
T. weissflogii	Cylinder	5.75	11.50	n/a	n/a	1194.49	NEPCC
P. tricornutum	Oblong	n/a	14.20	1.40	2.05	40.75	Popp *et al.* 1998
S. costatum	Cylinder	2.45	11.60	n/a	n/a	218.75	NEPCC
S. bacillaris	Sphere	0.68	n/a	n/a	n/a	1.32	Popp *et al.* 1998
D. tertiolecta	Sphere	4.10	n/a	n/a	n/a	288.70	NEPCC

Appendix B

Data Used for Modeling

Table B.1. Raw data used for modeling (continued). All cultures were *Thalassiosira pseudonana*. Steady state culture results were presented in Chapter 4. Multiple species data are for *T. pseudonana* only from Chapter 3. Units for light are μmol photons m^{-2} s^{-1}.

Experiment	Temp	Light	pH	μ ± 1 SD	[DIC]	[CO2]	Fract ± 1 SE	Ep	$K_{1/2}$DIC ± 1 SE	$K_{1/2}CO_2$ ± 1 SE
	°C			(d^{-1})	(mM)	(μM)	(‰)	(‰)	(μM)	(μM)
Steady State	18	200	8.2	1.09 ± 0.00	0.20	1.25	11.646 ± 0.453	1.886	85.90 ± 5.70	0.537 ± 0.036
Steady State	18	200	8.2	1.06 ± 0.42	0.45	2.81	14.255 ± 2.127	4.495	115.70 ± 4.90	0.723 ± 0.031
Steady State	18	200	8.2	1.45 ± 0.20	0.67	4.19	14.912 ± 1.109	5.152	124.80 ± 4.60	0.780 ± 0.029
Steady State	18	200	8.2	1.43 ± 0.40	1.00	6.25	16.848 ± 1.362	7.088	212.10 ± 15.90	1.326 ± 0.099
Steady State	18	200	8.2	1.26 ± 0.22	1.22	7.63	17.448 ± 0.000	7.688	260.00 ± 14.30	1.626 ± 0.089
Steady State	18	200	8.2	1.46 ± 0.26	1.33	8.32	18.970 ± 1.080	9.210	210.30 ± 8.70	1.315 ± 0.054
Steady State	18	200	8.2	1.37 ± 0.29	1.45	9.07	19.330 ± 0.407	9.570	244.30 ± 9.70	1.528 ± 0.061
Steady State	18	200	8.2	1.61 ± 0.10	1.60	10.00	17.930 ± 1.264	8.170	324.00 ± 12.00	2.026 ± 0.075
Steady State	18	200	8.2	1.42 ± 0.33	1.90	11.88	19.086 ± 0.232	9.326	433.60 ± 34.80	2.711 ± 0.218
Steady State	18	200	8.2	1.68 ± 0.20	2.00	12.51	21.548 ± 0.026	11.788	470.00 ± 20.00	2.939 ± 0.125
Steady State	18	200	8.2	1.50 ± 0.31	2.35	14.69	21.978 ± 0.630	12.218	260.70 ± 19.00	1.630 ± 0.119
Steady State	18	200	8.2	1.51 ± 0.14	2.75	17.20	21.628 ± 0.258	11.868	469.30 ± 28.70	2.934 ± 0.179
Mult. Species	18	200	8.2	1.68 ± 0.22	2.70	16.88	21.833 ± 0.493	12.073	817.39 ± 62.24	5.111 ± 0.389
Mult. Species	18	200	8.2	1.52 ± 0.27	0.50	3.13	15.760 ± 0.849	6.000	98.37 ± 7.85	0.615 ± 0.049

Table B.2. Raw data used for modeling. All cultures were *Thalassiosira pseudonana*. The temperature data are from Chapter 4 while the light level data are from Lee (1998). Units for light are μmol photons m^{-2} s^{-1}.

Experiment	Temp	Light	pH	μ ± 1 SD	[DIC]	[CO2]	Fract ± 1 SE	Ep	$K_{1/2}$DIC ± 1 SE	$K_{1/2}CO_2$ ± 1 SE
	°C	(μE)		(d^{-1})	(mM)	(uM)	(‰)	(‰)	(μM)	(μM)
Temperature	10	200	8.2	0.57 ± 0.04	0.42	3.13	21.223 ± 0.601	10.50300	317.80 ± 14.20	2.366 ± 0.106
Temperature	10	200	8.2	0.58 ± 0.07	1.68	12.51	29.615 ± 0.346	18.89500	544.10 ± 40.90	4.051 ± 0.304
Temperature	14	200	8.2	1.20 ± 0.21	0.46	3.13	18.739 ± 0.440	8.49900	203.40 ± 9.70	1.398 ± 0.067
Temperature	14	200	8.2	1.48 ± 0.08	1.82	12.51	27.225 ± 0.154	16.98500	549.70 ± 17.50	3.777 ± 0.120
Temperature	18	200	8.2	1.76 ± 0.07	0.50	3.13	16.900 ± 1.042	7.14000	140.10 ± 7.10	0.876 ± 0.044
Temperature	18	200	8.2	1.59 ± 0.24	2.00	12.51	21.640 ± 0.079	11.88000	436.80 ± 24.70	2.731 ± 0.154
Temperature	22	200	8.2	2.00 ± 0.46	0.52	3.13	14.197 ± 0.394	4.88700	255.80 ± 5.70	1.532 ± 0.034
Temperature	22	200	8.2	1.99 ± 0.34	2.09	12.51	21.621 ± 0.059	12.31100	432.10 ± 9.40	2.588 ± 0.056
Light	18	25	8.2	0.65 ± 0.13	0.50	3.13	16.390 ± 0.300	6.63000	38.40 ± 7.51	0.240 ± 0.047
Light	18	50	8.2	0.86 ± 0.22	0.50	3.13	19.480 ± 0.130	9.72000	69.04 ± 6.17	0.432 ± 0.039
Light	18	75	8.2	1.30 ± 0.13	0.50	3.13	18.740 ± 0.190	8.98000	67.23 ± 4.26	0.420 ± 0.027
Light	18	200	8.2	2.00 ± 0.28	0.50	3.13	16.670 ± 0.420	6.91000	126.90 ± 4.26	0.793 ± 0.027
Light	18	25	8.2	0.63 ± 0.10	1.00	6.25	20.890 ± 0.380	11.13000	108.58 ± 8.94	0.679 ± 0.056
Light	18	50	8.2	0.86 ± 0.25	1.00	6.25	20.590 ± 0.070	10.83000	179.63 ± 9.03	1.123 ± 0.056
Light	18	75	8.2	1.29 ± 0.11	1.00	6.25	18.520 ± 0.470	8.76000	194.42 ± 19.53	1.216 ± 0.122
Light	18	200	8.2	1.68 ± 0.24	1.00	6.25	15.340 ± 0.040	5.58000	249.08 ± 47.88	1.557 ± 0.299
Light	18	25	8.2	0.57 ± 0.07	2.00	12.51	24.510 ± 0.080	14.75000	199.35 ± 14.75	1.247 ± 0.092
Light	18	50	8.2	1.08 ± 0.08	2.00	12.51	20.890 ± 0.150	11.13000	182.31 ± 28.28	1.140 ± 0.177
Light	18	75	8.2	1.22 ± 0.10	2.00	12.51	19.230 ± 0.090	9.47000	303.35 ± 19.20	1.897 ± 0.120
Light	18	200	8.2	1.60 ± 0.04	2.00	12.51	16.990 ± 0.500	7.23000	332.44 ± 20.30	2.079 ± 0.127

Appendix C

Diffusion Model # 1

Source : Raven *et al.* (1993)

Equations :

$$\frac{C_C}{C_B} = \frac{[(\Delta+1)-\alpha_{diff}]}{[\alpha_{carbox}-\alpha_{diff}]} \quad (15)$$

$$\text{Limitation by diffusion} = 1 - \frac{C_C}{C_B} \quad (16)$$

$$\Delta = \frac{\varepsilon_P}{1000} \quad (17)$$

Where :

$C_C = [CO_2]$ at carboxylation site (mol m^{-3})

$C_B = [CO_2]$ in the bulk medium (mol m^{-3})

$\alpha_{diff} = 1.0007$ (unitless)

$\alpha_{carbox} = 1.029$ (unitless)

Δ = fractionation (unitless)

Note : $\text{Limitation by carboxylation} = \frac{C_C}{C_B}$

Figure : Figure 5.8

Appendix D

Diffusion Model # 2

Source : Hinga *et al.* (1994); Farquhar *et al.* (1982)

Equation :

$$\frac{C_i}{C_e} = \frac{\left[\left(\delta^{13}_{plant} - \delta^{13}CO_2\right) + d\right]}{\left[d + f\right]} \qquad (18)$$

Where : C_i = internal $[CO_2]$ (mol m^{-3})

C_e = external $[CO_2]$ (mol m^{-3})

d = fractionation during CO2 diffusion (‰)

f = fractionation by RuBisCO + other enzymes (‰)

Note : This is a variation of equation 15 presented in Appendix C.

Figure : Figure 5.9

Appendix E

Diffusion Model # 3

Source : Rau *et al.* (1996)

Equations :

$$\varepsilon_p = \varepsilon_f + \frac{b}{C_e} \tag{19}$$

$$b = -(\varepsilon_f - \varepsilon_d)\, Q_s \left[\frac{r}{D_T (1 + r/r_k)} + \frac{1}{P} \right] \tag{20}$$

$$Q_s = \frac{Q_r}{4\pi r^2} \tag{21}$$

$$D_T = D_{T(\text{FreshWater})} \times \left[0.9508 - \left(7.389 \times 10^{-4}\, T_C \right) \right] \tag{22}$$

$$D_{T(\text{FreshWater})} = 5.019 \times 10^{-6}\, e^{-\left(\frac{E_d}{RT_K} \right)} \tag{23}$$

$$r_k = \sqrt{\frac{D_T}{k'}} \tag{24}$$

$$Q_r = \gamma_c \times \mu_i \tag{25}$$

$$\mu_i = \mu \times \frac{L + D}{L} \tag{26}$$

$$k' = k_{1(T_K)} [OH^-] + k_{2(T_K)} \tag{27}$$

$$k_{1(T_K)} = k_{1(T_{Ko})} \frac{e^{-\left(\frac{E_k}{RT_K} \right)}}{e^{-\left(\frac{E_k}{RT_{Ko}} \right)}} \tag{28}$$

$$k_{2(T_K)} = k_{2(T_{Ko})} \frac{e^{-\left(\frac{E_k}{RT_K}\right)}}{e^{-\left(\frac{E_k}{RT_{Ko}}\right)}} \quad (29)$$

$$[OH^-] = \frac{K_W}{[H^+]} \quad (30)$$

$$[H^+] = 10^{-pH} \quad (31)$$

$$K_W = 10^{-pK_W} \quad (32)$$

$$pK_W = \frac{3441.0}{T_K} + 2.241 - \left(0.09415\sqrt{S}\right) \quad (33)$$

Related Equations :

$$\delta^{13}C_{Ce} = \delta^{13}C_{\Sigma CO_2} + 23.644 - \frac{9701.5}{T_K} \quad (34)$$

$$C_r = C_e - \frac{Q_r}{4\pi r D_T \left(1 + r/r_k\right)} \quad (35)$$

$$C_i = C_r - \frac{Q_s}{P} \quad (36)$$

$$\gamma_c = 3.154 \times 10^{-14} V^{0.758} \quad (37)$$

Note : - This model assumes fractionation by RuBisCO to be 25‰ and a fractionation of 0.7‰ for CO_2 diffusion.

Figure : Figure 5.10

Table E.1. Brief description of the equations used in the model of carbon isotope fractionation described in this appendix.

Equation #	Function of Equation
1	Calculate the fractionation relative to external CO_2 concentration
2	Calculate the constant 'b' for the Farquhar *et al.* (1982) model
3	Calculation of CO_2 uptake rate per unit cell surface area
4	Calculate temperature sensitive diffusivity of CO_2 in seawater (Li and Gregory 1974)
5	Calculate temperature sensitive diffusivity of CO_2 in fresh water (Jahne *et al.* 1987)
6	Calculate reacto-diffusive length
7	Calculate CO_2 uptake rate per cell to support a given growth rate
8	Convert per day growth rate to instantaneous growth rate ($\mu_i = \mu$ when 24 h Light)
9	Rate coefficient calculation
10	Correct k_1 to appropriate temperature
11	Correct k_2 to appropriate temperature
12	Calculate hydroxide ion concentration
13	Calculate hydrogen ion concentration
14	Calculate K_W
15	Calculate pK_W for given temperature and salinity
16	Calculate isotope content of CO_2 based on total DIC isotope content (Mook *et al.* 1974)
17	Calculate CO_2 concentration at cell surface
18	Calculate CO_2 concentration inside cell
19	Estimation of cell carbon content based on volume (Strathmann 1967)

Table E.2. Listing of parameters, definitions, and base values used in the carbon isotope fractionation model described in this appendix.

Variable	Definition	Source	Value	Units
B	$(\varepsilon_p - \varepsilon_f)\ C_e$	Calculated		‰ µM
C_e	Ambient CO_2	Input	Variable	mol m^{-3}
C_I	Intracellular CO_2	Calculated		mol m^{-3}
C_r	CO_2 at cell surface	Calculated		mol m^{-3}
D	Dark period	Input	0	H
$\delta^{13}C_{Ce}$	Isotope content of C_e	Calculated		‰
$\delta^{13}C_{Ci}$	Isotope content of C_I	Calculated		‰
$\delta^{13}C_{phyto}$	Isotope content of POC	Calculated		‰
$\delta^{13}C_{DIC}$	Isotope content of total DIC	Input	0	‰
$\Delta\ \delta$	$\delta^{13}C_{DIC} - \delta^{13}C_{phyto}$	Output		‰
D_T	D_T corrected for salt water	Calculated		$m^2\ s^{-1}$
$D_{T(Fresh\ Water)}$	Temp sensitive diffusivity of CO_2	Calculated		$m^2\ s^{-1}$
ε_d	Diffusion isotope fractionation	Assumed	0.70	‰
ε_f	Enzymatic isotope fractionation	Assumed	25.00	‰
ε_p	$\delta^{13}C_{Ce} - \delta^{13}C_{phyto}$	Output		‰
E_d	Activation energy (diffusion)	Constant	19,510	J mol^{-1}
E_k	Activation energy (reaction)	Constant	62,800	J mol^{-1}
γ_c	Carbon content per cell	Input	5.00×10^{-13}	mol C
k'	Rate coefficient	Calculated		s^{-1}
$k_{1(Tko)}$	Rate coefficient at 25C	Constant	8,500	$m^3\ mol^{-1}\ s^{-1}$
$k_{2(Tko)}$	Rate coefficient at 25C	Constant	3×10^{-5}	s^{-1}
$k_{1(TK)}$	Rate coefficient	Calculated		$m^3\ mol^{-1}\ s^{-1}$
$k_{2(TK)}$	Rate coefficient	Calculated		s^{-1}
K_w	Constant	Calculated		Unitless
L	Light period	Input	24	H
μ	Specific growth rate	Input	Variable	d^{-1}
μ_i	Instantaneous growth rate	Calculated		s^{-1}
π	Constant	Constant	3.1416	Unitless
P	Membrane permeability to CO_2	Assumed	1.0×10^{-4}	m s^{-1}
pH	pH of growth medium	Input	8.2	Unitless
pK_w	Calculated Value	Calculated		Unitless
Q_r	CO_2 uptake rate per cell	Calculated		mol C s^{-1}
Q_s	CO_2 uptake per unit surface area	Calculated		mol C $m^{-2}\ s^{-1}$
r	Surface area equivalent radius	Input	2.54×10^{-6}	M
R	gas constant	Constant	8.3143	J K^{-1} mol^{-1}
r_k	Reacto-diffusive length	Calculated		M
S	Salinity	Input	35	Psu
T_c	Temperature	Input	Variable	°C
T_k	Temperature (273.15 + T_c)	Calculated		°K
T_{ko}	Temperature in °K at 25°C	Constant	298.15	°K
V	Cell volume	Input	n/a	μm^3

Appendix F

Active Uptake Model # 1

Source : Laws *et al.* (1997)

Equation :

$$\frac{\mu}{C_e} = 0.225\left(\frac{\varepsilon_2' - \varepsilon_p}{\varepsilon_p - \varepsilon_1'}\right) \qquad (38)$$

Where μ = growth rate (d^{-1})

C_e = external CO_2 concentration ($\mu mol\ kg^{-1}$)

ε_p = observed fractionation relative to CO_2 (‰)

ε_1' = minimum possible ε_p value presumably due to uptake fractionation (‰)

ε_2' = maximum possible ε_p value presumably due to fixation fractionation (‰)

Note :

- ε_1' and ε_2' are parameters fitted through regression.
- Linear regression is for C_e>10 $\mu mol\ kg^{-1}$. Non-linear regression (above model) is for entire range of C_e.

Figure : Figure 5.11

Appendix G

Active Model # 2

Source : Sharkey and Berry (1985)

Equation : $$D = d + b_3 \frac{F_3}{F_1} \quad (39)$$

Where D = observed fractionation by the phytoplankton relative to dissolved CO_2 in the medium (‰)

d = equilibrium fractionation associated with hydration of CO_2 (‰)

b_3 = fractionation by RuBisCO (‰)

F_1 = influx rate of carbon (relative)

F_3 = efflux rate of carbon (relative)

$\frac{F_3}{F_1}$ = leakiness of the cell.

Figure : Figure 5.13

Appendix H

Active Model # 3

Source : Keller and Morel (1999)

Equation :

$$\varepsilon_p = \varepsilon_t + \left(\frac{\gamma}{\frac{[CO_2]_o \times P \times A}{\mu \times Q_c} + \gamma} \right) \left(\delta^{13}C_{CO_{2,o}} - \delta^{13}C_{source} \right) + \frac{1 + (\gamma - 1)\left(\frac{\mu \times Q_c}{[CO_2]_o \times P \times A} \right)}{1 + \gamma \left(\frac{\mu \times Q_c}{[CO_2]_o \times P \times A} \right)} \left(\varepsilon_{fix} - \varepsilon_{diff} \right) \quad (40)$$

Where See Table H.1

Note : - Relationship between $\delta^{13}C$ of DIC and CO_2 is described by Equation 34 of Appendix E.

- ε_{fix} assumed to be 29‰ and ε_t to be 0‰

Figure : Figure 5.13

Table H.1. Listing of parameters, definitions, and base values used in the carbon isotope fractionation model described in this appendix.

Parameter	Description	Source	Value	Units
A	Cell surface area	Input	8.13×10^{-11}	m^2
$[CO_2]_o$	External CO_2 concentration	Input	Variable	mol m^3
$\delta^{13}C_{CO2,o}$	$\delta^{13}C$ of the external CO_2	Input	-7.5	‰
$\delta^{13}C_{source}$	$\delta^{13}C$ of either CO_2 or HCO_3^- actively transported	Input		‰
ε_{diff}	Diffusion fractionation relative to CO_2	Assumed	0.70	‰
ε_{fix}	Fixation fractionation relative to CO_2	Assumed	29.00	‰
ε_p	Observed fractionation relative to CO_2	Output		‰
ε_t	Active uptake fractionation relative to source carbon (CO_2 or HCO_3^-)	Assumed	0.00	‰
γ	Active carbon uptake ratio	Fitted		Unitless
μ	Growth rate	Input	Variable	s^{-1}
P	Membrane permeability	Fitted		m s^{-1}
Q_c	Cellular carbon content	Input	5.00×10^{-13}	mol

Appendix I

Active Model # 4

Source : Keller and Morel (unpublished)

Equation :

$$\varepsilon_p = -\left(1 - \frac{[CO_2]_o \times P \times A}{\mu \times Q_c + ([CO_2]_i \times P \times A)}\right)\left(\delta^{13}C_{source} - \varepsilon_t\right)$$

$$-\left(\frac{[CO_2]_o \times P \times A}{(\mu \times Q_c) + ([CO_2]_i \times P \times A)}\right)\left(\delta^{13}C_{CO_{2,o}} - \varepsilon_{diff}\right)$$

$$+\left(\frac{1}{1 + \left(\frac{\mu \times Q_c}{[CO_2]_i \times P \times A}\right)}\right)\left(\varepsilon_{fix} - \varepsilon_{diff}\right)$$

$$+ \delta^{13}C_{CO_{2,o}} \qquad (41)$$

$$[CO_2]_i = [CO_2]_{i,critical} \text{ if } [CO_2]_o \leq [CO_2]_{i,critical} + \frac{\mu \times Q_x}{P \times A}$$

$$[CO_2]_i = [CO_2]_o - \frac{\mu \times Q_x}{P \times A} \text{ otherwise} \qquad (42)$$

$$[CO_2]_{i,critical} = \frac{V \times Km}{V\,max - V} \qquad (43)$$

$$V = Q_c \times \mu \qquad (44)$$

Table I.1. Listing of parameters, definitions, and base values used in the carbon isotope fractionation model described in this appendix.

Parameter	Description	Source	Value	Units
A	Cell surface area	Input	8.13×10^{-11}	m^2
$[CO_2]_I$	Internal CO_2 concentration	Input	8.33×10^{-3}	mol m^3
$[CO_2]_{I,critical}$	Critical internal CO_2 concentration	Input	Variable	mol m^3
$[CO_2]_o$	External CO_2 concentration	Input	Variable	mol m^3
$\delta^{13}C_{CO2,o}$	$\delta^{13}C$ of the external CO_2	Input	-7.5	‰
$\delta^{13}C_{source}$	$\delta^{13}C$ of either CO_2 or HCO_3^- actively transported	Input		‰
ε_{diff}	Diffusion fractionation relative to CO_2	Assumed	0.70	‰
ε_{fix}	Fixation fractionation relative to CO_2	Assumed	29.00	‰
ε_p	Observed fractionation relative to CO_2	Output		‰
ε_t	Active uptake fractionation relative to source carbon (CO_2 or HCO_3^-)	Assumed	0.00	‰
γ	Active carbon uptake ratio	Fitted		Unitless
Km	Half saturation constant of RuBisCO	Assumed	40*	μM
μ	Growth rate	Input	Variable	s^{-1}
P	Membrane permeability	Fitted		m s^{-1}
Q_c	Cellular carbon content	Input	5.00×10^{-13}	mol
V	Minimum photosynthetic rate required to support a given growth rate	Calculated	8.10×10^{-18}	mol s^{-1}
Vmax	Maximum photosynthetic rate	Input	4.70×10^{-17}	mol s^{-1}

* From Badger (1998) for *Phaeodactylum tricornutum*

Note : - Relationship between $\delta^{13}C$ of DIC and CO_2 is described by Equation 34 of Appendix E.

- ε_{fix} assumed to be 29 ‰ and ε_t to be 0 ‰

Figure : Figure 5.14